

VYSOKÉ UČENÍ TECHNICKÉ V BRNĚ  
BRNO UNIVERSITY OF TECHNOLOGY



FAKULTA STROJNÍHO INŽENÝRSTVÍ  
ÚSTAV PROCESNÍHO A EKOLOGICKÉHO INŽENÝRSTVÍ  
FACULTY OF MECHANICAL ENGINEERING  
INSTITUTE OF PROCESS AND ENVIRONMENTAL ENGINEERING

# NUMERICAL MODELLING OF GRATE COMBUSTION

## NUMERICKÉ MODELOVÁNÍ SPALOVÁNÍ NA ROŠTU

DIZERTAČNÍ PRÁCE  
DOCTORAL THESIS

AUTOR PRÁCE  
AUTHOR

Ing. TOMÁŠ JUŘENA

VEDOUČÍ PRÁCE  
SUPERVISOR

doc. Ing. JIŘÍ HÁJEK, Ph.D.

BRNO 2012



## **Abstract**

The present work is focused on numerical modelling of grate combustion of solid fuels by means of computational fluid dynamics (CFD) methods. Since CFD results from simulations of grate combustion depend on the quality of input data including information on temperature, mass flux and chemical composition of flue gas leaving a fuel bed, the attention is turned to modelling of processes, that take place within the fuel bed on a grate. A great part of the work is devoted to development of a reliable numerical model of packed-bed combustion as it may help improve both results from simulations and knowledge of principles of solid fuel combustion in fixed or moving beds.

A one-dimensional transient numerical model of combustion in an experimental reactor is developed and implemented into a computer program called GRATECAL 1.3 with a graphical user interface. A special emphasis is put on the conservativeness property of the model. Therefore, a method for control of mass and energy balance over the system is developed and applied to a series of case studies, which have revealed certain errors in definitions of mass source terms, so that data adopted from literature have been reconciled.

The model is used for analysis of propagation of drying and char combustion reaction fronts in a bed of wheat straw particles. It is suggested to include modelling of particle internal porosity change in order to obtain correct reaction zone thickness, if porosity of the bed is allowed to change during combustion. The balance-based method is also used to analyse effects of convergence criteria on mass and energy imbalance of the modelled system. It is found that all the scaled residuals must drop to as low as  $10^{-6}$  or lower in order to obtain sufficiently accurate results from in-bed simulations in terms of mass and energy conservation within the packed bed.

The second part of the work is devoted to development of a library of user-defined functions for the commercial CFD software ANSYS FLUENT for coupling the bed model with a freeboard model of a real combustion unit in order to specify the boundary conditions indirectly using results from in-bed simulations. The created interface is general enough to be used for a wide range of models of grate furnaces.

The presented results contribute to better understanding of numerical modelling of grate combustion, especially in the setup of a numerical model and parameters of solver for the control of the convergence.

## **Keywords**

Computational Fluid Dynamics, numerical modelling, grate combustion, solid fuels, packed-bed model, scaled residuals, mass and energy balance, coupled models, user defined function

## Abstrakt

Předkládaná práce je zaměřena na numerické modelování spalování tuhých paliv na roštu metodami výpočtové dynamiky tekutin (CFD). Jelikož výsledky CFD simulací roštového spalování závisí na kvalitě vstupních dat, která zahrnují i údaje o teplotě, hmotnostním toku a chemickém složení spalin vystupujících z lože, pozornost je věnována především procesům, probíhajícím v loži během spalování na roštu. Velká část práce je věnována vývoji spolehlivého modelu spalování v sypaných ložích, jelikož může napomoci zkvalitnit výsledky simulací i rozšířit znalosti principů spalování tuhých paliv v sypaných ložích.

V rámci práce byl vyvinut jednorozměrný nestacionární model spalování v experimentálním reaktoru a implementován do počítačového programu GRATECAL 1.3 včetně grafického uživatelského rozhraní. Zvláštní důraz byl kladen na konzervativnost modelu. Proto byla vyvinuta metoda pro kontrolu hmotnostní a energetické bilance systému a následně aplikována v řadě studií, v rámci nichž byly odhaleny některé chyby týkající se definic zdrojových členů, které byly převzaty z literatury a opraveny.

Pomocí modelu byla provedena analýza šíření čela sušení a reakce hoření koksu po výšce lože pšeničné slámy. Na základě výsledků těchto analýz bylo doporučeno zahrnout i modelování změny porozity částic paliva, aby šířka reakční zóny byla predikována korektně v případě, že je uvažována změna porozity celého lože. Rovněž vyvinutá bilanční metoda byla použita k analýze vlivu kritérií konvergence na hmotnostní a energetickou nerovnováhu simulovaného systému. Bylo zjištěno, že škálovaná rezidua rovnic všech veličin by měla poklesnout aspoň na hodnotu  $10^{-6}$ , aby bylo dosaženo nízké hmotnostní a energetické nerovnováhy a tudíž uspokojivě přesných výsledků ze simulací v loži.

Druhá část práce je věnována vývoji a implementaci knihovny uživatelem definovaných funkcí pro komerční CFD nástroj ANSYS FLUENT, které slouží k propojení modelu lože s modelem komory reálné spalovací jednotky, aby byla umožněna dynamická změna okrajových podmínek na vstupu do komory v závislosti na výstupech ze simulací v loži. Vytvořené rozhraní pro propojení těchto dvou modelů je dostatečně obecné pro aplikaci na širokou škálu modelů roštových kotlů.

Popsané výsledky přispívají k lepšímu porozumění numerickému modelování spalování na roštu, a to zejména ve fázi sestavování numerického modelu a nastavení parametrů řešiče pro kontrolu konvergence.

## Klíčová slova

výpočtová dynamika tekutin, roštové spalování, tuhá paliva, model sypaného lože, škálovaná rezidua, hmotnostní a energetická bilance, propojené modely, uživatelem definovaná funkce

JUŘENA, T. *Numerical modelling of grate combustion*. Brno: Vysoké učení technické v Brně, Fakulta strojního inženýrství, 2012. 97 s. Vedoucí disertační práce doc. Ing. Jiří Hájek, Ph.D.

**Prohlášení o původnosti práce**

Prohlašuji, že dizertační práci jsem vypracoval samostatně pod vedením doc. Ing. Jiřího Hájka, Ph.D. a s použitím uvedené literatury.

V Brně 9.10.2012

Ing. Tomáš Juřena



## **Acknowledgements**

I would like to thank to my supervisor doc. Ing. Jiří Hájek, Ph.D. for his guidance, countless inspiring discussions and neverending optimism, all of which have helped me to finish the thesis. Thanks also to prof. Ing. Petr Stehlík, CSc. for allowing me to study and work in scientific research at the Institute of Process and Environmental Engineering.

My special thanks belong to my parents, close friends and especially my girlfriend Eva for her patience and support she has given me during my studies. Without that, the work would have been experienced much worse.

I would also like to thank to South Moravian Centre for International Mobility for their great financial support within the framework of the program Brno Ph.D. Talent.

## **Poděkování**

Tímto bych rád poděkoval svému školiteli doc. Ing. Jiřímu Hájkovi, Ph.D. za odborné vedení, nesčetné podnětné diskuse a nekončící optimismus, což vše mi pomohlo dokončit tuto práci. Také děkuji prof. Ing. Petru Stehlíkovi, CSc. za to, že mi umožnil studovat a věnovat se vědecké činnosti na Ústavu procesního a ekologického inženýrství.

Zvláštní poděkování patří mým rodičům a blízkým a zejména mé přítelkyni Evě za trpělivost a podporu, kterou mi věnovala v průběhu studia a bez níž by se pracovalo o poznání hůře.

Chci také poděkovat Jihomoravskému centru pro mezinárodní mobilitu za velkou finanční podporu v rámci programu Brno Ph.D. Talent.

Ing. Tomáš Juřena





# Contents

<b>1</b>	<b>Introduction</b>	<b>1</b>
1.1	Utility of numerical modelling in combustion science . . . . .	1
1.1.1	CFD in solid fuel combustion applications . . . . .	1
1.2	Approaches to CFD modelling of grate combustion . . . . .	2
1.2.1	Empirical approach - profiles along the grate length . . . . .	2
1.2.2	Modelling approach - porous-zone CFD model . . . . .	4
1.2.3	Modelling approach - stand-alone numerical bed model . . . . .	4
1.3	Objectives and scope of the thesis . . . . .	5
1.3.1	Report structure . . . . .	6
<b>2</b>	<b>Review of packed-bed combustion modelling approaches</b>	<b>7</b>
2.1	Classification of bed models . . . . .	7
2.2	Mathematical description . . . . .	9
2.2.1	Source terms . . . . .	11
2.2.2	Process rate models . . . . .	11
2.3	Representation of a moving grate . . . . .	13
2.4	Summary . . . . .	14
<b>3</b>	<b>Mathematical model setup of packed-bed combustion</b>	<b>17</b>
3.1	Class of the models . . . . .	17
3.2	Governing equations . . . . .	18
3.2.1	One-dimensional transient model . . . . .	18
3.3	Boundary conditions . . . . .	21
3.4	Coefficients of process rates . . . . .	21
3.4.1	Drying rate . . . . .	21
3.4.2	Pyrolysis rate . . . . .	22
3.4.3	Combustion reaction rates . . . . .	23
3.4.4	Two-dimensional steady model . . . . .	23
3.5	Summary . . . . .	25
<b>4</b>	<b>Physical and chemical properties of solid fuels for CFD modelling of grate combustion</b>	<b>27</b>
4.1	Biomass characteristics . . . . .	27
4.1.1	Moisture . . . . .	28
4.1.2	Volatile matter . . . . .	29
4.1.3	Packing conditions . . . . .	29
4.1.4	Thermophysical and heat and mass transfer parameters . . . . .	31

4.2	Summary . . . . .	36
<b>5</b>	<b>Numerical solution technique for the packed-bed model</b>	<b>37</b>
5.1	Discretization . . . . .	37
5.1.1	Note on discretization of effective dispersion coefficients . . . . .	40
5.2	Controlling the convergence . . . . .	41
5.2.1	Convergence criterion . . . . .	41
5.2.2	Relaxation . . . . .	42
5.2.3	Adaptive time stepping . . . . .	42
5.2.4	Linearization . . . . .	43
5.2.5	Special treatment of process rates . . . . .	43
5.3	Overall solution algorithms . . . . .	45
5.3.1	SIMPLE co-located algorithm . . . . .	45
5.3.2	1D flow algorithm . . . . .	46
5.4	Summary . . . . .	47
<b>6</b>	<b>Simulation tool with GUI</b>	<b>49</b>
6.1	General comments on GRATECAL . . . . .	49
6.1.1	Running GRATECAL 1.3 . . . . .	49
6.1.2	Limitations . . . . .	50
6.2	Description of graphical user interface . . . . .	50
6.2.1	Main window . . . . .	51
6.2.2	Gas & fuel properties . . . . .	51
6.2.3	Bed & furnace properties . . . . .	53
6.2.4	Processes . . . . .	55
6.2.5	Solver settings . . . . .	55
6.3	Summary . . . . .	56
<b>7</b>	<b>Analysis of some specific modelling issues</b>	<b>59</b>
7.1	Physical issues . . . . .	59
7.1.1	Effects of drying models . . . . .	60
7.1.2	Effects of variable porosity . . . . .	60
7.2	Numerical issues . . . . .	64
7.2.1	Sources of errors in numerical simulations . . . . .	64
7.2.2	Balance-based control method . . . . .	65
7.2.3	Test studies . . . . .	67
7.2.4	Effects of convergence criteria . . . . .	68
7.2.5	Inverse application of the method . . . . .	69
7.3	Summary . . . . .	70
<b>8</b>	<b>C library of functions for coupled bed-freeboard modelling in ANSYS FLUENT</b>	<b>71</b>
8.1	Generation of C code from MATLAB code of GRATECAL . . . . .	71
8.1.1	Fluent data . . . . .	72
8.1.2	GRATECAL data . . . . .	72
8.1.3	User data . . . . .	72
8.1.4	Generated code . . . . .	73
8.2	Coupled modelling methodology in detail . . . . .	74
8.2.1	Placement of the interface . . . . .	74

8.2.2	Radiation heat flux . . . . .	74
8.2.3	Main descriptive parameters of a grate . . . . .	75
8.3	Working with UDF . . . . .	75
8.4	Summary . . . . .	78
<b>9</b>	<b>Conclusions and future work</b>	<b>79</b>
9.1	Future work . . . . .	80
	<b>References</b>	<b>81</b>
	<b>Nomenclature</b>	<b>89</b>
	<b>Annex I – List of author’s publications</b>	<b>93</b>
	<b>Annex II – Source codes of GRATECAL</b>	<b>95</b>
	<b>Annex III – Source codes of UDF</b>	<b>97</b>



# Chapter 1

## Introduction

During the past twenty years, grate-fired systems have received significant attention by researchers involved in combustion science. It is not only because renewable and environmentally friendly energy sources such as biomass have been found as a promising alternative to fossil fuels. Also incineration in grate-type furnaces has become a widely-used method of municipal solid waste disposal.

Many experimental measurements have been carried out in order to improve the effectiveness of energy utilization as well as to reduce the pollutant emissions and undesirable effects of combustion products on heat transfer surfaces. However, due to the difficulty and increasing costs of experiments, the research has also been focused on development of a reliable computational model as a supporting tool for design and optimization of combustion systems.

### 1.1 Utility of numerical modelling in combustion science

Modelling methods provide for a cost-effective and safe analysis of various phenomena encountered in real systems. In particular, several types of modelling tools are available for combustion analysis from simple heat and mass balance models through chemical equilibrium models to advanced numerical models, for solutions of which Computational Fluid Dynamics (CFD) tools are utilized [69].

Based on the purpose of modelling, one can choose the most appropriate tool. While heat and mass balance models provide for a fast calculation of e.g. adiabatic flame temperature, they cannot resolve the problem to greater details. Common interests of analysis include computation and visualisation of local flow and temperature distribution, level of mixing of gas species in a combustion chamber or examining the effects of operational conditions on combustion parameters. In such cases, numerical models are developed and solved mostly using CFD tools, see e.g. [31, 34, 90].

#### 1.1.1 CFD in solid fuel combustion applications

CFD modelling has become a standard supporting tool for design and optimization of all kinds of solid fuels utilization systems. The area of applications ranges from small-scale units such as domestic wood stoves and biomass pellet boilers (e.g. [8, 33]), to medium-to-large-scale units such as dryers, gasifiers, fluidized bed and pulverized-fuel furnaces as

well as municipal solid waste (MSW) grate and rotary kiln incinerators (for instance, see [9, 36, 55, 56]), etc.

Numerical modelling using CFD techniques has been found helpful in troubleshooting and identification of controlling parameters. For example, high amounts of unburnt carbon in fly ash during grate combustion of biomass is attributed mainly to poor mixing in the freeboard [31]. Since slagging and fouling of heat transfer surfaces caused by ash deposition is a severe problem not only in straw-fired boilers, quite a lot of effort has been made to model and predict deposit formation on superheaters, e.g. [30, 32]. Further, grate combustion of straw under oxygen-enriched conditions as well as effects of auxiliary gas burners on temperature and flow distribution during straw combustion have also been investigated numerically in [79, 89], respectively. CFD tools have also been used to model the effects of transition from pulverized-coal combustion to pulverized coal and biomass co-firing [22, 35].

It can be concluded that current CFD codes such as ANSYS FLUENT [14] have become very practical tools for analysis of combustion systems. However, quality of simulation results is strongly affected by the quality of input data. Therefore, in order to develop a reliable CFD model, care must be taken when preparing the mesh and defining not only physical and chemical models, but also boundary conditions and additional models (such as the model of deposit formation), which are sometimes necessary to incorporate into the CFD code to adjust the solution procedure and enhance capabilities of the CFD modelling tool [5, 87].

## 1.2 Approaches to CFD modelling of grate combustion

This work concerns CFD modelling of grate combustion as widely used technology in biomass and municipal solid waste combustion for heat and power production [86]. A typical model of a grate combustor consists of a grate with primary air inlets, freeboard with secondary (and possibly tertiary) air inlets and heat exchangers in radiation and convection shafts. One of the key issues in the modelling is the degree of approximation of processes, that take place in a fuel layer on the grate. As combustion proceeds in the fuel layer, various gaseous products leave the bed entering the freeboard, for which values of gas species concentrations, temperatures and mass fluxes must be supplied as inlet boundary conditions. The situation is schematically shown on the Figure 1.1.

Specification of the type and values of boundary conditions is crucial in any numerical problem. Especially, in case of grate combustion modelling, where there is a strong coupling between processes occurring inside the fuel layer and in the over-bed region, inappropriate treatment of the boundary conditions may lead to inaccurate results of a simulation, mainly in the vicinity of the fuel bed [87]. The following sections discuss three different ways, that have been previously reported in literature and can be used for the treatment of boundary conditions at the grate.

### 1.2.1 Empirical approach - profiles along the grate length

The most frequently used method for setting up the boundary conditions is based on an experience and design of a real furnace. As shown on the Figure 1.2, a grate is divided along its length into four sections, for each of which profiles of temperature, mass flux and

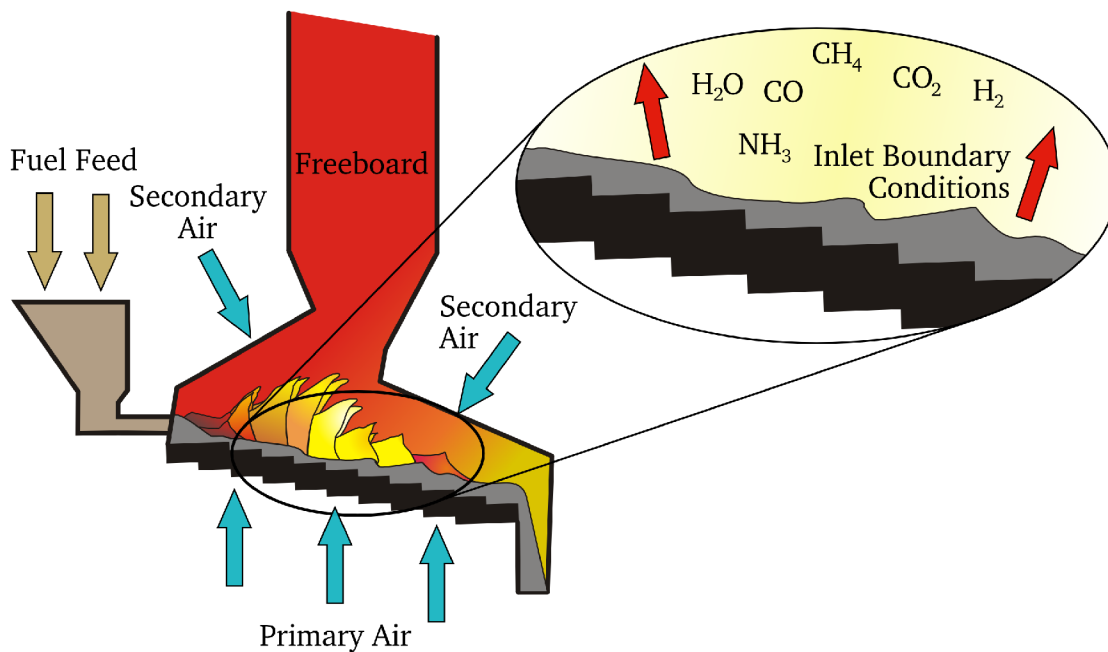


Figure 1.1: A scheme of a typical grate-fired incinerator. The detail depicts boundary conditions at the grate.

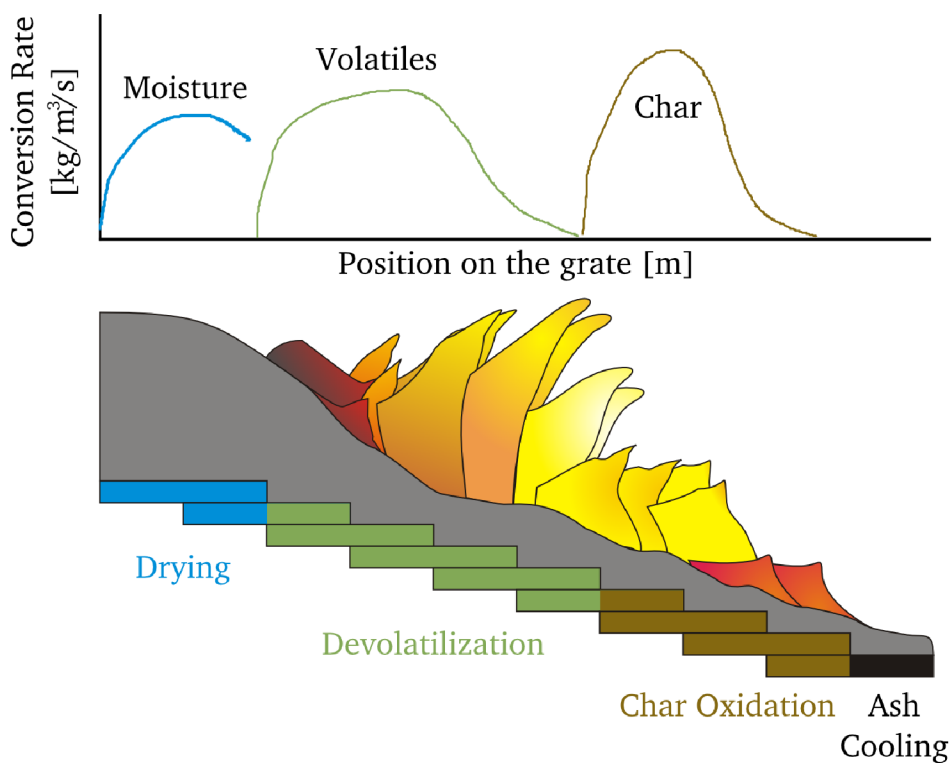


Figure 1.2: Illustrative drying, devolatilization, char combustion and ash cooling zones on the grate.

concentrations of gas species are prescribed as they are either measured in a real unit or calculated from mass and energy balance of the fuel.

This approach has been used in many works, e.g. [57, 58]. Although calculated results have been reported as satisfactory compared to measured data, the method lacks the capability to predict combustion in the phase of design of a new furnace. The reason is that while measurements of required profiles are mostly impossible to carry out on real combustion furnaces, mass and energy balance, on the other hand, is calculated using an estimate of the grate sections, where drying, devolatilization and char oxidation take place. Such an assumption may deviate from reality.

### 1.2.2 Modelling approach - porous-zone CFD model

Some CFD codes (e.g. ANSYS FLUENT) allow user to define a porous zone within the computational domain. The porous zone creates resistance to fluid flow and generates a pressure drop. Therefore, it is suitable for modelling of gas flow through a porous fuel layer. Various source terms, which arise, for example, due to drying, devolatilization and char oxidation, and additional governing equations for solid fuel variables (i.e. mass fractions of solid species and temperature) must be defined within the porous zone to fully describe processes inside the fuel bed. Solution of the equations is left to the CFD code during the overall solution procedure.

Since solutions of gas species concentrations, gas temperature and mass flux are obtained by the CFD code within the porous zone, there is no need to define profiles of these variables for boundary conditions. Instead, properties of primary air must be specified. However, as the top of the fuel layer is heated up by radiation from hot gases in the free-board, the radiation must be taken into account in the boundary condition for the porous zone. The modelling concept is shown on the Figure 1.3a).

The method has been successfully demonstrated e.g. in [11]. Compared to previous method, CFD model with a fuel bed treated as a porous zone is much more complicated and requires longer computational time to complete the simulation. On the other hand, it is also capable to predict combustion and processes inside the fuel bed.

### 1.2.3 Modelling approach - stand-alone numerical bed model

The attention of researchers has recently been attracted to development of a stand-alone numerical model of bed combustion, that describes and predicts all the processes inside the bed in more detail (e.g. [18, 65, 68, 74, 91]). The model is based on the same principles as porous zone bed model. However, several advantages of the stand-alone model over the porous zone model can be drawn:

- **Independence.** Development of a stand-alone bed model is independent of the CFD code, for which it is intended to be coupled with. This has an important implication: in order to couple the bed model with a CFD code, only an interface has to be programmed as a function or procedure, by means of which these two separate models share and interchange data. Definitions of various boundary conditions on the common boundary of the two models are essential parts of the function, see Figure 1.3b).
- **Extendibility.** While various CFD codes may not provide a complete set of functions for the definition of all porous zone properties of interest, the stand-alone bed model



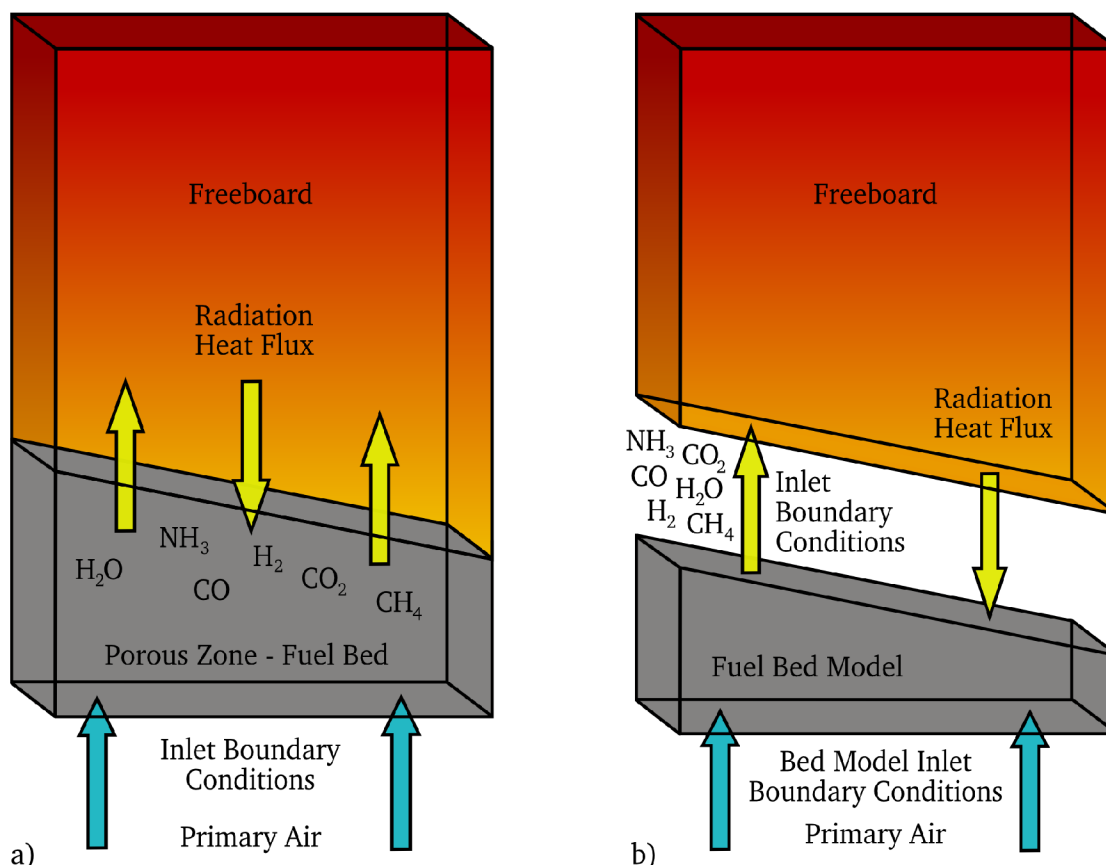


Figure 1.3: Modeling approaches: a) Porous zone CFD model. b) Stand-alone bed model coupled with freeboard model.

can be extended for any additional functionality. A well-structured code is flexible to be accommodated for a specific modelling requirements and needs.

- **Analysis.** Once the bed model is developed, it can be used apart from a CFD code for a detailed study of in-bed processes without a need to run the whole coupled simulation. Also various physical models can be tested more easily by means of parametric studies to further improve the modelling methodology.

As it is stressed in [88], it is crucial to ensure, that the bed model is conservative, i.e. the model obeys essential physical principles such as conservation laws of mass and energy. Although a natural requirement it may seem, it is not precisely fulfilled in numerical simulations due to various sources of errors, see e.g. [12]. An imperfect conservation implies that the gas does not carry the right amount of mass and energy and therefore such a model cannot improve the estimate of boundary values at the inlet of a freeboard model. This may lead to inaccurate results of freeboard combustion predictions as the accuracy depends, among others, on the quality of input data [87].

### 1.3 Objectives and scope of the thesis

This work is focused on numerical modelling of grate combustion. The first objective is to develop and implement a stand-alone conservative numerical model of packed-bed com-

bustion such that it may serve as a tool for both study and analysis of various processes in the bed and calculation of boundary values in the coupled-model methodology. The emphasis is put on the conservativeness property of the model. Therefore, a method for control of mass and energy balance over the system is developed, by means of which the model can be checked and corrected for various errors to yield a conservative model. The method is also applied to several of simulations to determine a suitable value of convergence criteria in order to produce acceptably low mass and energy imbalance. Such a parametric study has, to the author's knowledge, not been performed yet and therefore the result contributes to better understanding of numerical modelling of grate combustion, especially in the setup of a numerical model and parameters of solver for the control of the convergence. Other physics-related issues including propagation of drying and char oxidation reaction fronts are addressed and investigated by means of numerical simulation using the computer code developed within this work.

The second objective is to develop a library of user-defined functions for the commercial CFD software ANSYS FLUENT for coupling the bed model with a freeboard model of a real combustion unit in order to specify the boundary conditions indirectly using results from in-bed simulations. The library of functions should be general enough to be easily applied for a wide range of grate furnace models.

### 1.3.1 Report structure

The thesis is organized as follows:

Chapter 2 reviews existing bed models and describes their common features such as mathematical equations, modelling assumptions, various physical models included in the bed model, etc.

Two mathematical models of packed bed combustion are presented and described in detail in the chapter 3. Selection of physical models is based on chapters 2 and 4.

Chapter 4 summarizes available data on physical and chemical properties of biomass and municipal solid waste, that are needed for CFD modelling of grate combustion. Discussion is made on the generality and validity of parameters under combustion conditions.

Numerical methods, that are used to discretize governing equations, are described in the chapter 5. Especially, methods that were found helpful in obtaining convergence are discussed in more detail.

The developed computer code is introduced in the chapter 6. A graphical user interface, which makes setting the model parameters easier is described as well as some general information on the application such as prerequisites to run the program or limitations of the code.

Analysis of some physical and numerical modelling issues is presented in chapter 7. Also the mass and energy balance control method is described and demonstrated on a series of case studies.

A way for coupling of the two separate CFD models is outlined in the chapter 8. A library of user-defined functions, that has been developed in order to serve as an interface for coupling the bed model and the commercial CFD package ANSYS FLUENT, is described here.

Conclusions are made in the chapter 9. Main results are summarized and future work is proposed.

## Chapter 2

# Review of packed-bed combustion modelling approaches

As documented in [72] numerous models of combustion in packed beds have been developed during the last 50 years, from simple ones with many simplifying assumptions to very sophisticated models with detailed description of phenomena occurring during the combustion process. These models can be classified according to various aspects, for instance four classes of bed models can be found in [82], a different classification is given in [68].

This chapter describes common features of all bed models. Section 2.1 presents a classification of bed models, which is suitable with respect to the purpose of this work. A general mathematical description is provided in the section 2.2 and two different techniques for modelling of moving beds are described in the section 2.3.

### 2.1 Classification of bed models

The complexity of processes occurring inside a fuel bed is one of the reasons why authors created different classifications of existing models. In this work, use is made of the fact that all models can be characterised by a common feature - a level of approximation. The choice of the level of approximation is an important step in development of any mathematical model as it determines, what details are important to be solved and to what extent and degree of precision should these details be solved. The level of approximation defines a general way of classification, by which all bed models can be sorted. These include models whose common feature is the degree of homogeneity (homogenous models, heterogenous, pseudo-homogenous, etc.) as described in [19], models that are sorted according to the solution method (analytical/numerical), which is mainly affected by the complexity of governing equations, or the purpose for which models were developed [68].

For practical reasons, it is useful to divide models into classes according to the scale of modelling. The scale of the whole bed is defined as macroscale, while microscale is reserved for a single porous fuel particle [72]. Depending on whether the intra-particle effects are significant or not, a particle-resolved modelling approach must be used, or the packed bed can be treated as a continuous porous medium, respectively. The latter assumption seems to be reasonable for use in simulations of industrial grate furnaces, since a bed in such

furnaces occupies large volume with a vast number of particles. Therefore, modelling of individual particles would be an enormous task in terms of computational requirements.

However, the nature of combustion in packed beds depends on a host of parameters, one of which is the size of fuel particles. This is especially important for situations in which the bed consists of rather large fuel particles, so the continuous model may produce highly inaccurate results due to significant intra-particle gradients. In this respect, fuel particles are considered to be large if temperature gradient inside a particle cannot be neglected, i.e. when Biot number  $Bi \gg 1$ , [28]. Modelling of a bed of thermally-thick biomass particles is presented in [83], where it is concluded that particles over 35 mm can develop very steep temperature gradients (the temperature difference between the centre and surface of a particle is over 400 K) corresponding with  $Bi > 2$ . Hence the suitable level of approximation for such cases is a combination of micro- and macroscale models, i.e. a model of a single particle incorporated into the bed model, which is considered a continuous porous medium. Five major effects of fuel size on combustion in packed beds are summarised in [80], where the significance of this combustion parameter is assessed both by simulations and experiments.

The classification of bed models according to the scale of modelling can be summarised as follows:

- **Microscale models.** The combustion process is described within an individual solid particle as shown on Figure 2.1. Additionally, governing equations for the liquid phase can be considered as well to account for effects of free water inside a particle. Microscale models can be used for detailed study of heat and mass transfer and fluid flow as well as propagation of reaction fronts inside a particle.

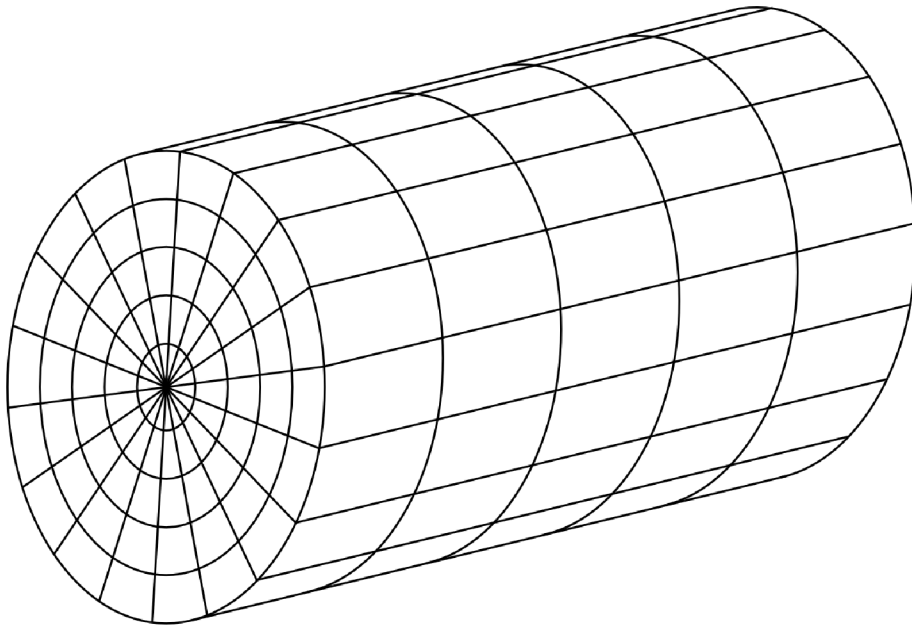


Figure 2.1: A computational grid applied to a microscale model of a wood log.

- **Macroscale models.** The bed is considered a continuous porous medium which consists of gas and solid phase and the combustion process is described within the entire fuel bed. The intra-particle effects are neglected. This assumption can be applied to

beds of thermally-thin solid particles. A mesh of a typical macroscale model is shown on Figure 2.2.

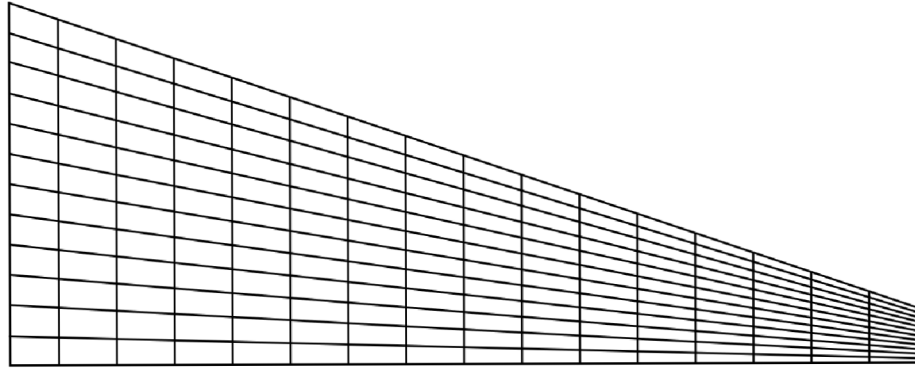


Figure 2.2: A computational grid of a macroscale model. The model is typically applied to beds of fine wood chips or wheat straw.

- **Particle-resolved macroscale models.** The packed bed is treated as in macroscale models. However, the solid phase is represented by a specific number of fuel particles, each of which is described individually by a microscale model, see Figure 2.3. The particle model is coupled with the entire bed model through boundary conditions. No limitations due to fuel particle size arise and its effect on combustion behaviour in the bed can be considered.

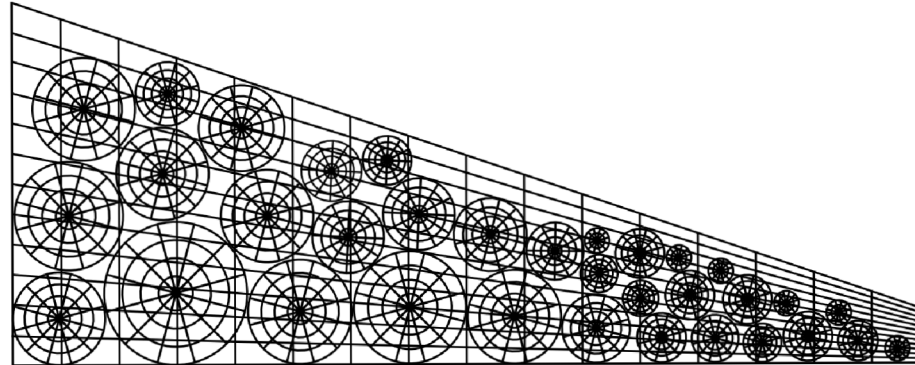


Figure 2.3: Particle-resolved macroscale model.

## 2.2 Mathematical description

The combustion process is governed by basic physical principles known as conservation laws of mass, momentum and energy. In a general form, these laws are mathematically described by a system of transient partial differential equations denoted as governing equa-

tions. An unsteady bed model is described by a set of governing equations in the form [63, 88]

$$\underbrace{\frac{\partial (\epsilon \rho \phi)}{\partial t}}_{\text{unsteady term}} + \underbrace{\nabla \cdot (\epsilon \rho \mathbf{v})}_{\text{convection term}} = \underbrace{\nabla \cdot (\Gamma \nabla \phi)}_{\text{diffusion term}} + \underbrace{S_\phi}_{\text{source term}}, \quad (2.1)$$

which is commonly called a general transport equation, where  $\epsilon$  [-] is porosity,  $\rho$  [kg/m<sup>3</sup>] is density,  $\mathbf{v}$  [m/s] is a vector of interstitial velocity,  $\phi$  is transported (scalar) quantity,  $\Gamma$  is diffusion coefficient and  $S_\phi$  includes all source terms. The product  $\epsilon \rho$  is called bulk density. By giving the variables  $\phi$ ,  $\Gamma$ , and  $S_\phi$  physical meanings with appropriate units, the equation (2.1) becomes a governing equation for heat, mass or momentum transfer. Examples of substitutions for the general coefficients by certain physical quantities commonly encountered in bed models are listed in the Table 2.1. Models in which heat and mass transfer are described by separate equations for each phase are called heterogenous. Contrary to heterogenous models, if temperature and species concentration gradients at the fuel particle surface are negligible (usually in beds of fine fuel particles), the bed model can be further simplified to a homogenous model (i.e. one-phase model) [19, 64].

Equation	$\phi$	$\Gamma$	$S_\phi$
Continuity	1 [-]	0 [kg/m s]	Sum of heterogenous reaction rates $r$ [kg/m <sup>3</sup> s]
Species	Mass fractions of $i$ -th species $Y_i$ [kg/kg]	Product of bulk density and effective mass dispersion coefficient $\epsilon \rho D_i$ [kg/m s]	Rate of production or consumption of species $r_i$ [kg/m <sup>3</sup> s]
Energy	Specific enthalpy $h$ [J/kg]	Effective thermal conductivity divided by specific heat capacity $\lambda/c_p$ [kg/m s]	Heat transfer rates $\dot{q}$ [W/m <sup>3</sup> ]
Momentum	Velocities $v_j$ [m/s]	Dynamic viscosity $\epsilon \mu$ [kg/m s]	Pressure gradient $\nabla p$ , gravity force, interphase momentum transfer $f$ [N/m <sup>3</sup> ]

Table 2.1: Physical meanings of coefficients of the general governing equation with corresponding physical units for transport equations in bed models.

It is important to note that due to various modelling assumptions, bed models differ not only in description of the coefficients, but also in the set of governing equations being solved. For example, some transient 1D models of MSW and biomass combustion in an experimental reactor [81] include a solution of gas flow using the momentum equation, while other 1D models (e.g. [29, 91]) assume a plug flow with constant pressure in the reactor and therefore the gas flow is calculated directly from the continuity equation.

Inconsistencies in modelling assumptions in case of two-dimensional models are even larger. For instance, two different 2D models of wheat straw combustion can be found in literature - a steady homogenous 2D model with constant pressure assumption [67]

and an unsteady heterogenous 2D model, which is described by a full system of Navier-Stokes equations (i.e. the continuity equation coupled with momentum, energy and species transport equations) [79]. Moreover, a different approach to model momentum transfer within the gas phase is used in [2], where an equation for solution of pressure raised to the second power is derived from Darcy's law combined with continuity equation.

According to Yin et al. [88], a description of a reliable bed model should be based on a generally accepted set of governing equations similar to those used for modelling of fluidized bed combustion in an open source MFX software [63]. Furthermore, it should be ensured that the model itself is conservative, i.e. mass and energy is conserved within the bed, so flue gas leaving the bed transports a correct amount of mass and energy into the freeboard.

### 2.2.1 Source terms

Whatever cannot be fitted into the unsteady, convection or diffusion terms of the equation (2.1), is considered a part of the source term. For the energy equation, heat transfer rates always include interphase convective heat transfer and heat release or consumption of chemical reactions. Radiation heat transfer is usually described by a separate system of ordinary differential equations (mostly using a flux model based on the model published in [62]) and the radiation heat flux enters the energy transport equation through the source term [29, 52, 75], or the radiation contribution is lumped into the effective thermal conductivity [79, 91].

Pressure drop due to resistance of the bed to gas flow is usually modelled by Ergun equation. Other volumetric forces are usually neglected in momentum equations.

For calculation of source terms in continuity, species and energy equations, rates of production/consumption of species are needed.

### 2.2.2 Process rate models

The combustion process can be divided into four sub-processes: evaporation of moisture from the fuel, volatile release/char formation, combustion of volatiles and combustion of char.

#### Models of moisture evaporation

According to [4], the drying models may be sorted into three different types.

1. **Heat sink model.** The model is based on the assumptions that drying occurs at a fixed boiling temperature and that the drying zone is infinitely thin. This means that there is no resistance to mass transfer and that the water vapour instantaneously leaves the particle. The drying rate is then completely controlled by the heat transfer. Various approaches to the implementation of this model exist, see for example [4, 49, 54].
2. **First-order kinetic rate model.** It is assumed that water vapour is not limited by saturation pressure, hence it leaves the fuel particle instantaneously depending only

on the fuel particle temperature and moisture content. The kinetically controlled rate of evaporation of moisture from solid is calculated by an Arrhenius-type expression:

$$r_{\text{dry}} = A \exp\left(-\frac{E_a}{RT_s}\right) \rho_{\text{sb}} Y_{\text{H}_2\text{O},s} \quad [\text{kg}/\text{m}^3 \text{ s}], \quad (2.2)$$

where  $A$  [1/s] is pre-exponential factor,  $E_a$  [J/mol] is the activation energy,  $R$  [J/molK] is the universal gas constant,  $T_s$  [K] and  $\rho_{\text{sb}}$  [kg/m<sup>3</sup>] are solid phase temperature and bulk density, respectively, and  $Y_{\text{H}_2\text{O},s}$  [kg/kg] is mass fraction of water contained in the fuel. The model is easy to implement as it is sufficient to add water and its vaporisation heat to the kinetic scheme. This scheme is generally unable to describe condensation. The model is applied in numerous works, e.g. [29, 65].

3. **Equilibrium model.** It is based on the hypothesis, that water vapour is in equilibrium with the liquid. Therefore the partial pressure of water vapour is fixed by the saturation pressure. This assumption is typical of models for low-temperature drying. Equilibrium models depend not only on heat transfer but also on mass transfer.

$$r_{\text{dry}} = k_d A_p (\rho_{\text{H}_2\text{O},\text{surf}} - \rho_{\text{H}_2\text{O},g}), \quad [\text{kg}/\text{m}^3 \text{ s}] \quad (2.3)$$

where  $k_d$  [m/s] is mass transfer coefficient,  $A_p$  [m<sup>2</sup>/m<sup>3</sup>] is volumetric particle surface area and  $C_{\text{H}_2\text{O},\text{surf}}, C_{\text{H}_2\text{O},g}$  [kg/m<sup>3</sup>] are densities of water vapour at particle surface and in the gas phase, respectively. Examples of application of this type of model may be found in [2, 72, 75].

It is worth to mention a possible combination of the heat sink and equilibrium models to emphasize the rate of drying at the boiling temperature, e.g. [79].

### Model of pyrolysis

Biomass contains large proportion of volatile matter which is gradually released as gaseous products. It starts as the fuel is heated up to a certain temperature after the moisture evaporation is finished. The solid fuel is thermally decomposed and since an external oxidizing agent cannot penetrate into particle pores due to the flow of released volatiles, the devolatilization is also referred to as pyrolysis. If sufficient oxygen is present, gaseous products burn (provided that a minimal temperature needed for ignition is reached), when the temperature exceeds a certain level. The rate of devolatilization depends on heating rate and the type of the fuel. The devolatilization of most solid fuels can be described by a one-step global reaction [85]



Devolatilization is often considered to be globally almost neutral with respect to heat release or consumption [6]. The pyrolysis rate  $r_{\text{pyr}}$  is proportional to the volatile matter remaining in the fuel, thus the first-order kinetic rate model is employed again as in the equation (2.2), where the mass fraction of moisture  $Y_{\text{H}_2\text{O},s}$  is replaced by mass fraction of volatiles  $Y_{\text{vol},s}$  [79, 91].



### Combustion reaction models

Gaseous products of pyrolysis must first mix together with the combustion air before homogenous reactions can take place. After that, reactions in the gas phase are kinetically controlled, so the reaction rates for particular reactions can be estimated by taking the minimum of the mixing rate and kinetic rate as obtained from an Arrhenius-type expression. Other chemistry modelling approaches as known in the area of turbulent combustion so far haven't been used, to the author's knowledge. However, it is important to note, that under typical operating conditions, large amount of volatile gases leave the bed unburnt due to fuel-rich combustion mode in the bed, which is inversely proportional to the initial moisture content of the fuel [85]. Therefore, burnout of gases takes place mainly in the over-bed area, if enough secondary air is supplied [68], so modelling of the reactions can be left for the freeboard model, for which a commercial CFD packages with more detailed reaction schemes such as ANSYS FLUENT are usually employed.

When pyrolysis is finished, only char (fixed carbon) and ash remain in the fuel and the surrounding gas can diffuse through the boundary layer of a solid particle to react with the carbon. Char may be fully or partially oxidized according to



where  $\alpha$  is determined from product formation ratio  $r_{CO}/r_{CO_2}$ , which depends on the fuel temperature and is usually expressed [30, 91] as

$$\frac{r_{CO}}{r_{CO_2}} = A \exp\left(\frac{-E_a}{RT_s}\right). \quad [\text{mol/mol}] \quad (2.6)$$

The rate of char oxidation is limited both by diffusion and chemical kinetics, therefore it is modelled as a combination of the kinetic reaction rate and the rate of oxygen diffusion to the particle surface. The rate  $r_c$  can be expressed generally as [6, 14]

$$r_c = A_p \frac{k_c k_D}{k_c + k_D} p_{O_2}, \quad [\text{kg/m}^3 \text{ s}] \quad (2.7)$$

where  $A_p$  [ $\text{m}^2/\text{m}^3$ ] is volumetric surface of the particle,  $k_c$  [ $\text{kg}/\text{m}^2 \text{ s atm}$ ] is Arrhenius-type kinetic rate constant,  $k_D$  [ $\text{kg}/\text{m}^2 \text{ s atm}$ ] is coefficient of mass transfer and  $p_{O_2}$  [atm] is partial pressure of oxygen in gas phase.

Parameters needed for the reaction modelling were reported e.g. in [85, 91].

## 2.3 Representation of a moving grate

Industrial furnaces are usually equipped with moving grates to provide for fuel transport from the stoker to the ash pit, while achieving better burnout of the fuel which is typical for forward or reverse reciprocating grates [88]. There are two modelling approaches for representation of the grate movement.

The first one can be considered more general as the grate movement is directly incorporated into the bed model through boundary conditions. The model can be two- or three-dimensional. This approach is general enough to be suitable for all kinds of grate systems. Fuel mixing can be taken into account either by empirical mixing coefficients, if

a macroscale model is used [77], or it can be modelled using a particle discrete method [47, 48], in which forces acting on each individual particle are resolved. While the former brings to the simulation additional factor of uncertainty in the form of the empirical mixing coefficient, the latter is computationally much more demanding.

The second approach, the so called walking-column method, is shown on the Figure 2.4. The fuel is fed from the left onto the grate and is ignited from the top of the layer. By taking a thin vertical slice of the bed at a position  $x_1$  and following the slice as it is moved on the grate towards the ash pit by known velocity  $v_G$ , the reaction front travels down from the top of the column. In this manner, transient solution of a one-dimensional reactor can be related with a corresponding position on the grate by the simple relation

$$x = v_G t, \quad [\text{m}] \quad (2.8)$$

so a continuous operation is represented by a transient one-dimensional batch-type simulation [19]. The walking-column method is based on several assumptions. First of all, the

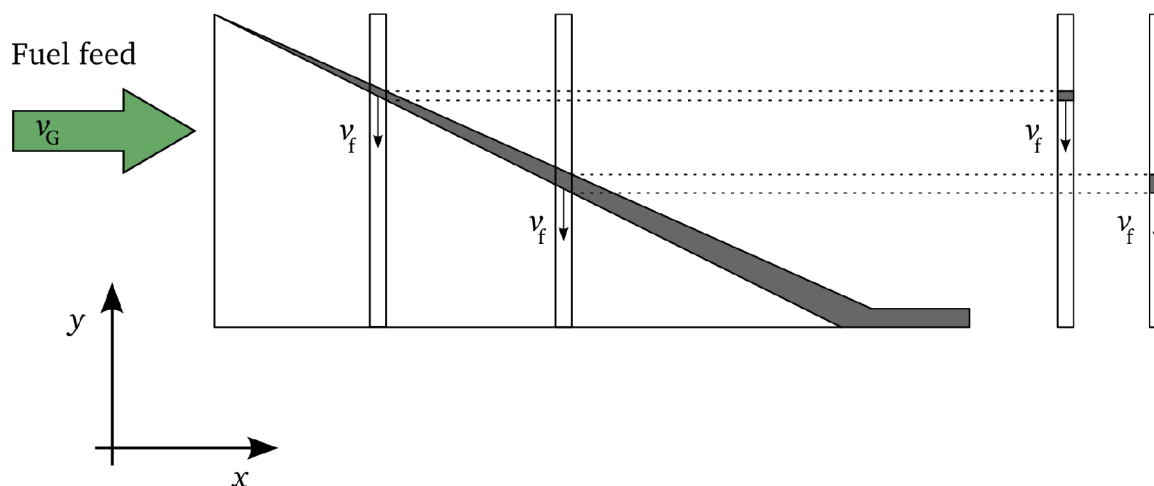


Figure 2.4: Walking-column approach. A fuel is moved on the grate with velocity  $v_G$ . As the combustion proceeds, the reaction front travels down with unknown velocity  $v_f$ .

entire bed is treated as a plug-flow reactor, which can be justified only when cross-flow gradients are negligible, especially when the heat flux due to thermal conduction is much smaller than the convective heat flux. This condition is expressed by the Peclet number for which it must hold  $Pe \gg 1$ . However, under most of the typical operating conditions it can be shown that the assumption is satisfied (as demonstrated e.g. in [30, 67]).

Another assumption is related to fuel mixing, which can be taken into account only by introducing some empirical mixing coefficient. However, effects of fuel mixing are neglected in all existing one-dimensional models.

## 2.4 Summary

A review on approaches to model packed-bed combustion has been presented. Bed models have been classified according to a level of approximation, so that three different classes have been described, namely microscale models, macroscale models and particle-resolved macroscale models. Classes differ in the extent of details, that are required for

---

a proper description of the packed-bed. All models are mathematically described by a set of governing equations of the same form, which is described by a single general transport equation. Assumptions on modelling have also been discussed. Commonly used physical models of in-bed processes have been briefly described and specific approaches including the walking-column method for modelling of moving beds have been presented.



## Chapter 3

# Mathematical model setup of packed-bed combustion

Two mathematical models of packed-bed combustion are developed based on the review presented in the chapter 2. One-dimensional transient (1D) and two-dimensional steady (2D) models are described in this chapter. These models differ mainly in the description of fluid flow, i.e. transport equations used for the solution of flow field. Physical models and chemical kinetics, otherwise, are common to both bed models. From this point of view, the 2D model can be considered as an extended version of the 1D model and therefore development of 1D model has become crucial and a base in development of the latter.

### 3.1 Class of the models

The first step in development of a model is to choose a suitable level of approximation with respect to purposes and needs of modelling. Selection of the class of the model and included physical models is made on the following requirements:

- **Coupled simulation.** The stand-alone bed model should be suitable for coupled simulation of grate combustion, preferably in (but not limited to) units with continuous feeding. The model is expected to improve quality of input data for a freeboard CFD model of a grate combustor. In most part, this is concerned with calculation of mass and heat fluxes entering the freeboard, which otherwise would be only roughly estimated in the absence of the bed model.
- **Level of approximation.** The bed model should allow to analyse main combustion parameters including various process rates, heat transfer rates, temperatures, mass fluxes, concentrations of flue gas species and amount of mass of constituents remaining in the fuel. On the other hand, too much detailed and complex model could be computationally very demanding leading to considerably longer computational times, which is typical for particle-resolved macroscale models.
- **Conservativeness.** In order to achieve improved quality of input data, the bed model must be conservative, i.e. the gas must carry a correct amount of mass and energy. This is an essential requirement as any kind of model must obey basic principles of physics such as conservation laws.

According to foregoing requirements, it is necessary to treat gas and solid as two separate, though coupled, phases and represent their physical properties by specific variables. Since fuel beds in industrial grate furnaces occupy large volume with a vast number of particles, it is reasonable to consider the bed a continuous porous layer, as modelling of individual particles would be an enormous task in terms of computational requirements. For these reasons, the class of macroscale heterogeneous models is chosen as suitable level of approximation, see the section 2.1.

## 3.2 Governing equations

Governing equations of both models have the same form and can be expressed by a general transport equation (2.1). Since diffusion and source terms are defined the same for both models, 1D model is described first with all coefficients, while for equations of the 2D model only additional coefficients not included in the 1D model are described exclusively.

### 3.2.1 One-dimensional transient model

The model corresponds with an experimental fixed-bed reactor, that belongs to a group of so-called large reactors [27] and can be schematically sketched as in the Figure 3.1. They

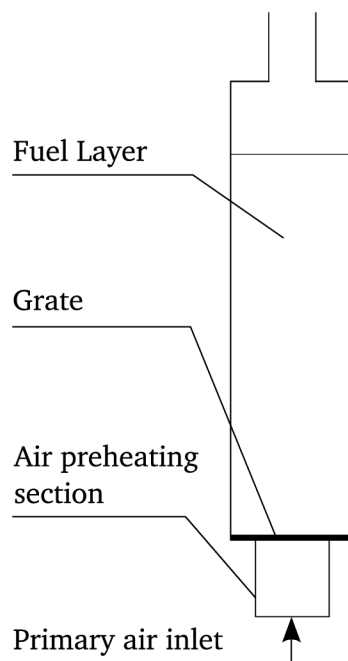


Figure 3.1: Schematic diagram of an experimental reactor.

consist of a thermally insulated cylinder where all processes take place in one direction only. The (possibly preheated) primary air enters the bed through a grate at the bottom of the furnace and flows in plug flow through the fuel layer to the top. The fuel is ignited by a burner or an electric heating device placed above the top of the bed. Such type of a reactor is suitable for batch-type experiments and can be found, for instance, in Lyngby (Denmark), Sheffield (Great Britain) and Taejon (Korea), where many experimental works have been

carried out [53, 59, 92]. However, as described in the section 2.3, transient solutions of such a system can also be transformed to represent a 2D bed.

### Model assumptions

The assumptions made upon the model are summarized:

1. The fuel bed can be considered a continuous porous layer consisting of gas and solid phases.
2. Fuel particles are thermally thin, i.e. intra-particle temperature gradients are negligible.
3. Fuel consists of four major species - moisture, volatile matter, char and ash.
4. Combustion can be divided into four sub-processes: moisture evaporation, volatile release/char formation, combustion of volatiles and combustion of char.
5. Gas flow is incompressible, gas is in plug flow and can be described by the ideal gas law.
6. Pressure drop along the bed height is neglected.
7. The gas is a mixture of species  $H_2O$ ,  $O_2$ ,  $CO_2$ ,  $CO$ ,  $H_2$ ,  $N_2$ , light hydrocarbons and tar represented by  $CH_4$ ,  $C_xH_yO_z$ , respectively.
8. The radiative heat transfer inside the bed can be modelled by effective thermal conductivity.

The model is based on the reference [91], however, several modifications are introduced regarding definition of source terms, boundary conditions and empirical formulas for calculation of certain physical quantities. Governing equations of 1D packed-bed combustion model of an experimental unit as in the Figure 3.1 are formulated as follows:

### Gas phase equations

$$\frac{\partial (\epsilon_b \rho_g)}{\partial t} + \frac{\partial (\epsilon_b \rho_g v_g)}{\partial y} = r_{dry} + r_{pyr} + r_C \quad [\text{kg}/\text{m}^3 \text{ s}], \quad (3.1)$$

$$\frac{\partial (\epsilon_b \rho_g Y_{g,i})}{\partial t} + \frac{\partial (\epsilon_b \rho_g v_g Y_{g,i})}{\partial y} = \frac{\partial}{\partial y} \left( \epsilon_b \rho_g D_{g,i} \frac{\partial Y_{g,i}}{\partial y} \right) + r_i + \epsilon_b \sum_j r_{i,j} \quad [\text{kg}/\text{m}^3 \text{ s}], \quad (3.2)$$

$$\begin{aligned} \frac{\partial (\epsilon_b \rho_g h_g)}{\partial t} + \frac{\partial (\epsilon_b \rho_g v_g h_g)}{\partial y} &= \frac{\partial}{\partial y} \left( \frac{\epsilon_b \lambda_g}{c_{p,g}} \frac{\partial h_g}{\partial y} \right) + h_c A_p (T_s - T_g) + (r_{dry} + r_{pyr} + r_C) h_s \\ &\quad - \epsilon_b \sum_{j \in G} \Delta h_j r_j - 4 \epsilon_b \lambda_w \frac{T_g - T_{amb}}{d_{in,r}^2 \ln(d_{out,r}/d_{in,r})} \quad [\text{W}/\text{m}^3]. \quad (3.3) \end{aligned}$$

While the right-hand side of the continuity equation (3.1) represents the total rate of species formation in heterogenous processes, the continuity equation (3.2) written for the  $i$ -th gas specie,  $i \in G = \{\text{H}_2\text{O}, \text{O}_2, \text{CO}, \text{CO}_2, \text{H}_2, \text{CH}_4, \text{C}_x\text{H}_y\text{O}_z\}$  contains mass source terms from both heterogenous and  $j$  homogenous reactions.

Source terms in the energy transport equation (3.3) have the following meanings:

- $h_c A_p (T_s - T_g)$  is heat gain due to interphase convective heat transfer,
- $(r_{\text{dry}} + r_{\text{pyr}} + r_c)h_s$  is heat transferred due to interphase mass transfer,
- $-\epsilon_b \sum_{j \in G} \Delta h_j r_j$  is total heat released in homogenous reactions
- $4\epsilon_b \lambda_w \frac{T_g - T_{\text{amb}}}{d_{\text{in},r}^2 \ln(d_{\text{out},r}/d_{\text{in},r})}$  is heat loss through a wall of the reactor [28].

It is assumed that energies of heterogenous reactions are released/consumed in the solid phase only.

### Solid phase equations

$$\frac{\partial (1 - \epsilon_b) \rho_s}{\partial t} = -r_{\text{dry}} - r_{\text{pyr}} - r_c \quad [\text{kg}/\text{m}^3 \text{ s}], \quad (3.4)$$

$$\frac{\partial (1 - \epsilon_b) \rho_s Y_{s,i}}{\partial t} = -r_i, \quad i \in \{\text{moisture, volatile matter, char}\} \quad [\text{kg}/\text{m}^3 \text{ s}], \quad (3.5)$$

$$\begin{aligned} \frac{\partial (1 - \epsilon_b) \rho_s h_s}{\partial t} = & \frac{\partial}{\partial y} \left( (1 - \epsilon_b) \frac{\lambda_s}{c_{p,s}} \frac{\partial h_s}{\partial y} \right) + h_c A_p (T_g - T_s) - r_c \Delta h_c - r_{\text{dry}} \Delta h_{\text{vap}} \\ & - (r_{\text{dry}} + r_{\text{pyr}} + r_c) h_s - 4(1 - \epsilon_b) \lambda_w \frac{T_s - T_{\text{amb}}}{d_{\text{in},r}^2 \ln(d_{\text{out},r}/d_{\text{in},r})} \quad [\text{W}/\text{m}^3]. \quad (3.6) \end{aligned}$$

Source terms are defined as analogical to those in gas phase governing equations. Sensible enthalpies are related to temperatures through temperature-dependent specific heat capacities

$$h(T) = \int_{T_{\text{ref}}}^T c_p(\tilde{T}) d\tilde{T} + h_{\text{ref}}. \quad [\text{J}/\text{kg}] \quad (3.7)$$

The equation (3.5) is written for solid species  $i \in \{\text{moisture, volatiles, char}\}$ . In addition,  $-r_{\text{dry}} \Delta h_{\text{vap}}$  and  $-r_c \Delta h_c$  are heat rates of vaporization and char combustion, respectively. For physical meanings and units of coefficients appearing in equations (3.1)-(3.6), please refer to the list of symbols.



### 3.3 Boundary conditions

Boundary conditions at the grate are given by the operating conditions, i.e. primary air enthalpy (or temperature), mass flux and concentrations of species, whereas zero enthalpy gradient is prescribed for solid phase. At the bed top, zero gradients are assumed for gas enthalpy and species mass fractions, while radiation heat flux is prescribed for the solid enthalpy:

$$-\left( (1 - \epsilon_b) \frac{\lambda_s}{c_{p,s}} \frac{\partial h_s}{\partial y} \right)_{y_{\text{top}}} = \epsilon_{\text{rad}} \sigma \left( T_{s,\text{top}}^4 - T_{\text{env}}^4 \right), \quad [\text{W/m}^2] \quad (3.8)$$

where  $T_{\text{env}}$  and  $T_{\text{top}}$  [K] are temperatures of environment and solid at the top of the bed, respectively.

### 3.4 Coefficients of process rates

Process rates must be properly specified in order to solve equations (3.1)-(3.6). Other coefficients of governing equations are related to gas and fuel properties, for description of which the chapter 4 is devoted.

#### 3.4.1 Drying rate

Both diffusion-limited rate model (2.3) and first-order kinetic model are used and implemented in the numerical computer program. However, the temperature dependence of the kinetic rate model is emphasized by an additional term, so the evaporation rate, as applied to modelling of biomass combustion in [41], is expressed as

$$r_{\text{dry}} = 2.822 \cdot 10^{-4} \exp\left(-\frac{10584}{T_s}\right) (1 - \epsilon_b) \rho_s Y_{\text{H}_2\text{O},s} |T_s - 475|^7. \quad [\text{kg/m}^3 \text{s}] \quad (3.9)$$

Figure 3.2 shows temperature dependence of the evaporation rate as calculated according to (3.9) for  $Y_{\text{H}_2\text{O},s} = 0.1$ ,  $\rho_s = 160 \text{ kg/m}^3$ . It can be seen that drying becomes the most intensive around the boiling temperature at normal conditions. However, for temperatures higher than 475 K the equation (3.9) produces unrealistic rates, especially in simulations of high-temperature drying. An increase of temperature above 373.15 K causes at first the evaporation rate drop to zero (at  $T_s = 475 \text{ K}$ ) and then it again rises up with very steep gradient for temperatures  $T_s > 500 \text{ K}$  provided that some moisture content is left in the fuel. This effect can be seen on Figure 3.3 as drying peaks of two successive drying fronts, which have been obtained from simulations of hot primary air drying ( $T_{\text{air}} = 573.15 \text{ K}$ ). Obviously, this model is not suitable for such high temperatures, unless evaporation completes below 475 K.

The diffusion-limited rate model requires a correlation for Sherwood number for evaluation of coefficient of  $\text{H}_2\text{O}$  diffusion into air (see the chapter 4) and a relation for calculation of saturation pressure of water vapour at the fuel particle surface. A Goff-Gratch equation is employed for this purpose [17].

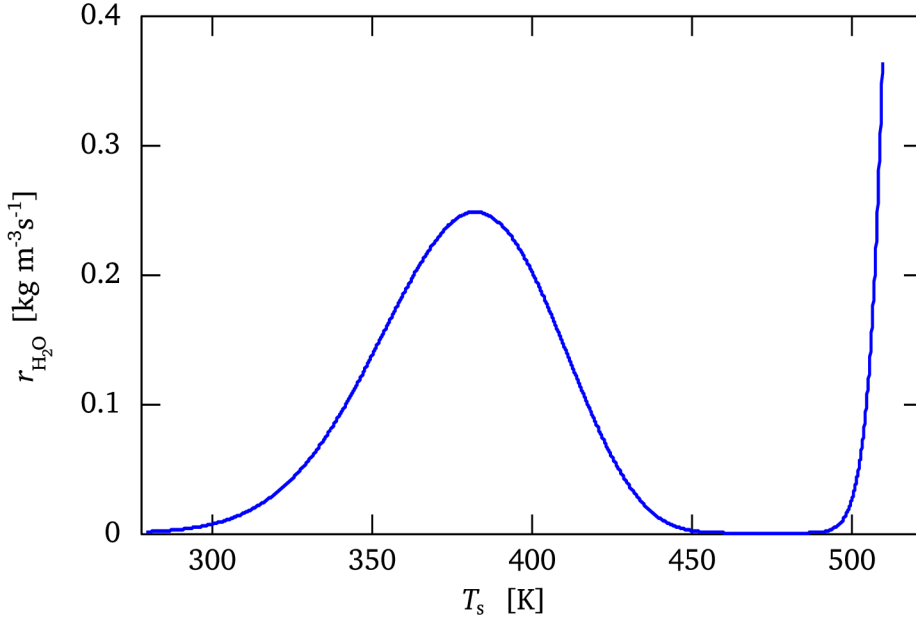


Figure 3.2: The first-order kinetic rate of moisture evaporation with modified temperature dependence.

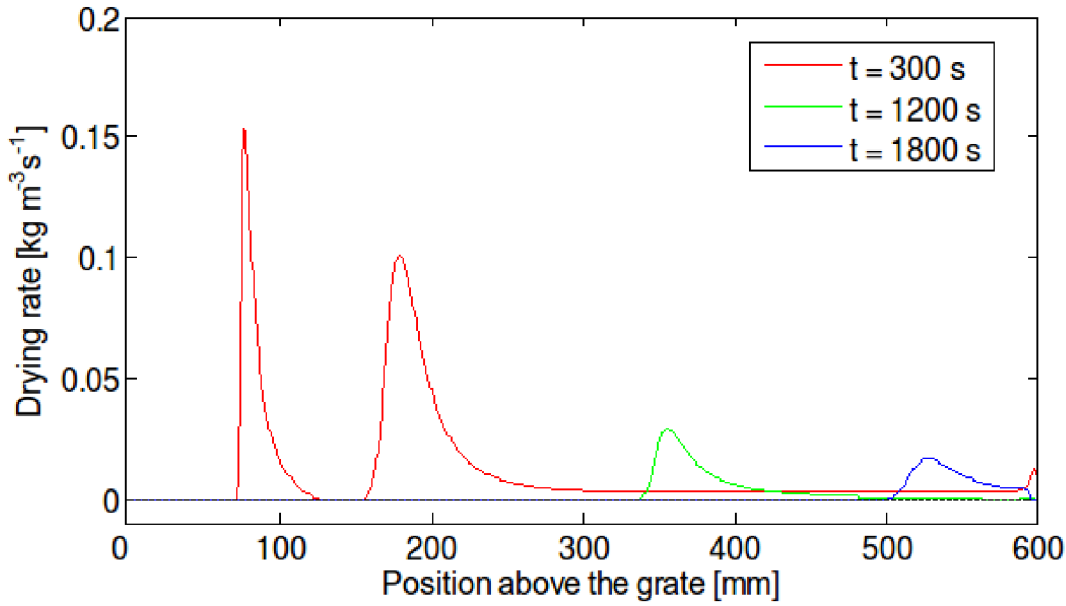


Figure 3.3: Propagation of drying front as predicted by the first-order kinetic rate model with modified temperature dependence.

### 3.4.2 Pyrolysis rate

Pyrolysis rate is given as a first-order reaction rate with Arrhenius reaction rate constant [79, 91]:

$$r_{\text{pyr},i} = 1.56 \cdot 10^{10} \exp\left(\frac{-16600}{T_s}\right) (1 - \epsilon_b) \rho_s Y_i, \quad [\text{kg}/\text{m}^3 \text{ s}] \quad (3.10)$$

where  $Y_i$  [kg/kg] is a mass fraction of volatile specie  $i \in \{\text{CO}, \text{CO}_2, \text{H}_2, \text{CH}_4, \text{C}_x\text{H}_y\text{O}_z\}$  left in the fuel. An example of volatile composition of wheat straw, which is also adopted in simulations in this work, is given in the Table 4.1.

### 3.4.3 Combustion reaction rates

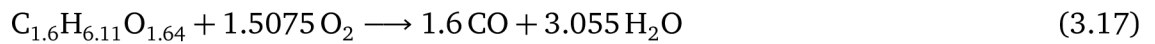
It is assumed, that char is oxidized according to equation (2.5) and all parameters in equations (2.6)-(2.7) are adopted from [30]:

$$\frac{r_{\text{CO}}}{r_{\text{CO}_2}} = 33 \exp\left(\frac{-4700}{T_s}\right), \quad [\text{mol/mol}] \quad (3.11)$$

$$k_c = 497 \exp\left(\frac{-8540}{T_s}\right), \quad [\text{kg/m}^2 \text{ s atm}] \quad (3.12)$$

$$k_d = \frac{2.53 \cdot 10^{-7}}{r_{\text{out}}} T_s^{0.75}. \quad [\text{kg/m}^2 \text{ s atm}] \quad (3.13)$$

For gas phase reactions, the following chemical reaction schemes are employed:



Modelling of pollutant species reactions such as for  $\text{NO}_x$  or  $\text{SO}_x$  is not considered in this work. The chemical formula of tar substitute in equation (3.17) is based on mass and energy balance of wheat straw given in the Table 4.1. Otherwise, rates of reactions (3.14)-(3.17) are taken from [91].

### 3.4.4 Two-dimensional steady model

In order to account for effects of moving grates, two-dimensional steady model has also been developed with a simplified description of the solid phase based on 1D model.

#### Model assumptions

Modelling assumptions are adopted from the one-dimensional model. However, the plug-flow assumption does not hold anymore for a two-dimensional bed, therefore the flow field must be described on basis of Navier-Stokes equations and pressure drop over the bed cannot be neglected.

**Gas phase equations**

$$\nabla \cdot (\epsilon_b \rho_g \mathbf{v}_g) = r_{\text{dry}} + r_{\text{pyr}} + r_C \quad [\text{kg}/\text{m}^3 \text{ s}], \quad (3.18)$$

$$\nabla \cdot (\epsilon_b \rho_g \mathbf{v}_g v_{g,x}) = -\frac{\partial p}{\partial x} + \nabla \cdot (\epsilon_b \mu \nabla v_{g,x}) - f_x \quad [\text{kg}/\text{m}^3 \text{ s}], \quad (3.19)$$

$$\nabla \cdot (\epsilon_b \rho_g \mathbf{v}_g v_{g,y}) = -\frac{\partial p}{\partial y} + \nabla \cdot (\epsilon_b \mu \nabla v_{g,y}) - f_y \quad [\text{kg}/\text{m}^3 \text{ s}], \quad (3.20)$$

$$\nabla \cdot (\epsilon_b \rho_g \mathbf{v}_g Y_{g,i}) = \nabla \cdot (\epsilon_b \rho_g D_{g,i} \nabla Y_{g,i}) + r_i + \epsilon_b \sum_j r_{i,j} \quad [\text{kg}/\text{m}^3 \text{ s}], \quad (3.21)$$

$$\begin{aligned} \nabla \cdot (\epsilon_b \rho_g \mathbf{v}_g h_g) &= \nabla \cdot \left( \frac{\epsilon_b \lambda_g}{c_{p,g}} \nabla h_g \right) + h_c A_p (T_s - T_g) + (r_{\text{dry}} + r_{\text{pyr}} + r_C) h_s \\ &\quad - \epsilon_b \sum_{j \in G} \Delta h_j r_j \quad [\text{W}/\text{m}^3]. \end{aligned} \quad (3.22)$$

**Solid phase equations**

$$\frac{\partial ((1 - \epsilon_b) \rho_s v_G)}{\partial x} = -r_{\text{dry}} - r_{\text{pyr}} - r_C \quad [\text{kg}/\text{m}^3 \text{ s}], \quad (3.23)$$

$$\frac{\partial ((1 - \epsilon_b) \rho_s v_G Y_{s,i})}{\partial x} = \nabla \cdot ((1 - \epsilon_b) D_{s,i} \nabla Y_{s,i}) - r_i \quad [\text{kg}/\text{m}^3 \text{ s}], \quad (3.24)$$

$$\begin{aligned} \frac{\partial ((1 - \epsilon_b) \rho_s v_G h_s)}{\partial x} &= \nabla \cdot \left( (1 - \epsilon_b) \frac{\lambda_s}{c_{p,s}} \nabla h_s \right) + h_c A_p (T_g - T_s) - r_C \Delta h_C - r_{\text{dry}} \Delta h_{\text{vap}} \\ &\quad - (r_{\text{dry}} + r_{\text{pyr}} + r_C) h_s \quad [\text{W}/\text{m}^3]. \end{aligned} \quad (3.25)$$

There are several qualitative differences in 1D and 2D models. The gas flow field is described by a system of Navier-Stokes equations, having an impact on the solution procedure, which must take into account an additional coupling of momentum and continuity equations (3.18)-(3.20). The pressure drop due to fuel bed resistance to gas flow is included in source terms  $f_x, f_y$  and can be approximated by e.g. the Ergun equation (see e.g. [83]) as

$$f_x = \frac{\Delta p}{L} = 150 \frac{\mu v_{g,x} (1 - \epsilon_b)^2}{d_p^2 \epsilon_b^3} + 1.75 \frac{\rho_g |v_{g,x}| v_{g,x} (1 - \epsilon_b)}{d_p \epsilon_b^3} \quad [\text{N}/\text{m}^3] \quad (3.26)$$

$$f_y = \frac{\Delta p}{L} = 150 \frac{\mu v_{g,y} (1 - \epsilon_b)^2}{d_p^2 \epsilon_b^3} + 1.75 \frac{\rho_g |v_{g,y}| v_{g,y} (1 - \epsilon_b)}{d_p \epsilon_b^3} \quad [\text{N}/\text{m}^3] \quad (3.27)$$

The pressure drop has influence on the local air-to-fuel ratio as it determines local air distribution. While the assumption of plug flow in 1D model is reasonable, because the gas

cannot escape to other directions (with small deviations due to channelling effect, see e.g. [76, 78] - however, the upward flow direction remains on the macroscale), the situation is different in a 2D bed.

The simplified approach to model fuel motion along the grate resides in two facts:

1. The effects of moving grates can be modelled by the diffusion coefficient  $D_{s,i}$  in the equation (3.24), see [77] and further discussion in the chapter 4, where the mixing effects are included in the effective thermal conductivity of the fuel.
2. The current model does not take into account the possible vertical motion of the fuel caused by bed volume reduction. It is only assumed, that fuel travels on the grate by known velocity  $v_G$  [m/s]. The bed volume reduction can be calculated based on the density and porosity of the bed. A comprehensive description of fuel motion would require an application of discrete element method on individual particles of the bed [47]. This method is, however, far more complicated and computationally demanding.

### Boundary conditions

Boundary conditions for 2D model are schematically shown on the Figure 3.4.

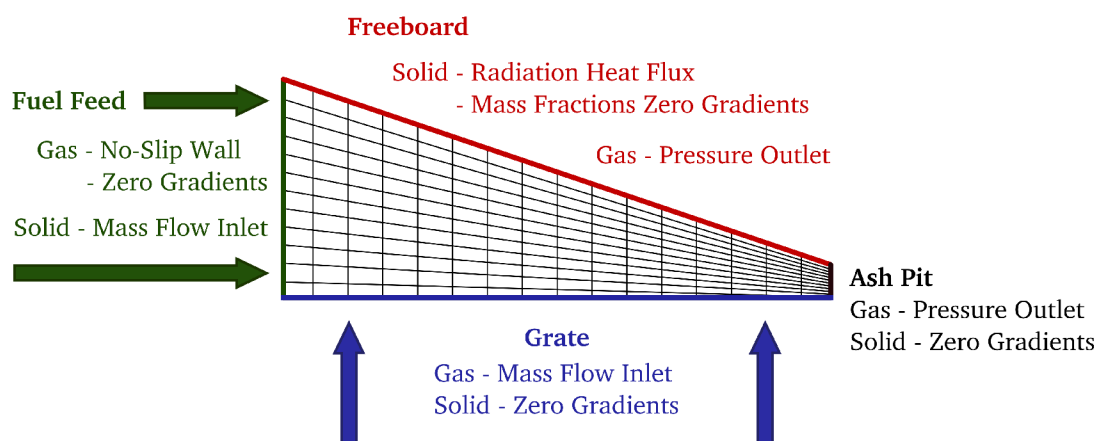


Figure 3.4: Boundary conditions for gas and solid employed for two-dimensional bed model.

## 3.5 Summary

Two mathematical models of packed-bed combustion have been developed and described. Both models are classified as macroscale heterogenous models, which treat a fuel bed as a continuous porous medium, that consists of gas and solid phase. Each phase is described by a separate set of governing equations, which, however, are coupled through various source terms. The source terms have also been described with focus on process rates, which form the solution by the most part. However, for a complete description of both models, relations for other parameters such as specific heat capacity, effective thermal conductivity, heat and mass transfer coefficients etc. must be defined. It is to this matter that the attention is turned in the next chapter 4.

The two models differ mainly in the description of the flow field, which is based on modelling assumptions. These have also been stated. Due to complexity, nonlinearity and coupling of equations, both models must be solved numerically. The chapter 5 is devoted to numerical methods and techniques.

## Chapter 4

# Physical and chemical properties of solid fuels for CFD modelling of grate combustion

A mathematical model of packed-bed combustion requires a large set of input parameters including physical and chemical properties of the fuel and flue gas. Some of these properties such as higher (or lower) heating value, bulk density or typical chemical composition are relatively well-documented and available from the literature. However, there are many other parameters that need to be properly specified in a bed model in order to obtain reliable results with sufficient accuracy. Not all of these properties (e.g. gas species diffusivities, fuel mixing coefficient) are well-documented unlike the basic parameters. This is partly due to the fact they are not valid over the entire range of temperatures, pressure and other physical quantities under combustion conditions.

This chapter aims at description of physical and chemical properties of both herbaceous and woody biomass, that are required in grate combustion modelling. Data are collected from existing literature and empirical formulas for calculation of coefficients in transport equations are discussed in terms of their generality and validity under combustion conditions. Especially, different approaches to model effective thermal conductivity and specific heat capacity are discussed as they belong to a set of parameters with significant effects on model predictions.

### 4.1 Biomass characteristics

Biomass fuels are typically characterized by varying moisture content, particle shapes and sizes, higher volatile matter content and smaller amount of nitrogen (N) and sulphur (S) compared to coal. It is also interesting to note, that higher concentrations of N, S and chlorine (Cl) are usually found in herbaceous biomass (e.g. wheat straw, miscanthus, switchgrass, olive residues) than in woody biomass (e.g. spruce, willow, beech). The elemental composition of the fuel has impact, for example, on a level of emission formation [44]. Biomass is usually processed prior to transportation and combustion by baling, pelleting or briquetting in order to increase energy density and make the fuel load more homogeneous in terms of shape and size. Therefore, fuel composition, lower heating value, particle dimensions and bulk density are basic parameters, which must be considered in

combustion system design [40, 69]. These parameters for various kinds of biomass can be found in several literature sources, e.g. [10, 23, 40, 45, 60, 88] or an online database (also for MSW) [1].

The following list summarizes all gas and fuel properties that are required for calculation of coefficients in governing equations of packed-bed combustion (not in order of their significance):

1. Fuel composition (both ultimate and proximate analysis and including yields of pyrolysis)
2. Material and bulk density of the fuel
3. Bed and fuel particle porosity
4. Fuel particle dimensions (mostly diameter and length), sphericity and shrinkage factors
5. Effective mass dispersion coefficient
6. Effective thermal conductivities of gas and fuel
7. Specific heat capacities of gas and fuel
8. Emissivity of fuel particles
9. Dynamic viscosity of gas

Additionally, there are parameters such as heat and mass transfer coefficients or gas mixing rate, for which an appropriate empirical formula has to be chosen. Discussion on significance, validity and generality of model parameters is provided in the following sections.

### 4.1.1 Moisture

Biomass mostly contains a sizeable amount of water including water vapour, which is in thermodynamic equilibrium with the liquid water (also called free water), which is stored in the pores due to capillary forces and also bound water that is built in the biomass structure by intra-molecular forces [4]. The amount of moisture in biomass is typically higher than in fossil fuels or municipal solid waste. Based on [4] the moisture content of wood chips made from green wood varies from 40 to 60%. After a year of covered storage, the moisture content may decrease to 30%. Even pellets, which are industrially dried during their manufacture, have a moisture content of approximately 10%. Hence, the moisture content is one of the key parameters of biomass fuel and it is of crucial importance to the grate combustion process in terms of both burning rate and energy generation rate. Water stored in biomass fuel has the effect of increased volume of flue gases and decreased flame temperature. It may not be critical for the efficiency of the boiler, because the heat of vaporization may be recovered by condensation from the flue gas, but it is extremely important for the combustion process and consequently for the design of combustors. Water content is also very important in the modelling of biomass combustion processes.



Moisture content  $Y_{\text{H}_2\text{O}}$  is usually expressed as a mass percentage (or fraction) on dry basis and it is defined as

$$Y_{\text{H}_2\text{O}} = \frac{m_{\text{H}_2\text{O}}}{m_{\text{fuel}}}, \quad [\text{kg/kg}] \quad (4.1)$$

where the components of the fraction are the total mass of water in a particle and the mass of the particle completely dried out at  $102^\circ\text{C} \pm 3^\circ\text{C}$ . But moisture content is often defined on a wet basis as well. Therefore one has to know the basis used for water content calculation when adopting data from literature, as a misinterpretation may produce large errors.

### 4.1.2 Volatile matter

Biomass contains large proportion of volatile matter which is gradually released as gaseous products when the temperature exceeds a certain level. The composition of volatiles (i.e. yields of pyrolysis) depends on the fuel type and local conditions under which it has been grown. Typical energy parameters of fifteen different samples of biomass grown in the Czech Republic can be found e.g. in [60], other may be found for instance in [53]. Volatile matter of biomass fuels usually consists of  $\text{CO}$ ,  $\text{CO}_2$ ,  $\text{H}_2$ ,  $\text{CH}_4$  and tar, which is a complex mixture of condensable hydrocarbons and therefore, for simplicity, is usually represented by a single compound  $\text{C}_x\text{H}_y\text{O}_z$ . The elemental composition and LHV of tar can be calculated based on mass and energy balance from the ultimate and proximate analysis and LHV of the fuel. The following formulae can be used to estimate HHV and LHV of the fuel [69]:

$$HHV = 0.3491Y_{\text{C}} + 1.1783Y_{\text{H}} + 0.1005Y_{\text{S}} - 0.0151Y_{\text{N}} - 0.1034Y_{\text{O}} - 0.0211Y_{\text{ash}}, \quad (4.2)$$

$$LHV = HHV (1 - Y_{\text{H}_2\text{O}}) - h_{\text{vap}} \left( Y_{\text{H}_2\text{O}} + Y_{\text{H}} \frac{M_{\text{H}_2\text{O}}}{M_{\text{H}_2}} (1 - Y_{\text{H}_2\text{O}}) \right), \quad (4.3)$$

where  $HHV$  [MJ/kg] is expressed on dry basis,  $LHV$  [MJ/kg] is expressed on wet basis,  $Y_{\text{C}}$ ,  $Y_{\text{H}}$ ,  $Y_{\text{S}}$ ,  $Y_{\text{N}}$ ,  $Y_{\text{O}}$ ,  $Y_{\text{ash}}$  [kg/kg] are mass fractions of carbon, hydrogen, sulphur, nitrogen, oxide and ash in fuel on dry basis, respectively,  $Y_{\text{H}_2\text{O}}$  [kg/kg] is a mass fraction of moisture in fuel on wet basis,  $h_{\text{vap}}$  [MJ/kg] is enthalpy of vaporization and  $M_{\text{H}_2\text{O}(\text{H}_2)}$  [kg/kmol] is molecular weight of water (hydrogen). Table 4.1 shows proximate and ultimate analysis of wheat straw with energy parameters of the fuel species (based on [91]). Note that calculated LHV of  $\text{C}_{1.6}\text{H}_{6.11}\text{O}_{1.64}$  is within a typical range of LHV of tars [3].

### 4.1.3 Packing conditions

Packing conditions refer to a set of parameters defining certain physical properties of the bed such as porosity, fuel particle shape and size, bulk density and bed volume. The structure of the bed and so the packing conditions change due to mass loss as particular combustion processes proceed. Thus, there is coupling between changes of packing conditions and heat and mass transfer and fluid flow and it should be considered in modelling of combustion in packed beds.

Species	Mass fraction in solid [kg/kg] w.b.	LHV [MJ/kg]	Standard state enthalpy of formation [kJ/mol]
H <sub>2</sub> O(liquid/gas)	0.091/0	0/0	-285.83/ -241.81
CO	0.0588	10.102427	-110.53
CO <sub>2</sub>	0.1287	0	-393.5
H <sub>2</sub>	0.0025	11.995258	0
CH <sub>4</sub>	0.0143	50.009163	-74.85
C <sub>1.6</sub> H <sub>6.11</sub> O <sub>1.64</sub>	0.5164	19.941459	-340.42
Char	0.1457	32.762454	0
Ash	0.0426	0	ND
Fuel	1	23.255205	ND
Ultimate analysis [kg/kg] on dry basis			
C			0.4725
H			0.0781
O			0.4494

Table 4.1: Composition of wheat straw and energy parameters of its constituents.

### Porosity

Porosity is defined as a part of a unit volume occupied by the gas phase:

$$\epsilon = \frac{V_g}{V}. \quad [-] \quad (4.4)$$

However, it is important to distinguish between porosity of the bed and particle porosity referred to as internal pores. While generation of internal pores is caused by mass loss of particles during individual combustion stages, bed porosity is determined from volumetric shrinkage of the particle [74]. For example, during drying, mass of particles is decreased about 10% depending on the initial moisture content, but there is only a little change in the size of the particle, thus the bed porosity remains unchanged. The volumetric shrinkage can lead both to an increase in the bed porosity and decrease of the bed height based on experimental observations.

Packing conditions change markedly as particular processes proceed. According to Zhou et al. [91], the fuel layer of wheat straw keeps its bulk volume. However, bed porosity must change due to particle shrinkage. In this respect, the change of bed porosity can be calculated using the relation [80]

$$\epsilon = \epsilon_0 + (1 - \epsilon_0) \sum_i f_i (X_{i,0} - X_i), \quad [-] \quad (4.5)$$

where  $\epsilon_0$  [-] is initial bed porosity,  $X_{i,0}$  [kg/kg] is initial mass fraction of the  $i$ -th solid component and  $f_i$  [-] is a shrinkage factor, which, for the two extreme cases, if  $f_i = 0$ , then the mass loss of the  $i$ -th solid component does not cause increase of bed porosity, if  $f_i = 1$ , then the bed porosity increases by the entire volume of the  $i$ -th solid component removed. Note that modelling of generation of internal particle pores is not considered in the present work.

Bed porosity also affects particle volumetric surface, which is an important parameter in heat and mass transfer between gas and solid phases.

### Particle shape, size and volumetric surface

If biomass is not processed to a form of either pellets or briquets, it has highly irregular shapes, which makes the geometry of a fuel particle difficult to describe for purposes of mathematical modelling. A common assumption in most of bed models is that the bed consists of spherical particles described by an equivalent diameter such that the surface-to-volume ratio remains the same as for the original irregular particle. The volumetric surface area of spherical solid particles can be calculated as [29]

$$A_p = \frac{6(1 - \epsilon_b)}{d_p}, \quad [\text{m}^2/\text{m}^3] \quad (4.6)$$

where  $d_p$  [m] is particle diameter.

However, as it is noted in [13], particles of herbaceous biomass such as wheat straw are rather hollow cylinders than spheres. Since volumetric surface area is a significant parameter of a bed model [29], more accurate estimate of the parameter for cylindrical particles is required. According to [30, 91], it may be expressed as a function of bed porosity and particle outer and inner diameters as follows

$$A_p = 2 \frac{r_{\text{out}} \rho_{\text{sb}}}{(r_{\text{out}}^2 - r_{\text{in}}^2) \rho_s} = 4 \frac{(1 - \epsilon_b) d_{\text{out}}}{d_{\text{out}}^2 - d_{\text{in}}^2}, \quad [\text{m}^2/\text{m}^3] \quad (4.7)$$

where  $\rho_s$  and  $\rho_{\text{sb}}$  [ $\text{kg}/\text{m}^3$ ] are material and bulk densities of solid phase, respectively. Note that the equation (4.7) can be applied also to a cylindrical pellet by taking  $d_{\text{in}} = 0$  m. Other particle shapes can be considered by introducing particle sphericity, which is defined as the ratio of surface area of a sphere with the same volume as the particle to actual surface area of the particle [3]. Sphericity can be calculated for well-defined geometries of particles from the definition. However, for most practical problems, an average value of sphericity must be obtained from measurements on a representative sample of individual fuel particles in the bed.

#### 4.1.4 Thermophysical and heat and mass transfer parameters

It is interesting to note that results from parametric studies on significance of various modelling parameters by different researchers are not consistent. For instance, Zhou et al. [91] studied wheat straw combustion and found that specific heat capacity of the fuel, bed porosity and effective thermal conductivity had significant effect on model predictions, while the rest of parameters were less important. On the other hand, Johansson et al. [29] concluded from the sensitivity analysis that only gas mixing rate, volumetric surface area and heat and mass transfer coefficients had significant effect on model predictions with respect to uncertainty of investigated parameters. Other studied parameters including bed porosity, effective mass dispersion coefficient and solid conductivity did not significantly affect the results in their simulations. It was also pointed out, that the two-flux radiation model could be substituted for less-demanding effective conductivity radiation model (the so called Roseland approximation [42]) due to relatively small differences in ignition rates and peak temperatures. However, when using the Roseland approximation model, effective thermal conductivity becomes in fact even more important parameter as the effects of solid conductivity and radiation are lumped into a single parameter.

### Effective thermal conductivity

Generally, two different approaches to model thermal conductivity (or thermal dispersion) of packed-beds can be found in literature on packed-bed combustion. The first one is applied mostly to homogenous models and it is based on a model of effective thermal conductivity of a quiescent bed (i.e. without fluid flow) corrected for the effect of fluid flow, which can be expressed as

$$\lambda_e = \lambda_{e,0} + aPrRe\lambda_g, \quad [\text{W/mK}] \quad (4.8)$$

where  $\lambda_{e,0}$  [W/mK] is the effective thermal conductivity of a quiescent bed,  $\lambda_g$  [W/mK] is thermal conductivity of the gas phase, Pr is Prandtl number, Re is Reynolds number and  $a$  takes the values of 0,1 or 0,5 for radial (along the bed length) or axial (along the bed height) heat conduction, respectively [71]. The inclusion of the additional term is based on heat and mass transfer analogy and describes effects of turbulent flow on the thermal dispersion. With an appropriate expression for  $\lambda_{e,0}$ , the equation (4.8) can be applied to any kind of fuel. However, Gort [19] pointed out that care must be taken, when a model of thermal conductivity with combined effects from both phases is applied to different types of bed models. Therefore, a few comments should be made on the applicability of the equation (4.8) to different classes of bed models.

Van der Lans et al. [67] used the equation (4.8) to describe an effective thermal conductivity of the bed in a homogenous model of wheat straw combustion. They suggested a temperature-dependent formula for  $\lambda_{e,0}$ . Indeed, the equation (4.8) can directly be used in homogenous models [71]. Yagi et al. [73] developed a model of effective thermal conductivity of a quiescent bed, which accounts for both gas and solid conductivities as well as radiation between solid particle surfaces and in the gas phase. Later, several extensions were introduced to this model to account for various effects on heat conduction, e.g. Fjellerup et al. [13] included effects of particle shape and fluid flow according to the equation (4.8) and applied the model for calculation of straw char bed conductivity. The homogenous bed model of van der Lans was then extended to a heterogenous model [91], using the conductivity model of Fjellerup for calculation of the solid phase conductivity, so the effects of eventual turbulent flow on heat transfer was included in the solid phase, while gas phase effective thermal dispersion coefficient included only thermal conductivity of fluid. On the other hand, effective mass dispersion in fluid was modelled with effects of turbulence (according to the equation (4.19)), so the approaches of modelling heat and mass transfer were inconsistent with respect to heat and mass transfer analogy.

Contrary to this, turbulence effects were included in the gas phase, while the turbulent term was not included in the effective solid phase conductivity in a heterogenous model of char particle combustion by Ryan et al. [51], where the original model of Yagi et al. [73] was also adopted.

To conclude discussion on the first approach of modelling the effective thermal conductivities, the equation (4.8) applied to the bed conductivity is suitable mainly for homogenous models, where the energy balance over the packed-bed is described by the only transport equation with conductivities and turbulence effects lumped into a single parameter (the effective thermal conductivity of the bed).

In the other approach, the solid conductivity is expressed as a weighted sum of conductivities of solid constituents (moisture, volatile matter, char, ash) plus contribution from radiation (in the radiation conductivity model) and possible solid particle mixing caused by

grate movement [7, 29, 77, 79]. However, since it is difficult to obtain thermal conductivity of volatile matter, species considered in the calculation of the thermal conductivity include virgin fuel and char. Values of the thermal conductivity are obtained by a linear interpolation between thermal conductivities of virgin fuel and char based on the degree of mass loss  $\eta$  [-]:

$$\lambda_s = \eta\lambda_{VF} + (1 - \eta)\lambda_C + \lambda_{rad} + \lambda_{mix}, \quad [\text{W/mK}] \quad (4.9)$$

$$\lambda_{rad} = 4\sigma\epsilon_{rad,p}d_p \left( \frac{\epsilon_b}{1 - \epsilon_b} \right) T_s^3, \quad [\text{W/mK}] \quad (4.10)$$

$$\lambda_{mix} = \rho_s c_{p,s} D_s, \quad [\text{W/mK}] \quad (4.11)$$

where  $T_s$  [K] is solid phase temperature,  $d_p$  [m] is solid particle diameter,  $\epsilon_{rad,p}$  [-] is solid particle emissivity,  $\sigma$  [W/m<sup>2</sup>K<sup>4</sup>] is Steffan-Boltzman constant and  $D_s$  [m<sup>2</sup>/s] is the particle diffusion coefficient, which has to be estimated based on the grate type and operational conditions. The species thermal conductivities  $\lambda_{VF}$ ,  $\lambda_C$  are usually constants or depend linearly on temperature and moisture content [7, 21, 47]. It is also interesting to note that the weighted sum of species conductivities in equation (4.9) is usually used for conductivity of woody biomass, whereas wheat straw conductivity is expressed as a single function of temperature and bulk density [79, 91]. Since wheat straw is used in all case studies in this work and thermal conductivity expressed in the form of equation (4.9) is in case of heterogenous model preferred to the equation (4.8), the following expression adopted from [79] is employed to model the fuel thermal conductivity:

$$\lambda_s = \left( \frac{\rho_s}{4511} \right)^{3.5} T_s^{0.5} + 2.27 \cdot 10^{-7} \left( \frac{d_p}{1 - \epsilon_b} \right) \left( \frac{\epsilon_{rad,p}}{2 - \epsilon_b} \right) T_s^3 \quad [\text{W/mK}] \quad (4.12)$$

Compared to the equation (4.8), the other approach (equation (4.9)) provides for an easier and faster calculation of the thermal dispersion, because the thermal conductivity of a quiescent bed is usually a complicated function of gas and fuel properties. However, information on the empirical parameter  $D_s$  in (4.11) is very scarce. The method for estimating of the effects of moving grates on mixing of fuel in a bed by diffusion coefficients (an analogy to Fick's law) was originally proposed by Yang et al. [77]. They ran a series of simulations in a certain range of the mixing coefficient and conducted experiments in furnaces with moving (reciprocating etc.) grates. Although simulations revealed a suitable range of the coefficient with respect to the optimal air-to-fuel ratio, it was not validated by measurements and more work has to be done in this area to fully account for effects of mixing by introducing diffusion coefficients. In spite of these facts, the mixing coefficient is included in the 2D model as it provides the easiest way for taking the mixing effects into account.

The temperature-dependent relation for the effective thermal conductivity of gas phase used in this work is given e.g. in [91] as

$$\lambda_g = 4.8 \cdot 10^{-4} T_g^{0.717}, \quad [\text{W/mK}] \quad (4.13)$$

and the effective thermal conductivity of the gas phase is given by (4.8) with  $\lambda_{e,0} = 0.8\lambda_g$  [29, 64, 71].

### Specific heat capacity of gas and fuel

The effect of solid specific heat capacity on wheat straw combustion was investigated in [91]. It was concluded, that it significantly affected the model results. On the other

hand, this parameter was not considered in the sensitivity analysis in [29]. Therefore, it would be interesting to perform such a parametric study in order to further examine the significance of the parameter. The specific heat capacities of both fuel and gas are usually expressed as a mass-weighted sum of specific heat capacities of species. While data for gas species are well-documented for a wide range of temperatures (e.g. [61]), specific heats of solid constituents are more difficult to determine. First, the specific heat capacity of wet biomass is greater than the simple sum of separate effects of dry biomass and moisture due to thermal energy absorbed by the biomass-water bonds [50]. Second, analogically to the thermal conductivity, the specific heat of volatile matter as a separate solid species is difficult to measure. Instead, specific heats of the virgin fuel and char are measured and the specific heat capacity is given as weighted average of virgin fuel and char based on the conversion degree  $\eta$  as [61]

$$c_{p,s} = \eta c_{p,VF} + (1 - \eta) c_{p,C} \quad [\text{J/kg K}] \quad (4.14)$$

Temperature-dependent specific heats of virgin fuel  $c_{p,VF}$  [J/kg K] and char  $c_{p,C}$  [J/kg K] are reported in the literature in the form similar to gas species heat capacities [7, 21, 24]:

$$c_{p,s}(T_s) = a + bT_s + cT_s^2 + dT_s^{-2} \quad [\text{J/kg K}] \quad (4.15)$$

Beside this widely used model of heat capacity of solids, the specific heats for certain kinds of fuels can also be found in literature expressed in other forms of nonlinear functions of the solid temperature such as the heat capacity of wheat straw in [91]

$$c_{p,s}(T_s) = 977.75 \ln(T_s) - 4144.4, \quad [\text{J/kg K}] \quad (4.16)$$

which is also used in this work for modelling of fuel specific heat capacity. Such an approach, however, does not provide for a description of the physical parameter on the basis of a general model such as equation (4.15), where only coefficients  $a, b, c, d$  instead of an entire relation need to be specified by a user. This approach is recommended for the future development of general codes.

For the sake of simplicity, instead of weighted sum of gas species capacities, the following relation for gas phase specific heat capacity is used in this work [91]:

$$c_{p,g}(T_s) = 990 + 0.122T_g - 5680 \cdot 10^3 T_g^{-2} \quad [\text{J/kg K}] \quad (4.17)$$

It is important to make a note on an inconsistency of physical units of heat capacities (4.16)-(4.17) given by the reference [91] as [J/molK]. The gas heat capacity numerically corresponds with values tabulated in literature, however, with units of [J/kgK]. Heat capacity of wheat straw could not be verified in the same way due to unavailable data. However, it is believed that both heat capacities were meant to be expressed in [J/kgK], so the equations are used with these units in this work.

### Heat and mass transfer coefficients

Based on [71], suitable correlations for coefficients of interphase heat and mass transfer in terms of Nusselt and Sherwood numbers in packed beds of spherical particles, which have been validated over different kinds of packing materials and wide range of Reynolds numbers, are as follows:

$$\begin{aligned} \text{Nu} &= 2 + 0.1\text{Pr}^{1/3}\text{Re}^{0.6}, & [-] \\ \text{Sh} &= 2 + 0.1\text{Sc}^{1/3}\text{Re}^{0.6}. & [-] \end{aligned} \quad (4.18)$$

The same correlations were used in the sensitivity analysis [29], where values of Nu and Sh were changed in the range of  $\pm 50\%$  of the reference values given by equation (4.18). Model predictions were significantly affected by the change of Nu and Sh. Therefore, similarly to the volumetric surface area, it can be concluded that other correlations for Nu and Sh should be considered for particle shapes different from a sphere. [30] describes a Sherwood number correlation for a cylinder as for a typical shape of wheat straw fuel particles. Otherwise, the particle sphericity can again be used to modify heat and mass transfer coefficients of spherical particles to be applied for other particle shapes.

### Effective mass dispersion coefficient

The coefficient for mass dispersion in gas phase consists of diffusional and turbulent contributions as described in [71]. The formula is analogical to the equation (4.8):

$$D_{i,e} = D_{i,0} + ad_p |\mathbf{v}_g|, \quad [\text{m}^2/\text{s}] \quad (4.19)$$

where  $D_{i,0}$  [ $\text{m}^2/\text{s}$ ] is the coefficient of diffusion of gas species  $i$ . Massman [37] studied molecular diffusivities of  $\text{H}_2\text{O}$ ,  $\text{CO}_2$ ,  $\text{CH}_4$ ,  $\text{CO}$ ,  $\text{O}_3$ ,  $\text{SO}_2$ ,  $\text{NH}_3$ ,  $\text{N}_2\text{O}$ ,  $\text{NO}$  and  $\text{NOO}$  in air,  $\text{O}_2$  and  $\text{N}_2$  and found a correlation for the diffusion coefficient as

$$D_{i,0} = D_i^0 \left( \frac{T_g}{273.15} \right)^{1.81}, \quad [\text{m}^2/\text{s}] \quad (4.20)$$

where  $D_i^0$  is the coefficient of diffusivity of species  $i$  under normal conditions (i.e.  $T_g = 273, 15 \text{ K}$ ,  $p = 1 \text{ atm}$ ). The correlation provides for an easy calculation of the coefficient, however it is valid only for temperatures up to  $373, 15 \text{ K}$ . Furthermore, diffusivity of hydrogen as one of gas species that is released during pyrolysis, is not provided in [37], it can be concluded, that further investigation is needed for determination of the mass diffusion coefficients calculated by this model under combustion conditions.

A different method is used in [30] for modelling of wheat straw combustion. The so-called Wilke and Lee equation (for detailed description, see e.g. [20]) is valid for wider range of conditions, however, the formula for estimation of gas diffusivity is much more complicated than (4.20).

### Pressure drop

It is worth noting that very little or no attention is given in the published experimental works to the investigation of flow resistance in the fuel bed. This problem is rather pressing, because flow resistance of the bed in real combustors has decisive role in determining the local air-fuel ratio in the bed and thus influences all other processes through local heat generation rates. It has been either completely disregarded as in [67, 74, 91] or a simple approximation assuming bed of spherical particles described by Ergun equation was adopted as in [79, 81]. The reason for adoption of such simplified approaches is the lack of experimental data both for model development and for its validation.

However, biomass particle shapes are far from being spherical. For instance, wheat straw particles are usually described as hollow cylinders. In spite of this fact, the Ergun equation with coefficients derived from measurements on spheres is still adopted for the

description of local pressure drop in the bed of cylindrical particles, although it has been found inaccurate in case of a bed of non-equilateral cylinders [15]. More attention should be paid to this issue both in experimental and modelling works. For the case of cylindrical particles with diameter  $d_p$  [m], the following expression can be used to calculate the pressure drop across a bed of the length  $L$  [m] and [15]:

$$\frac{\Delta p d_p^2 \epsilon_b^3}{L \mu v (1 - \epsilon_b)^2} = \left( 3.81 - \frac{5.265}{d_t/d_{p,e}} - \frac{7.047}{(d_t/d_{p,e})^2} \right) \frac{\rho_g v d_p}{\mu (1 - \epsilon_b)} + 211, \quad (4.21)$$

where  $\mu$  [N/m s] is gas viscosity,  $\rho_g$  [kg/m<sup>3</sup>] gas density,  $\Delta p$  [Pa] is pressure drop across the length  $L$  [m] of the bed with mean porosity  $\epsilon_b$  [-] and a tube diameter  $d_t$  [m]. Particles are characterized by particle and equivalent diameters  $d_p, d_{p,e}$  [m], respectively. The equivalent diameter is given by the particle volume-to-surface ratio  $d_{p,e} = 6V_p/S_p$ .

## 4.2 Summary

Physical and chemical properties of solid fuels that are needed as input parameters in CFD simulations have been described. Among all the parameters, different models of effective thermal dispersion and specific heat capacity have been discussed in terms of their validity, generality and applicability to various classes of bed models. Care must be taken when applying relations for effective mass and thermal dispersion coefficients to heterogenous models, in which contributions of heat conductivity to the energy balance are treated separately in gas and solid energy transport equations. Effects of turbulence should be included in a consistent way according to heat and mass transfer analogy.

Since pressure drop dominates the flow distribution in packed beds, applicability of Ergun equation to beds of nonspherical particles has been discussed as well. Also it has been pointed out that particle-mixing (diffusion) coefficient and particle shrinkage factors require further experimental investigations due to their uncertainty.



# Chapter 5

## Numerical solution technique for the packed-bed model

Since governing equations of the bed model are coupled and nonlinear, numerical methods are employed to solve the system of equations. Although there are plenty of books written on discretization and numerical solutions of various systems of differential equations, there is no general recipe to solve any kind of problem without considering some modifications to the solution algorithm or special setup of the solver parameters due to diversity of problems.

This chapter provides for the description of various techniques, that have been used for discretization and solution of packed-bed model equations. Especially, a comprehensive discussion is carried out on methods, that have been found helpful in obtaining the convergence. The overall solution algorithms are outlined at the end of the chapter.

### 5.1 Discretization

The equations are discretized by the finite volume method, which has become a standard method in CFD applications for solving problems involving both reacting and nonreacting fluid flows and heat and mass transfer in complex geometries. Since discretization is derived from the integral form of physical conservation laws, quantities such as energy, mass and momentum remain conserved at the discrete level as well [25] (this, however, holds on theoretical level only - for detailed discussion, see the chapter 7).

Since both governing equations (3.1)-(3.6) and (3.18)-(3.25) can be expressed by the general transport equation (2.1), discretization can generally be demonstrated using the equation and afterwards general coefficients be substituted for specific coefficients from gas and solid governing equations. Discretization and solution techniques are based on methods described e.g. in [38, 46, 63]. For a complete description of the discretization procedure, the continuity equation is needed as well. Therefore, it is recalled here:

$$\frac{\partial (\epsilon_b \rho)}{\partial t} + \nabla \cdot (\epsilon_b \rho \mathbf{v}) = r. \quad [\text{kg}/\text{m}^3 \text{ s}] \quad (5.1)$$

The bed is represented by a rectangle and the computational domain is divided into a number of non-overlapping control volumes forming a regular uniform-spaced grid. The equation (2.1) is discretized over time and space. Convective term is approximated by

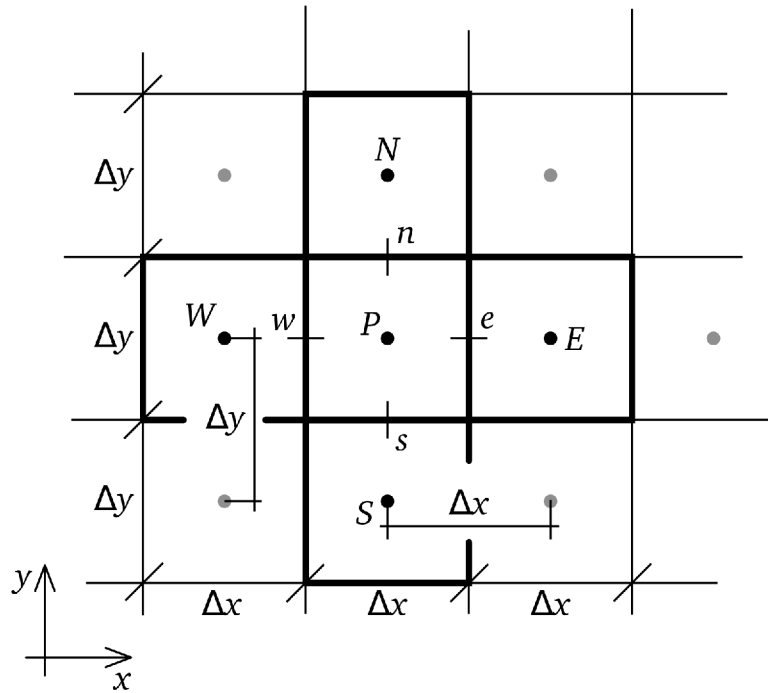


Figure 5.1: A part of a computational grid. While primitive variables are stored at cell centroids  $P, E, W, N, S$ , fluxes are evaluated at face centroids  $e, w, n, s$ . Points  $E, W, N, S$  are called neighbours of  $P$ .

the first-order upwind scheme (or eventually power law scheme [46], which is, however, first-order accurate as well), the diffusion term is treated by the central-difference scheme (second-order accurate) and the implicit Euler method is used for approximation of time integrals. If the source term is linearized as

$$S_\phi = S_C - S_P \phi_P, \quad (5.2)$$

then, discretization leads to a set of nominally linear equations of the form (5.3), where cardinal points notation is used for computational nodes (cell centroids) as commonly used in literature on CFD. For the explanation of indices and symbols, see Figure 5.1.

$$a_P \phi_P = a_E \phi_E + a_W \phi_W + a_N \phi_N + a_S \phi_S + b_P \quad (5.3)$$

$$a_E = \max(-F_e, 0) \Delta y + \Gamma_e \frac{\Delta y}{\Delta x} A(\text{Pe}_e) \quad a_N = \max(-F_n, 0) \Delta x + \Gamma_n \frac{\Delta x}{\Delta y} A(\text{Pe}_n)$$

$$a_W = \max(F_w, 0) \Delta y + \Gamma_w \frac{\Delta y}{\Delta x} A(\text{Pe}_w) \quad a_S = \max(F_s, 0) \Delta x + \Gamma_s \frac{\Delta x}{\Delta y} A(\text{Pe}_s)$$

$$a_P^0 = \epsilon_{b,P}^0 \rho_P^0 \frac{\Delta x \Delta y}{\Delta t}$$

$$b_P = a_P^0 \phi_P^0 + S_C \Delta x \Delta y + \max(-r, 0) \phi_P^* \Delta x \Delta y$$

$$a_P = a_E + a_W + a_N + a_S + a_P^0 + S_P \Delta x \Delta y + \max(r, 0) \Delta x \Delta y \quad (5.4)$$

The additional source term in  $a_P$  and  $b_P$  coefficients results from the continuity equation (5.1), which has been introduced into the discretization of the general transport equation

(2.1) in the same manner as in [46, 63]. The quantity  $F = \epsilon_b \rho v$  is mass flux, by which a scalar quantity  $\phi$  is convected through the domain. If a flow field does not satisfy the continuity equation, incorrect mass flux is substituted for the convection term leading to incorrect solutions. For this reason, it is extremely important to ensure, that the discrete continuity equation is satisfied at every iteration identically. Due to the plug-flow assumption in 1D model, the mass flux on a cell face is obtained directly from the discretized continuity equation as

$$F_n = F_s + r\Delta y - (\epsilon_{b,p}\rho_p - \epsilon_{b,p}^0\rho_p^0) \frac{\Delta y}{\Delta t}. \quad (5.5)$$

Gas velocities are calculated from (5.5) by interpolation of the face fluxes into the cell centroid and then by dividing by gas density. This is applicable to the 1D model only. Two-dimensional flow field (in 2D model) is solved using the algorithm SIMPLE for colocated grids [43].

Since the value of the rate  $r$  might become negative during the solution procedure, it must be ensured that the diagonal coefficient  $a_p$  in equations (5.4) does not become negative either, which is handled by max function. Should such situation arrive, the rate is added to  $b_p$ . In this case, the transported quantity  $\phi_p^*$  is treated explicitly using a value from the previous iteration. If the equations (5.3)-(5.4) are applied to discretized two-dimensional steady bed model, the unsteady coefficient  $a_p^0$  is omitted, since it vanishes as  $\Delta t \rightarrow \infty$ , while in the case of 1D transient model, coefficients  $a_N = a_S = 0$  and  $\Delta x = 1$ .

The quantity  $A(\text{Pe})$  is a function of Peclet number (defined as  $\text{Pe} = \rho v L / \Gamma$  [-]) and it depends on a numerical scheme used for discretization of convection problems. In particular, two numerical schemes are considered in this work, namely the first-order upwind scheme and the power-law scheme (respectively):

$$A(\text{Pe}) = 1, \quad A(\text{Pe}) = \max\left(0, (1 - 0.1|\text{Pe}|)^5\right).$$

For larger Peclet numbers the power-law scheme produces better results as the first-order scheme overestimates effects of diffusion [46].

Discretized boundary conditions enter the equation (5.3) through  $S_C$  and  $S_p$  coefficients as additional parts of source terms of boundary cell centroids. The contribution to  $S_C$  and/or  $S_p$  depends on the actual type of the boundary condition. A special treatment of a boundary condition is required if the radiation heat flux is specified as given by (3.8), because the boundary condition is nonlinear, so its value, i.e. the heat flux must be iteratively updated until convergence is reached. In order to do that, the derivative of the boundary condition (3.8) is first expressed in terms of temperature, discretized and rearranged to a general form of a nonlinear equation  $f(T) = 0$  (the subscript for solid phase is omitted for clarity):

$$\begin{aligned} - \left( (1 - \epsilon_b) \frac{\lambda}{c_p} \frac{\partial h}{\partial y} \right)_{y_{\text{top}}} &= - \left( (1 - \epsilon_b) \lambda \frac{\partial T}{\partial y} \right)_{y_{\text{top}}} \\ &\approx 2(1 - \epsilon_b) \lambda_{\text{top}} \frac{T_P - T_{\text{top}}}{\Delta y} = \epsilon_{\text{rad}} \sigma \left( T_{\text{top}}^4 - T_{\text{env}}^4 \right). \end{aligned} \quad (5.6)$$

$$f(T_{\text{top}}) = 2(1 - \epsilon_b) \lambda_{\text{top}} \frac{T_P - T_{\text{top}}}{\Delta x} - \epsilon_{\text{rad}} \sigma \left( T_{\text{top}}^4 - T_{\text{env}}^4 \right) = 0. \quad (5.7)$$

The equation is solved by Newton iteration method. Since the accuracy of temperatures is important as almost all parameters are temperature-dependent, the equation (5.7) is solved with a relative error of  $10^{-6}$ . This, however, does not slow down the iterative procedure significantly as it takes only a few iterations (typically around seven) to reach the limit.

The system of equations (5.3) is solved either by direct or indirect method. Indirect (iterative) methods are preferred for several reasons:

1. Governing equations are coupled and nonlinear, so a number of the so-called outer iterations must be performed at each time step to obtain a converged solution. Therefore it is usually worthless to solve the system of discretized equations to machine accuracy by using a direct method such as Gauss elimination method (GEM) or LU decomposition. Instead, the system can repeatedly be solved just to a certain level of accuracy (or with a fixed number of the so-called inner iterations) and the tentative values used as a guess for the next iteration until a convergence criterion is met.
2. Iterative methods are memory-efficient as they take advantage of sparsity of the resulting matrix of the system.
3. Iterative methods are easier to implement into a computer code.

In spite of these reasons, direct methods may become handy in certain problems, especially if a number of control volumes is not large or the problem is simplified in a sense. For instance, among easy-to-implement and computationally low-demanding non-iterative methods, the so-called Tri-Diagonal Matrix Algorithm (TDMA) (see e.g. [70]) can be employed in one-dimensional problems providing for calculation of the exact solution, while preserving advantages of iteration methods at the same time. The algorithm can also be applied to higher-dimensional problems, though on a basis of an iterative calculation.

### 5.1.1 Note on discretization of effective dispersion coefficients

For the description of gas thermal and species diffusion, the effective dispersion coefficients (4.8) and (4.19), respectively, are needed. From discretization point of view, both coefficients are covered by the general diffusion coefficient  $\Gamma$  in the general transport equation (2.1). The second-order central differencing is a standard way for discretization of such terms, i.e. terms with the second derivative of the transported property  $\phi$  providing for stable numerical calculation. However, it has been found during testing simulations, that significantly less iterations are needed to obtain a converged solution, when the turbulent term in the dispersion coefficients is omitted. This behaviour is believed to be caused by an inappropriate interpolation of  $\Gamma$  to the cell faces, which is needed after integration of the diffusion term. The diffusion term is of the form (in 1D case)

$$\frac{\partial}{\partial y} \left( (\Gamma_m + \Gamma_t(v)) \frac{\partial \phi}{\partial y} \right) = \left( \frac{\partial \Gamma_m}{\partial y} + \frac{\partial \Gamma_t(v)}{\partial y} \right) \frac{\partial \phi}{\partial y} + (\Gamma_m + \Gamma_t(v)) \frac{\partial^2 \phi}{\partial y^2}, \quad (5.8)$$

where  $\Gamma$  is split into two parts with a molecular contribution denoted by  $\Gamma_m$  and turbulent contribution  $\Gamma_t(v)$ , which is a function of velocity  $v$ . The turbulent part is now much like the convection term of the general transport equation (2.1), for which an upwind discretization scheme must be used in order to obtain physically realistic and stable solutions. However, the diffusion term is interpolated by arithmetic or harmonic mean as it is common for

diffusion coefficients, so the effect can be similar to central-differencing scheme, if it is applied to the convection term. A remedy could be to interpolate the turbulent part using an upwinding technique.

## 5.2 Controlling the convergence

Since the governing equations are solved sequentially in a decoupled manner, several outer iterations must be performed at each time step to obtain a converged solution. During these outer iterations, coefficients are updated according to the most current values of solution variables (solid and gas temperatures, mass of solid and gas species, gas mass flux or velocity). This strategy has been found helpful for its stabilizing effect on successive iterations. Furthermore, it is an efficient method in terms of computer memory, although this advantage comes at the expense of longer computational times [66]. Alternatively, the governing equations could be solved in a coupled way (different to the SIMPLE algorithm, e.g. [46]), which means that all equations are solved simultaneously. The rate of convergence of this method is reportedly slightly better when compared to that of the decoupled algorithm [14, 66]. On the other hand, it is much less memory-efficient and more difficult to implement into a computer program.

It is important to control the overall progress of iterations by adjusting the rate of change of various variables so that a sequence of intermediate solutions finally converge. This is accomplished by several methods that are described in detail in the following sections.

### 5.2.1 Convergence criterion

Of course, a criterion to decide whether the iterations are converged, must be defined first. The convergence of outer iterations is judged by scaled residuals (nondimensional) as described in [14], It is a standard method in CFD applications, which is based on the imbalance of the set of discretized equations (5.3) evaluated with instantaneous values of coefficients and solution variables. The imbalance of the discretized equation for a scalar variable  $\phi$  is given by the unscaled residual as

$$R_u^\phi = \sum_{\text{cells } P} |a_E \phi_E + a_W \phi_W + a_N \phi_N + a_S \phi_S + b_p - a_P \phi_P|, \quad (5.9)$$

The scaled residual can be defined in various ways. Here, the scale factor is given by the cell content, thus the scaled residual is calculated as

$$R_s^\phi = \frac{R_u^\phi}{\sum_{\text{cells } P} |a_P \phi_P|}. \quad (5.10)$$

Additionally, it is often useful to measure a decrease of the scaled residual as another convergence criterion. Therefore, the relative (normalized) scaled residuals are also defined and calculated by dividing the scaled residual by the residual value after the first iteration:

$$R_r^\phi = \frac{R_s^\phi}{R_{s,1}^\phi}. \quad (5.11)$$

Residuals of the continuity equation in 1D model are defined by analogy, scaling factor is the maximum value of cell face mass fluxes:

$$R_u^F = \sum_{\text{cells } P} \left| \left( \epsilon_{b,P} \rho_P - \epsilon_{b,P}^0 \rho_P^0 \right) \frac{\Delta y}{\Delta t} + F_n - F_s - r \Delta y \right|, \quad (5.12)$$

$$R_s^F = \frac{R_u^F}{\max_{\text{faces } f} F_f}. \quad (5.13)$$

The equation is said to be converged, if either of the scaled or relative (normalized ) scaled residual drops below a pre-defined value. For example, ANSYS FLUENT uses default values  $10^{-6}$  for the scaled residual of the energy equation and  $10^{-3}$  for the scaled residual of species transport and velocity equations [14].

### 5.2.2 Relaxation

Relaxation is a basic method for controlling the rate of change of various variables and consequently the rate of convergence. Through the so-called relaxation factor  $\alpha$ , the change of a value of a variable per iteration may be either increased for  $\alpha \in (1, 2)$ , or decreased for  $\alpha \in (0, 1)$  (of course, if  $\alpha = 1$ , the variable is not relaxed) [12, 26]. The choice depends on the actual problem being solved. In most cases of CFD simulations, it is necessary to slow down the changes of variables in order to stabilize the progress of iterations. Any variable  $\phi$  can be under-relaxed by

$$\phi = \alpha \phi^{\text{new}} + (1 - \alpha) \phi^*, \quad (5.14)$$

where  $\phi^{\text{new}}$  denotes new (i.e. true or previously updated) value of the variable and  $\phi^*$  is the old value from the previous iteration. It can be seen, that when the solution comes to convergence, so  $\phi^* = \phi$ , the effect of relaxation vanishes. This is an important property, which any kind of relaxation must possess to obtain relaxation-independent solutions [43]. Even though dependent variables such as temperature can be underrelaxed using (5.14), it is better to underrelax discretized equations as it makes the matrix of the system more diagonal-dominant, having a stabilizing effect on the successive iterations. Equations (5.3) are underrelaxed in the following way [43]:

$$\frac{a_p}{\alpha} \phi_p = a_E \phi_E + a_W \phi_W + a_N \phi_N + a_S \phi_S + b_p + \frac{1 - \alpha}{\alpha} a_p \phi^*. \quad (5.15)$$

### 5.2.3 Adaptive time stepping

Although the implicit (backward) Euler method is unconditionally stable with respect to the time step length, outer iterations are not guaranteed to converge for all possible cases. Too long time steps may produce oscillatory results of the iterations due to large source terms. Shorter time steps often help to solve such situations. On the other hand, computational times are longer. Adaptive time stepping can be used to let the solver choose a suitable length of a time step. While professional ODE (ordinary differential equation) solvers use sophisticated algorithms for adaptive time stepping, the method used here is

rather heuristical, based on experiences from simulations. The time steps are adapted according to the number of iterations, that have been needed in the current time level. When the convergence is not reached within the given maximum number of iterations, the time level is recomputed with a half of the previous time step. If the convergence is reached in less than 75% of the maximum number of iterations, the time step for the next time level is doubled.

Although the method has been found helpful in certain simulation cases, especially at the beginning of a simulation, when steep gradients arise, it is usually more efficient to allow more iterations per a fixed time step of suitable length (for instance 0.1-0.5 s or less) to resolve the initial gradients.

### 5.2.4 Linearization

If a source term is a nonlinear function of the dependent variable, it must be properly linearized in order to stabilize the iterative process. Linearization may be viewed as a kind of relaxation, because it has an effect on rates of change of dependent variables. A basic rule of linearization is to set coefficients of (5.3) such that  $S_p \geq 0$  at all circumstances, while  $S_C \geq 0$  for always-nonnegative dependent variables, e.g. temperatures or mass fractions. A generally recommended way of linearization is to expand a source term into Taylor series around the last known value  $S^* = S(\phi^*)$  and let

$$S_C = S^* - \left( \frac{\partial S}{\partial \phi} \right)^* \phi^* \quad S_p = - \left( \frac{\partial S}{\partial \phi} \right)^* . \quad (5.16)$$

The derivative must be nonpositive to satisfy conditions made on  $S_C, S_p$  coefficients. It is difficult to evaluate derivatives of some source terms defined in the chapter 3 due to complicated expressions (for instance, temperature-dependent terms in energy equations are in fact enthalpy-dependent, but the inverse of  $h \sim T$  relation would have to be found). Therefore, linearization based on Taylor series expansion is not used. Instead, the source terms are split into the always positive parts and always negative parts as  $S = S^+ + S^-$ , so the linearized source term is [46].

$$S_C = S^+ \quad S_p = - \frac{S^-}{\phi^*} . \quad (5.17)$$

It is clear, that coefficients  $S_p, S_C$  are always nonnegative. If a source term is a linear function of dependent variable such as for enthalpy the heat source term due to interphase mass transfer, this linearization is the same as (5.16). The linearization has a stabilizing effect, however at the expense of slower convergence caused by artificially created linearity of  $S_p$ .

### 5.2.5 Special treatment of process rates

Treatment of process rates is separated from linearization, as it does not belong to conventional methods. Both diffusion limited drying rate and char combustion rate do not depend on the content of moisture and fuel, respectively. Let us concentrate on the drying rate only (the idea is the same for char combustion rate). The rate can become during iterations large enough to consume all the moisture in a control volume. If it becomes even

larger, then an appropriate method must be employed to handle potential negative values of mass. Following the discretization of the general transport equation and substituting coefficients for quantities from the governing equation (3.5), the following numerical formula is obtained (subscript  $P$  is omitted for clarity, because no neighbours are involved in the equation):

$$Y_{\text{H}_2\text{O}} = \frac{(1 - \epsilon_b^0)\rho^0 Y_{\text{H}_2\text{O}}^0 \frac{\Delta y}{\Delta t} + r Y_{\text{H}_2\text{O}}^* \Delta y}{(1 - \epsilon_b^0)\rho^0 \frac{\Delta y}{\Delta t} + \frac{r_{\text{dry}} \Delta y}{Y_{\text{H}_2\text{O}}^*}}. \quad [\text{kg/kg}] \quad (5.18)$$

Such a formula has an asymptotic behavior meaning, that successive iterations will gradually improve the solution and finally approach zero, whenever nonzero (and arbitrarily large) drying rate is calculated. However, the rate of convergence is slow and, more importantly, if mass of moisture in the fuel is less than the drying rate integrated over the cell and time, i.e.

$$r_{\text{dry}} \Delta t \Delta V > m_{\text{H}_2\text{O}}^0 \quad [\text{kg}], \quad (5.19)$$

then, after substitution into the water vapour transport equation, it overestimates the amount of vapour evaporated into the gas phase, resulting in both mass and energy imbalance of the system. This undesirable behavior is avoided, if an appropriate limiter is used for the drying rate. Therefore, based on the physical limitations, all process rates are limited and calculated by

$$r_{i,\text{lim}} = \min \left( r_i, \frac{m_i^0}{\Delta t \Delta V} \right). \quad [\text{kg/m}^3 \text{ s}] \quad (5.20)$$

It is important to note, that the limiter cannot be used in a steady calculation unless a time-marching scheme is employed, see e.g. [14]. This can be partly remedied by another limiter for gas species transport equations. The amount of water vapour is limited by saturation pressure, so if drying completes at low gas temperatures, the amount of evaporated water is limited in the gas phase through linearization for variables with physical limits such as mass fractions [46]. In order to use this linearization, upper and lower bounds of the dependent variable must be determined. While the lower bound is zero, the upper bound is given by mass fraction of saturated water vapour and can be expressed as

$$Y_{\text{H}_2\text{O}}^{\text{sat}} = \frac{\rho_{\text{H}_2\text{O}}^{\text{sat}}}{\rho_g} = \frac{p_{\text{H}_2\text{O}}^{\text{sat}} M_{\text{H}_2\text{O}}}{p_g \overline{M}_g}, \quad [\text{kg/kg}] \quad (5.21)$$

This leads to the following linearization, which depends on the sign of the source term (cell centroid subscripts  $P$  are again omitted for better readability):

$$\text{if } r_{\text{dry}}^* \geq 0, \text{ set } S_C = \frac{r_{\text{dry}}^* Y_{\text{H}_2\text{O}}^{\text{sat}}}{Y_{\text{H}_2\text{O}}^{\text{sat}} - Y_{\text{H}_2\text{O}}^*}, \quad S_P = \frac{r_{\text{dry}}^*}{Y_{\text{H}_2\text{O}}^{\text{sat}} - Y_{\text{H}_2\text{O}}^*}, \quad (5.22)$$

$$\text{if } r_{\text{dry}}^* < 0, \text{ set } S_C = 0, \quad S_P = -\frac{r_{\text{dry}}^*}{Y_{\text{H}_2\text{O}}^*}. \quad (5.23)$$



Obviously, for other compounds, a different treatment of source terms must be found. The first possible solution is to multiply the rates by the mass fraction of corresponding solid constituent. For instance, the modified diffusion-limited rate model is given as

$$r_{\text{dry}} = Y_{\text{H}_2\text{O}} k_d A_p (\rho_{\text{H}_2\text{O},\text{surf}} - \rho_{\text{H}_2\text{O},\text{g}}). \quad [\text{kg}/\text{m}^3 \text{ s}] \quad (5.24)$$

The extra term has a stabilizing effect on successive iterations. The method has been applied e.g. to a heat sink drying model in [84]. Although the modification slows down the rate, simulations show, that the overall drying time is close to that of the first-order kinetic rate as will be shown in the chapter 7.

The second variant is to employ a heavy under-relaxation on the source terms. Iterations may start with just a fraction, say a hundredth or a thousandth of the true process rate value, so that the response of other variables to the rate is very limited and the variables do not change much. Through the iterations, the fraction can be gradually, but slightly increased till the under-relaxed rate reaches its true value. Such a relaxation does not comply with the prescription (5.14), so it is important to perform enough iterations to let a source term grow to its unrelaxed value.

## 5.3 Overall solution algorithms

The overall solution algorithms for both models are finally described. The two algorithms differ mainly in the way by which the flow field is obtained. Since the energy equation is solved with respect to enthalpy, temperatures must be recovered using heat capacities and Newton method for a few iterations after energies are solved. The same applies for the boundary condition at the top of the bed, where radiation heat flux is prescribed. Bed top temperature is a solution to the equation (5.7) obtained by Newton iteration method.

### 5.3.1 SIMPLE co-located algorithm

For the two-dimensional bed model, the SIMPLE co-located algorithm is used, e.g. [43, 38]. The term co-located refers to grids, that are not staggered, i.e. all flow variables as well as other scalars are defined and stored in cell centroids contrary to staggered grids, in which velocities are defined at cell centroids of a main grid, however associated with the staggered grid, that is shifted a half the space step of the main grid. This makes the co-located formulation applicable also to unstructured grids without the necessity to store two different sets of indices of grid points.

Velocities and mass fluxes calculated by the SIMPLE co-located strategy are relaxation-dependent, if under-relaxation (5.15) is used. Therefore, momentum equations must not be under-relaxed. However, face velocities obtained later by momentum interpolation scheme in the step 3b can be under-relaxed using (5.14). The solution of momentum equations require proper linearization to stabilize progress through iterations due to the absence of momentum equation relaxation. The algorithm is as follows:

1. Setup grid, calculate coordinates of both cell and face centroids.
2. Initialize solution variables including pressure and velocity fields, coefficients, boundary conditions and source terms. The initial guess is set according to the values of boundary conditions.

3. Start outer iteration loop (SIMPLE).
  - (a) Guess the pressure and velocity field using prevailing values and solve unrelaxed momentum equations (3.19)-(3.20) to obtain velocities  $v_{x,P}^*, v_{y,P}^*$ .
  - (b) Calculate mass fluxes  $F_f^*$  and velocities  $v_{x,f}^*, v_{y,f}^*$  at face centroids using the momentum interpolation scheme.
  - (c) Solve pressure correction equation derived from the continuity equation (3.18) for  $p'$ .
  - (d) Using  $p'$ , correct face mass fluxes at face centroids, face and cell velocities. Use suitable value of the under-relaxation factor.
  - (e) Solve solid continuity equation (3.23) for mass flux as in discretized 1D gas continuity equation (5.5) and calculate solid density.
  - (f) Solve other gas and solid equations (3.21)-(3.22) and (3.24)-(3.25) using the updated flow field.
  - (g) Update boundary conditions, solve (5.7) to obtain the bed top temperatures.
  - (h) Update gas and solid properties, coefficients and source terms using the current values of transported quantities.
  - (i) Check for convergence. If all residuals have dropped below criterial values, stop iterations and go to step 4. Otherwise continue to step 3a.
4. Save solutions and rates and plot results. Additionally, check the steady state mass and energy balance.

### 5.3.2 1D flow algorithm

The flow algorithm for 1D model consists of steps similar to those of the SIMPLE co-located algorithm. This algorithm is simpler in that the flow field is obtained directly from the continuity equation. The algorithm reads:

1. Setup one-dimensional grid, calculate coordinates of cell centeroids.
2. Initialize solution variables including flow field, coefficients, boundary conditions and source terms according to initial conditions.
3. Initialize variables for calculation of mass and energy balance.
4. Start time loop for  $t = 0 \text{ s} \dots t_{\text{end}}$ .
  - (a) Update time level  $t \leftarrow t + \Delta t$ .
  - (b) Set initial values for the current time level.
  - (c) Calculate maximum rates according to (5.20).
  - (d) Start outer iteration loop.
    - i. Solve gas continuity equation (3.1) for mass fluxes  $F_f$  and velocities  $v_p$ .
    - ii. Solve solid continuity equation (3.4) for density.

- iii. Solve other gas and solid equations (3.2)-(3.3) and (3.5)-(3.6) using the most current mass flux.
  - iv. Update boundary conditions, solve (5.7) to obtain the bed top temperature.
  - v. Update gas and solid properties, coefficients and source terms using the current values of transported quantities.
  - vi. Check for convergence. If all residuals have dropped below criterial values, stop iterations and go to step 4e. Otherwise continue to step 4(d)i.
- (e) Update mass and energy balance variables (for details, see 7.2.2).
  - (f) Save solutions from the current time level. If the time  $t < t_{\text{end}}$ , go to step 4a. Otherwise, continue to step 5.
5. Evaluate mass and energy balance and save to a text file.
  6. Save all temporal solutions and plot results.

## 5.4 Summary

Numerical methods and algorithms used for the solution of bed models from the chapter 3 have been described. Besides common discretization techniques, that are generally recommended in literature to obtain a converged solution, some special methods have been introduced to treat nonlinear terms and couplings of the equations. These include process rate limiters based on physical limitations. These limiters are important controlling factors in the mass and energy balance because they ensure, that the same amount of mass released from the fuel is formed in the gas phase. Also, it has been pointed out, that central differencing of the turbulent parts of effective dispersion coefficients slows down the rate of convergence due to the analogy with a convection term. Finally, solution algorithms for both models have been outlined.



# Chapter 6

## Simulation tool with GUI

The governing equations together with all physical relations for equation coefficients from chapters 3, 4 and numerical methods and techniques mentioned in the chapter 5 have been implemented into a computer program, which has been named GRATECAL. It has been developed in the MATLAB system [39], which integrates a high-level programming language for technical computing with graphics and desktop tools into an environment in which it is easy to work intuitively with matrices and numerical algorithms generally.

The module-based computer program is capable to predict the drying, devolatilization and char oxidation as stand-alone combustion stages as well as to run a full batch-type simulation including all processes together. The drying module provides a choice of two different drying models (the first-order kinetic rate model and the diffusion-limited rate model). A graphical user interface (GUI) has also been implemented to make the application user-friendly. The program GRATECAL may serve as a tool for detailed analysis of physical and chemical phenomena, that take place in a packed bed during combustion. It can provide a deep insight into processes occurring inside the bed such as heat-up, drying, devolatilization and char oxidation. Through graphical tools, temperature, concentrations or flow fields can be viewed along the bed height as well as the propagation of reaction fronts.

The following sections describe the simulation tool in detail. First, general comments on the developed simulation tool involving prerequisites to run the application and limitations of codes are given in 6.1. The graphical user interface is presented in 6.2.

### 6.1 General comments on GRATECAL

There are two distinct versions of GRATECAL. One-dimensional transient and two-dimensional steady models are implemented into computer programs GRATECAL 1.3 and GRATECAL 2.0, respectively.

#### 6.1.1 Running GRATECAL 1.3

In order to run the application, MATLAB must be installed on the operating system. All GRATECAL 1.3 source codes are distributed within a single folder `GRATECAL_1.3` in three subfolders as shown in the Figure 6.1.

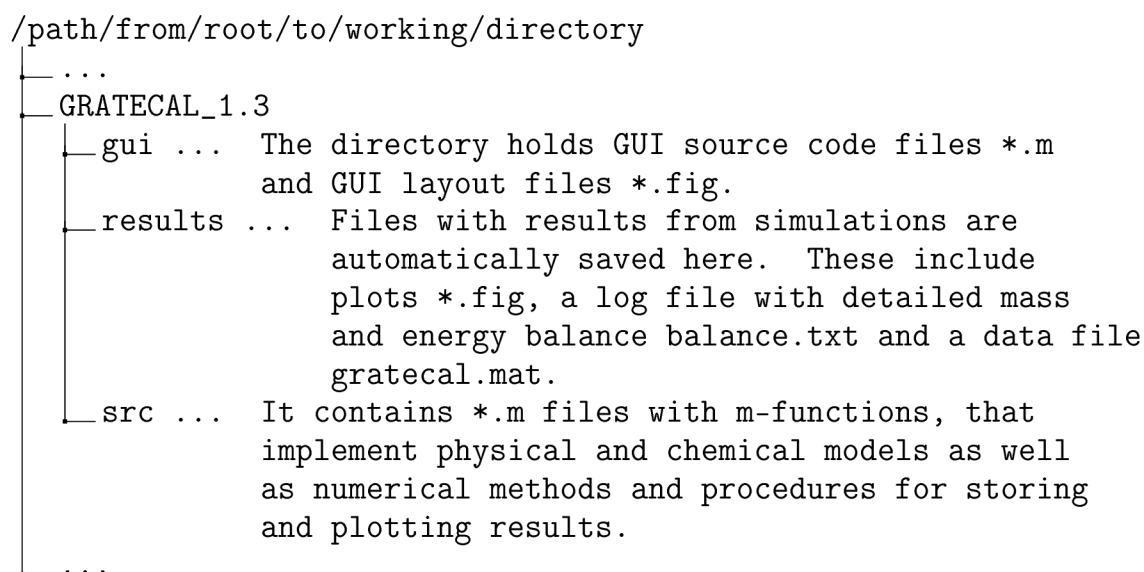


Figure 6.1: Hierarchy of GRATECAL 1.3 directories and source code files.

To execute the application from the MATLAB prompt, enter the following command with full path to the main .m-file:

```
run /path/from/root/to/working/directory/GRATECAL_1.3/gui/gratecal.
```

The application temporarily adds all needed directories to the MATLAB search path, so that this need not be done manually by a user.

### 6.1.2 Limitations

Although a many features are implemented in the resulting source codes, usage of programs is limited to a certain extent mainly due to convergence problems under some conditions. Gas phase reactions often cause troubles in obtaining convergence. Therefore, this module is switched off in all presented simulations and more work has to be done to get a stable and converging iteration process in simulations involving gas phase reactions. The solution to Navier-Stokes equations by co-located scheme is also prone to divergence in many situations. Therefore, 2D model is considered to be still in a stage of development. For these reasons, GUI has not been developed for the 2D version and the parameters can be set only by modifying the source code. GRATECAL 2.0 can be run from MATLAB prompt by `data=@gc2Ddata; gc2D(data);`. Parameters to the simulation of pure isothermal convection through 2D bed are preset such that iterations are slowly convergent (the progress of scaled residuals of pressure and velocity components through iterations is shown on the screen).

## 6.2 Description of grafical user interface

GRATECAL 1.3 is enhanced with a graphical user interface to make setting of model parameters easier. Values of all parameters are predefined for a simulation of wheat straw

combustion under typical experimental conditions. The following sections guide through the GUI and describe features and usage of its components within all windows.

### 6.2.1 Main window

As shown on the Figure 6.2 (left), the main window of the computer program consists of a menu bar and a button to start the simulation. Four child windows for specification of simulation parameters are accessible through the *Define* pull-down menu, see Figure 6.2 (right). These include setting the gas and fuel properties (initial conditions, primary air properties, composition, fuel type, proximate and ultimate analysis of the fuel, etc.), bed and furnace properties (geometry, physical properties of the bed, position of probes such as thermocouples, gas species analyzers, properties of the over-bed radiation heat source, etc.), processes and solver parameters. Whenever either of child windows is launched, it takes control over the application and the main window becomes inactive until the child window is closed. If *Plot*→*Residuals* is selected, scaled residuals of solution variables

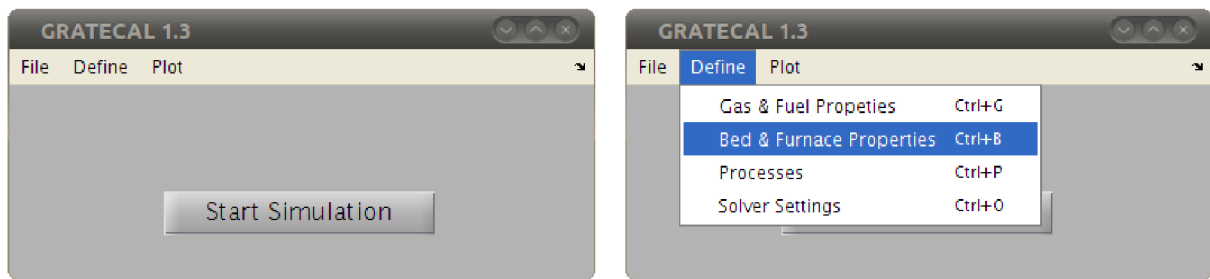


Figure 6.2: Main window of the program GRATECAL.

are plotted after each time step (the option is checked by default). It provides for a visual control of convergence of governing equations for gas and solid energies (denoted as *gasH* and *solidH*, respectively), gas mass flux (denoted as *gasmf*), solid density (*solidDens*) and gas species (denoted by the corresponding chemical formula or name of the specie, e.g. *O2*, *tar*, etc.), see Figure 6.3. The *Results* option from the *Define* pull-down menu is permanently disabled as results from the current version of the program are plotted automatically right after the simulation is completed.

### 6.2.2 Gas & fuel properties

**Gas & fuel properties** child window (Figure 6.4) is logically divided into two panels, each of which contains a number of edit boxes for entering values of gas and fuel properties. While properties of primary combustion air (i.e. the boundary conditions at the inlet) as well as initial conditions of gas within the bed are placed on the left panel, ultimate and proximate analyses and particle properties of fuel selected from the drop-down list can be entered on the right half of the window. Although selection of fuels with predefined typical values of properties is limited to wheat straw only in the current version of the program, the properties may be overwritten with any suitable values, for instance using the *Fuel Type*→*User Specified* option of the drop-down list.

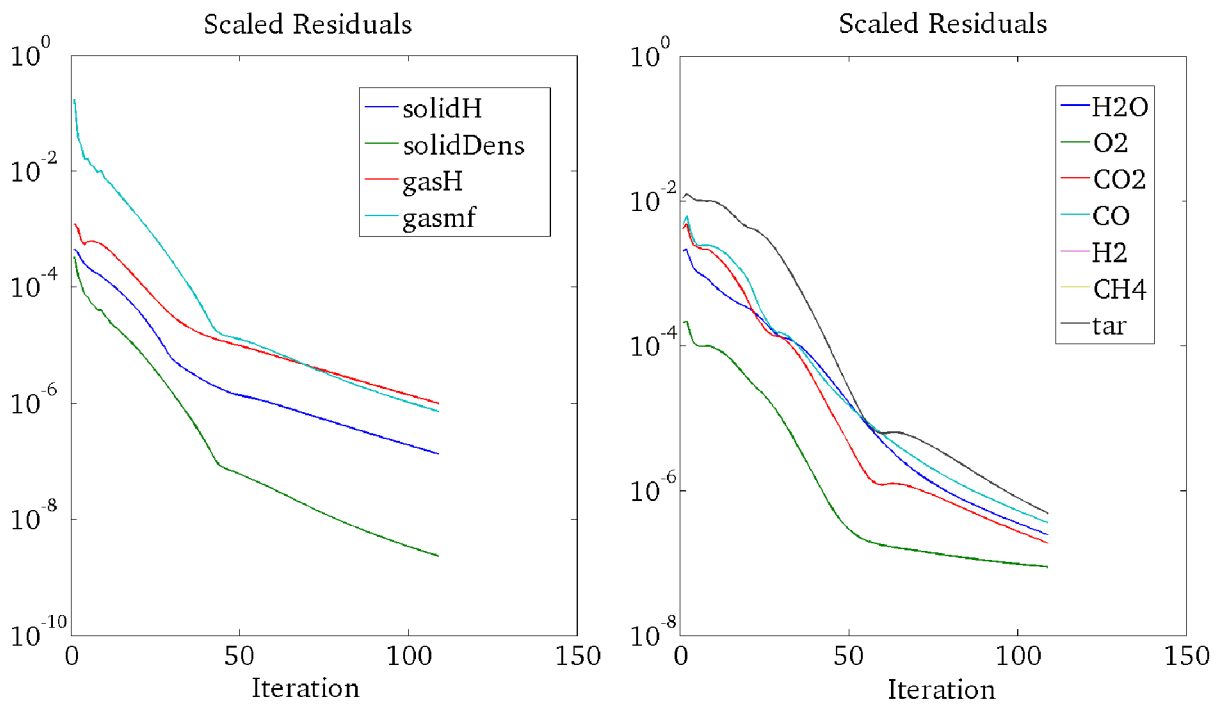


Figure 6.3: Plots of scaled residuals.

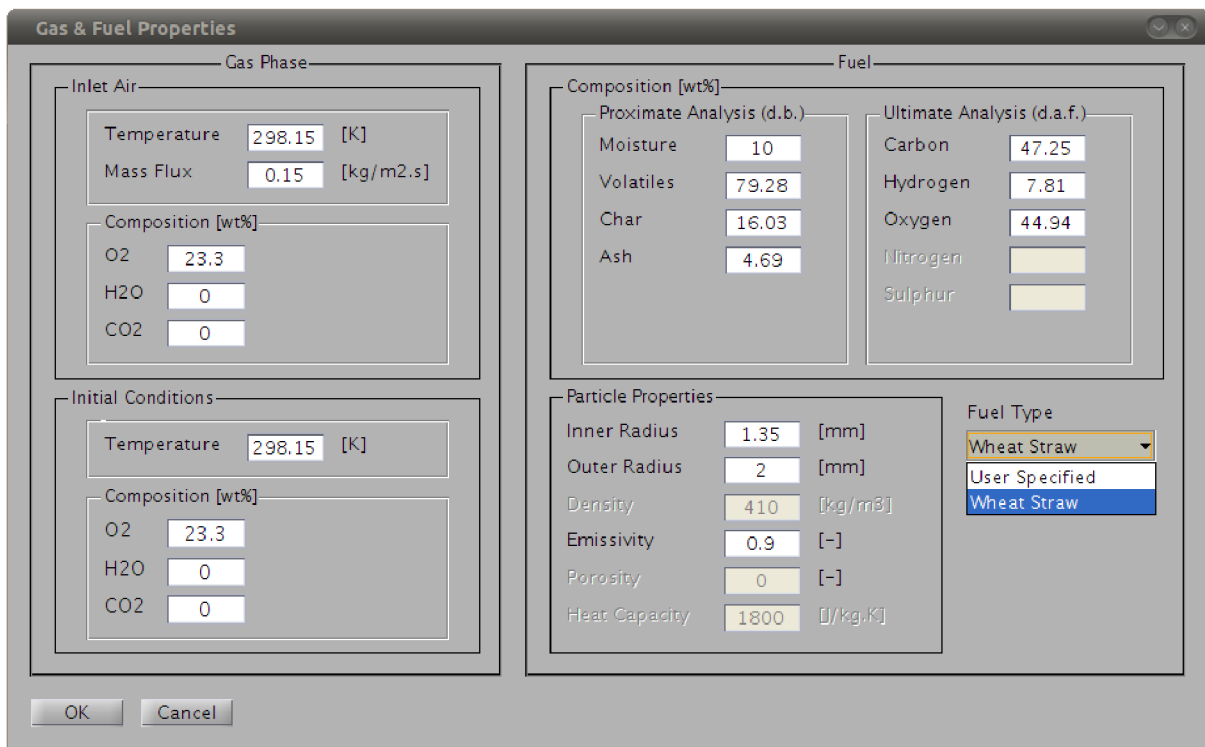


Figure 6.4: Gas & fuel properties child window.



### 6.2.3 Bed & furnace properties

Initial and boundary conditions for the fuel bed and certain properties of the reactor are defined in **Bed & furnace properties** window 6.5. Initial conditions for the bed are defined in terms of temperature and packing conditions, i.e. the fuel layer is described by initial porosity, bulk density and geometric dimensions (bed height and diameter which is defined by and equal to the diameter of the reactor). The boundary condition for the fuel at the top of the bed is given by radiation heat transfer between the bed and the over-bed area. Incident radiation is described by properties of radiation heat source, e.g. a burner or an electric heating device, which is installed in the reactor. A user must provide information on the emissivity and either temperature of the environment in units of [K] or power of the burner [W] by use of radio buttons placed in the Radiation Heat Source panel. Temperature, of course, must be a positive real number. However, if the power is set to 0 W, than the burner is switched off and it is assumed, that no radiation heat transfer takes place at the bed top, thus allowing to simulate a thermally insulated bed. In this case, processes can be initiated by the preheated primary air only. Additionally, the radiation boundary condition may be assumed non-constant throughout the simulation. Especially, if the series of one-dimensional transient solutions represent a real bed on moving grates as described earlier in the section 2.3, the radiation profile can be swithed from Constant to Time-dependent in the Profile drop-down list. The time-dependent profile is defined by a series of temperatures of the environment.

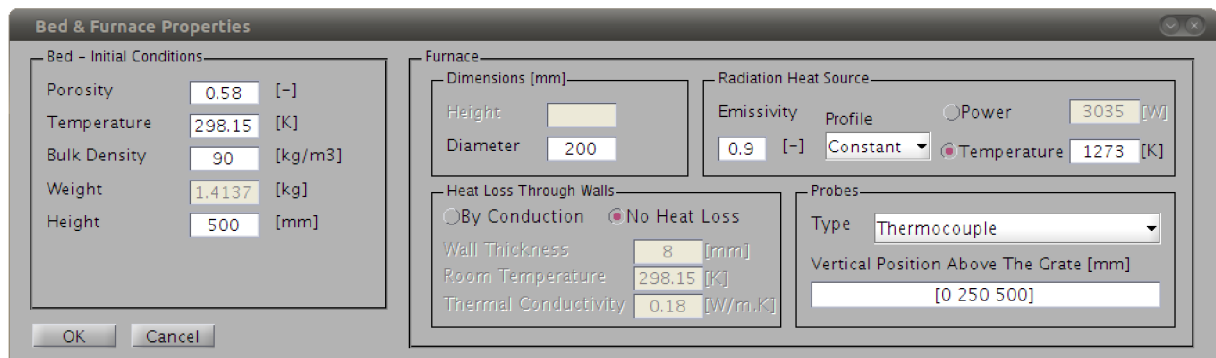


Figure 6.5: Bed & furnace properties child window.

Since an experimental reactor is equipped with various probes such as thermocouples, gas species concentration analysers, weighting scales etc., the used instrumentation can be selected from the drop-down list as it is shown on the Figure 6.6.

The selection of probes determines the kind of data that are recorded during the simulation and hence will be plotted after the simulation finishes. Positions of the probes in the reactor are defined in terms of vertical distances (in [mm]) from the grate as a set of space- or comma-delimited real numbers enclosed in square brackets. Empty brackets are used in case the probe is not installed. The Table 6.1 summarizes plotting options according to the type of the installed probe, where  $\Delta t$  [s] is the time step in temporal discretization. Process rates are plotted along the bed height, when reaction fronts reach the probe positions. The time instants are defined for drying/pyrolysis/char oxidation such that solid temperature  $T_s$  [K] at given positions reaches onset temperatures  $T_{\text{onset}} = 373.15/473.15/633.15$  K, re-

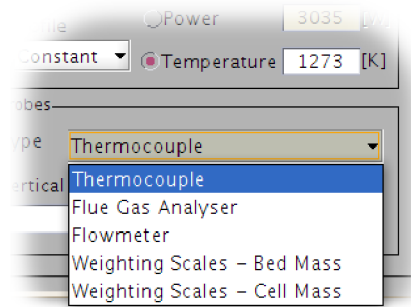


Figure 6.6: A list of probes available for data recording.

spectively. This allows for monitoring the propagation of various reaction fronts. Note that the reaction fronts can be plotted only if the corresponding process rate models are defined in **Processes** window 6.7. Likewise, only concentrations of gas species that are solved by transport governing equations can be displayed in result plots. The Table 6.2 maps various bed model settings to gas species for which the solution of transport governing equations is turned on.

Probe	Data Plots	Recording Time Instances
Thermocouple	Gas and solid temperatures.	$\Delta t_{\text{plot}} = \Delta t \max(1, \lfloor 1/\Delta t \rfloor)$
	Process rate plots along the bed.	First time when $T_s \geq T_{\text{onset}}$
Gas Species Analysers	Concentrations of gas species.	$\Delta t_{\text{plot}} = \Delta t \max(1, \lfloor 1/\Delta t \rfloor)$
Weighting Scales	Total mass of fuel and fuel species	$\Delta t_{\text{plot}} = \Delta t \max(1, \lfloor 1/\Delta t \rfloor)$
- Bed Mass	- above the probe position.	
- Cell Mass	- in the control volume	

Table 6.1: Probe types and corresponding data plots.

Bed Model Settings		Gas Species						
		H <sub>2</sub> O	O <sub>2</sub>	CO <sub>2</sub>	CO	CH <sub>4</sub>	H <sub>2</sub>	C <sub>x</sub> H <sub>y</sub> O <sub>z</sub>
Process Rate Models	None (Heat-up only)							
	Drying	✓						
	Pyrolysis			✓	✓	✓	✓	✓
	Char Oxidation		✓	✓	✓			
	Gas Phase Reactions	✓	✓	✓	✓	✓	✓	✓
Initial/Boundary Conditions [kg/kg]	Y <sub>O<sub>2</sub></sub> > 0		✓					
	Y <sub>H<sub>2</sub>O</sub> > 0	✓						
	Y <sub>CO<sub>2</sub></sub> > 0			✓				

Table 6.2: Sets of gas species transport equations to be solved according to specific settings of bed model parameters.

### 6.2.4 Processes

Although the computer program GRATECAL 1.3 is designated for a simulation of fixed-bed combustion, it may also be used for study of particular processes individually. Processes of interest can be included in the simulation by clicking on radio buttons in the Include panel of **Processes** window (Figure 6.7). Any combination of processes is allowed. Simulation of non-reactive fluid flow through a porous layer with interphase heat transfer is achieved by disabling all processes. For the simulation of drying, two different models become available, namely the first-order kinetic rate model with modified Arrhenius approach (see the equation (3.9), [41]), and a diffusion-limited rate model (2.3), when the drying process is selected. Since it is assumed that pyrolysis can be described by a one-step global Arrhenius-type reaction scheme, activation energy and preexponential factor are required as well as mass fractions of final pyrolysis yields. The rate of pyrolysis can be adjusted by means of activation energy and preexponential factor contrary to char and gas phase combustion reactions, which are described by equations (3.14)-(3.17) and no such options are available in order to keep settings of models as simple as possible.

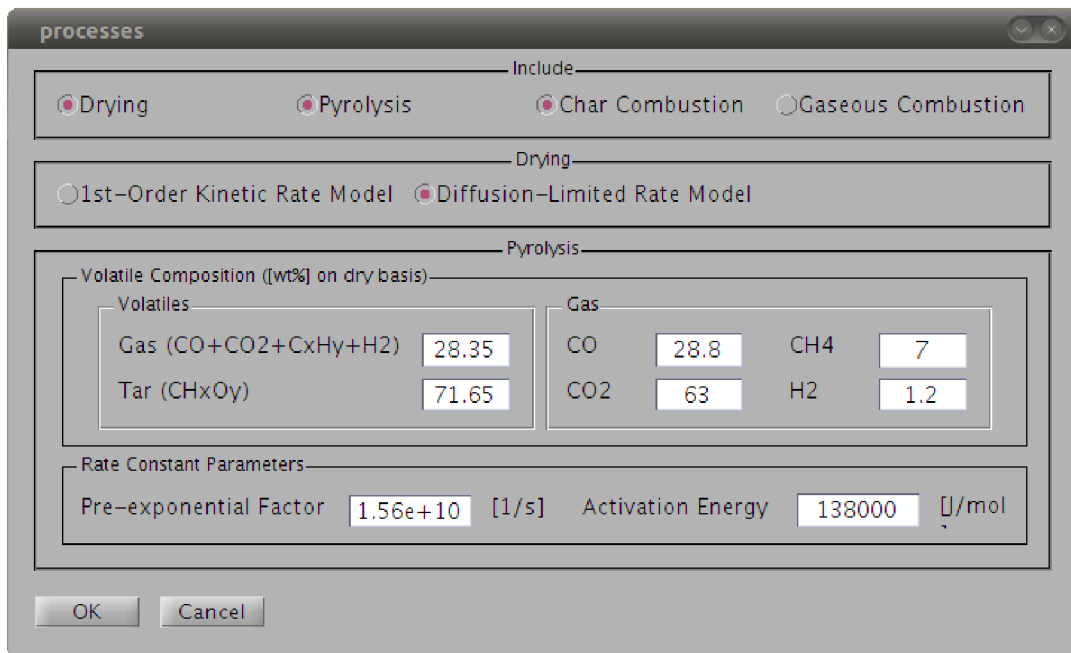


Figure 6.7: Processes child window provides for selection of combustion sub-models to be included in the simulation.

### 6.2.5 Solver settings

Information on temporal and spatial discretization, discretization schemes and computational algorithms and parameters for controlling the convergence are entered in **Solver settings** window (Figure 6.8). The computational domain can be extended to the over-bed region by introducing a number of control volumes above the top of the bed in the corresponding edit box. If Adaptive Time Stepping is enabled, the value in the Time step edit box represents the largest allowed length of time step and the value in the Max. No.

Of Iterations edit box is the maximum number of iterations permitted in a time step before it is reduced.

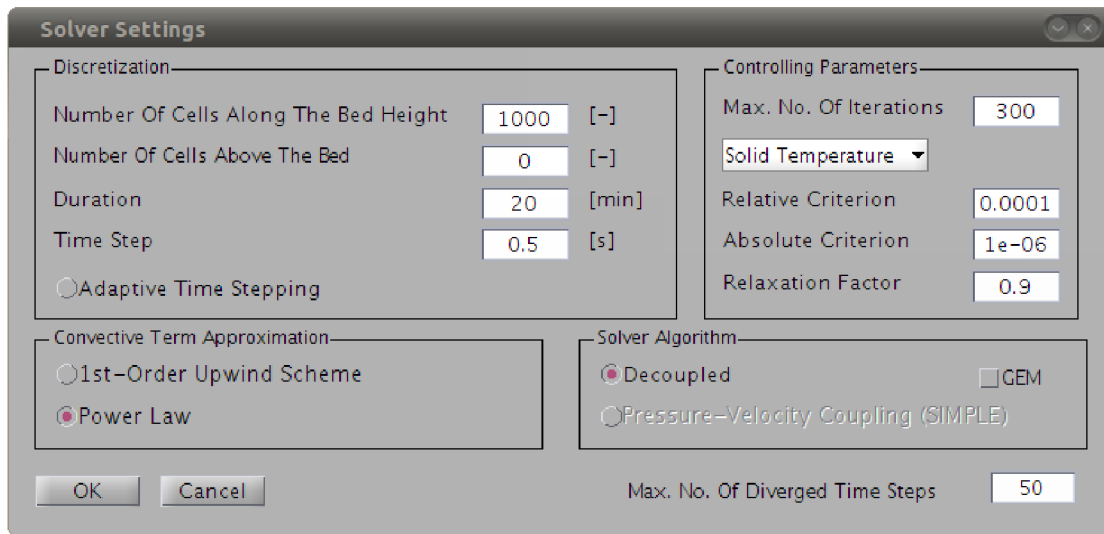


Figure 6.8: Solver settings child window.

For the convective term approximation, two discretization schemes are available. Although both are only first-order accurate, the power law scheme exhibits better accuracy in terms of mass and energy balance as it is discussed further in the chapter 7.

The current version of the computer program supports only the so called decoupled solver algorithm, which solves governing equations in a decoupled manner, i.e. sequentially one by one. The coupling of equations is resolved by performing a number of iterations. The maximum number of iterations per time step can be set in the Max. No. Of Iterations edit box under the Controlling Parameters panel. In addition, Gaussian elimination method can be used instead of the default Gauss-Seidel iterative method to solve the system of algebraic equations resulting from the discretization by checking GEM option under the Solver Algorithm panel.

Other controlling parameters include relaxation factors and convergence criteria, which must be set for each solution variable from the drop-down list, see the Figure 6.9. However, time solutions may be accepted irrespective of whether the convergence criteria during certain time steps are met after performing the maximum number of iterations. This can be controlled by the number of time steps, for which the solution does not fully converge. The number is specified in the Max. No. Of Diverged Time Steps edit box.

### 6.3 Summary

The 1D model of packed bed combustion and numerical methods for its solution have been implemented in a simulation tool GRATECAL 1.3. It has been developed in MATLAB environment and enhanced with a graphical user interface, through which setting of a large set of parameters needed for a CFD simulation of in-bed processes is made easier. Since the computer program is structured such that various physical models are implemented as standalone modules, it is possible to study particular processes such as heat-up, drying,

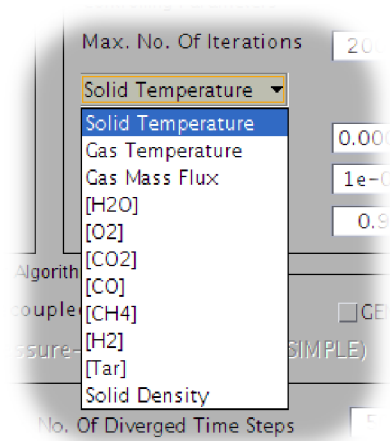


Figure 6.9: A list of solution variables, for which relaxation factors and convergence criteria must be set.

pyrolysis and char combustion independently as well as to run a complete simulation of combustion at once or any desired combination of processes.

The simulation tool provides for plotting results according to a selection of probes installed in the reactor (i.e. defined in the model). All parts of the GUI have been described in detail.



# Chapter 7

## Analysis of some specific modelling issues

The in-house computer program GRATECAL 1.3 may serve as a tool for analysis of physical and chemical processes taking place in a bed of an experimental reactor during combustion or its individual stages. The level of detail of information, that can be provided by a simulation is primarily determined by the type of the model, i.e. macroscale homogeneous model. It means that the model cannot simulate processes within an individual fuel particle, nor it can properly handle motion of particles within the bed due to bed volume reduction or mixing. For these details, one would have to develop a model from the class of particle-resolved macroscale models as described in 2.1.

However, a lot of other issues including propagation of reaction fronts, fuel mass loss rate, burn rates as well as distribution of temperatures and species concentrations can be studied by the present model. This chapter is devoted to results obtained from simulations conducted in order to analyse some specific modelling issues. These are divided into two groups - physical issues and numerical ones. In the absence of experimental work due to unavailability of a testing rig, the results were interpreted by physical reasoning and, where possible, qualitatively compared to those of other researchers.

From these results, recommendations are given regarding mainly the effectivity of simulations and quality of numerical results. The section 7.2 presents an original method for checking the conservativeness of a numerical model by means of additional mass and energy balance calculation. The method is applied to several case studies to demonstrate its capabilities. Finally, a parametric study of effects of convergence criteria on the mass and energy balance of the system is carried out and new findings are summarized.

Wheat straw has been used as a fuel common to all simulations. Chemical composition of the fuel as used in all cases is given in the Table 4.1. Other relevant parameters of simulations are mentioned in corresponding sections.

### 7.1 Physical issues

Two simulation cases are introduced. Both studies are devoted to analysis of propagation of reaction fronts. First one concerns drying stage, while the other one combustion of char.

### 7.1.1 Effects of drying models

In order to compare the available types of drying models, two models adopted from the literature are used to compute the drying rate, namely the first-order kinetic rate model (3.9), and the modified diffusion-limited rate model (5.24). Since a batch-type simulation of drying is considered, the propagation of the drying front can be observed in the fuel bed until all moisture contained in the fuel is evaporated. Steady state is reached after a certain period depending on the temperature and velocity of the primary air. Cut straw has been used as the fuel and its properties were taken from [91]. Computational conditions are listed in the Table 7.1. Figure 7.1 shows propagation of the drying front along the fuel

Property	Value
Biomass fuel [-]	Wheat straw
Bed height [m]	1
Bed diameter [m]	0.154
Primary air-flow rate [ $\text{kg}/\text{m}^2 \text{s}$ ]	0.18
Primary air temperature [K]	373.15
Initial (ambient) temperature [K]	293.15
Initial moisture in fuel [wt%] (dry basis)	10
Bed porosity [-]	0.6
Particle emissivity [-]	0.9
Particle diameter [mm]	1.4
Time step [s]	0.02
Space step [m]	0.001

Table 7.1: Computational conditions in simulations of moisture evaporation from wheat straw.

bed. It can be seen that both models predict almost identical propagation rates. Thus the steady state is reached after the same time as may be easily seen in Figure 7.2, which shows total mass of solid as a function of time. However, the drying fronts of the two models are different in terms of both intensity and thickness. While the first-order kinetic rate model predicts non-zero drying rate values wherever solids contain any moisture, the diffusion-limited model significantly bounds the zone to much thinner domain. Also maxima of the drying rates differ by one order of magnitude.

### 7.1.2 Effects of variable porosity

It has been concluded from both experimental and theoretical studies that the local bed porosity has impact on ignition and burning rates (e.g. [53, 81, 91]). Nevertheless, inconsistencies can be found in the literature concerning combustion of wheat straw. The volume reduction was neglected in [91], while a local volume shrinkage was assumed in [79]. Furthermore, the effect of bed porosity on ignition flame front rate was shown to be significant in [91]. However, neither the bed height decrease nor bed porosity change were taken into account in the mathematical model. The effects of particle size as well as bed porosity on combustion of wheat straw are investigated through a series of numerical simulations.



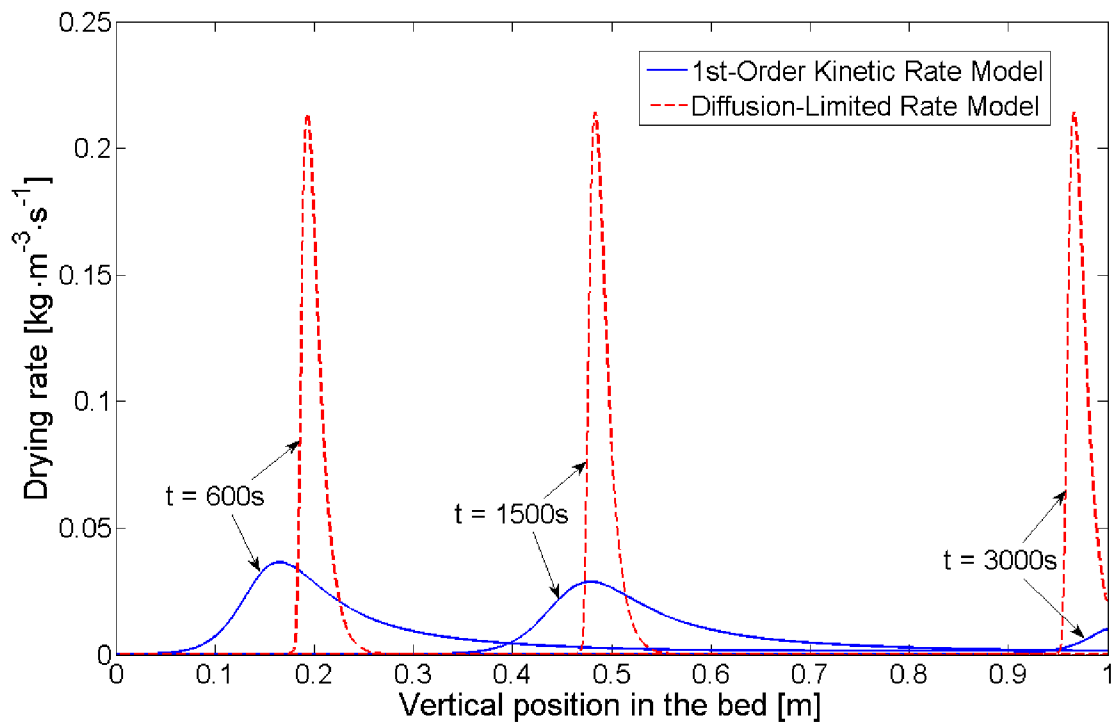


Figure 7.1: Propagation of drying front as predicted by the first-order kinetic rate model and modified diffusion-limited rate model.

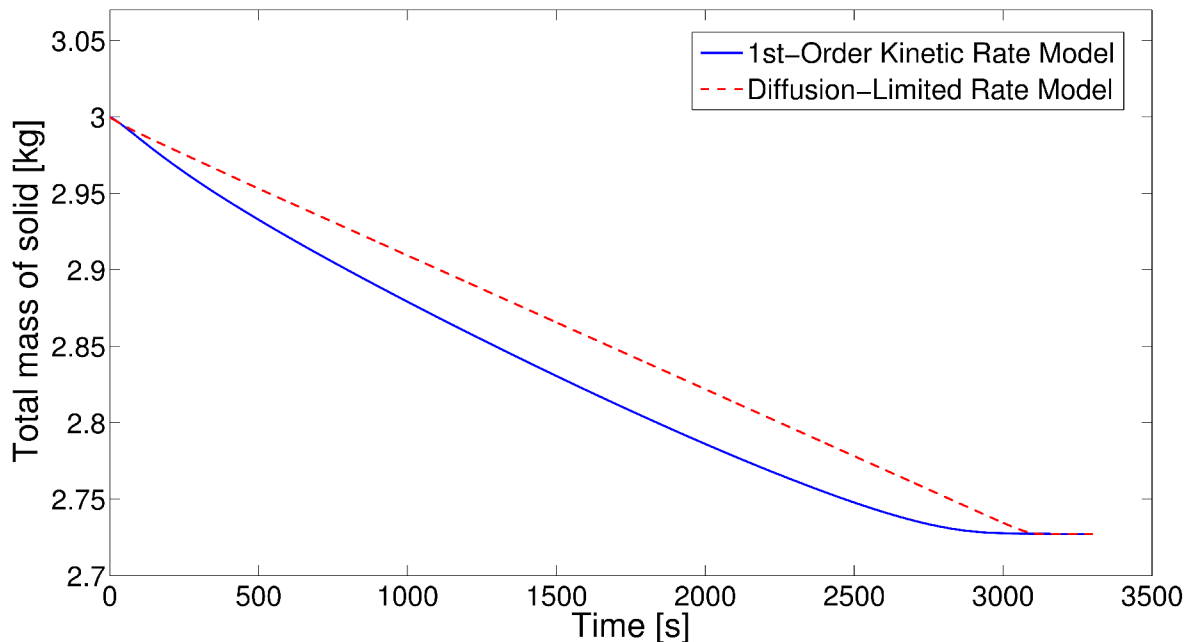


Figure 7.2: Solid mass loss curves as predicted by the first-order kinetic rate model and modified diffusion-limited rate model.

In order to assess the approach for modelling the change of bed porosity and particle size during wheat straw combustion, several simulations have been performed, three of

which are discussed in more detail in this section. Initial and operating conditions of these simulations are the same for each case and are listed in the Table 7.2. The difference between simulations is in the initial size of a solid particle and whether the change of bed porosity was taken into account or not. Discussion of results from simulations is based on physical reasoning and qualitative comparison to both theoretical and experimental results of other authors. The effects of porosity on burning rate with respect to the primary air

Property	Value
Bed height [m]	0.5
Bed diameter [m]	0.2
Primary air-flow rate [kg/m <sup>2</sup> s]	0.1
Primary air temperature [K]	298.15
Initial (ambient) temperature [K]	298.15
Initial moisture in fuel [wt%] (dry basis)	10
Initial volatile matter in fuel [wt%] (dry basis)	79.28
Initial char in fuel [wt%] (dry basis)	16.03
Initial ash in fuel [wt%] (dry basis)	4.69
Initial bed porosity [-]	0.58
Shrinkage factors for individual processes [-]	0-drying, 1-else
Particle diameter [mm]	4 or 20

Table 7.2: Initial and operating conditions in simulations with constant- and variable-porosity models.

flow rate were studied in [81]. At low air flow rates (around 0.1 kg/m<sup>2</sup> s), the burning rate decreases as the bed porosity increases. A similar trend was obtained from the model of van der Lans et al. [67]. As for the particle size, larger fuel particles cause lower burning rates, thicker reaction zone and higher bed temperatures. Figure 7.3 illustrates propagation of char combustion reaction fronts for a case of particles of the same initial size ( $d_p = 4$  mm) as calculated during simulations with constant porosity (solid line) and variable porosity (dash-dotted line).

It is important to note that burning rate is different to char combustion reaction rate. Burning rate is defined as mass of solid fuel that is converted into gas phase per unit time and unit area [68]. However, mass loss is proportional to the sum of reaction rates. Since drying and devolatilization fronts pass a certain position in the bed before the char combustion reaction front, the propagation of char combustion reaction front can be used as an indicator of the burning rate. It can be seen from the Figure 7.3, that the reaction front as predicted by the model with variable bed porosity moves downward the bed with lower velocity than the reaction front in case of the constant porosity model. This corresponds with the aforementioned results of other authors, because the bed porosity increases during straw combustion. The value of the char combustion reaction rate predicted by the variable-porosity model is lower than the value obtained by the constant-porosity model, because volumetric surface of particles decreases with increasing porosity. Figure 7.4 shows propagation of reaction front in the bed of particles with  $d_p = 20$  mm. The variable-porosity model has been used. The reaction front travels down with considerably lower speed than in the bed of 4-mm particles. A thicker reaction zone can be seen as well. This corresponds well with experimental results ([80, 81]). However, a thicker reaction zone can also be

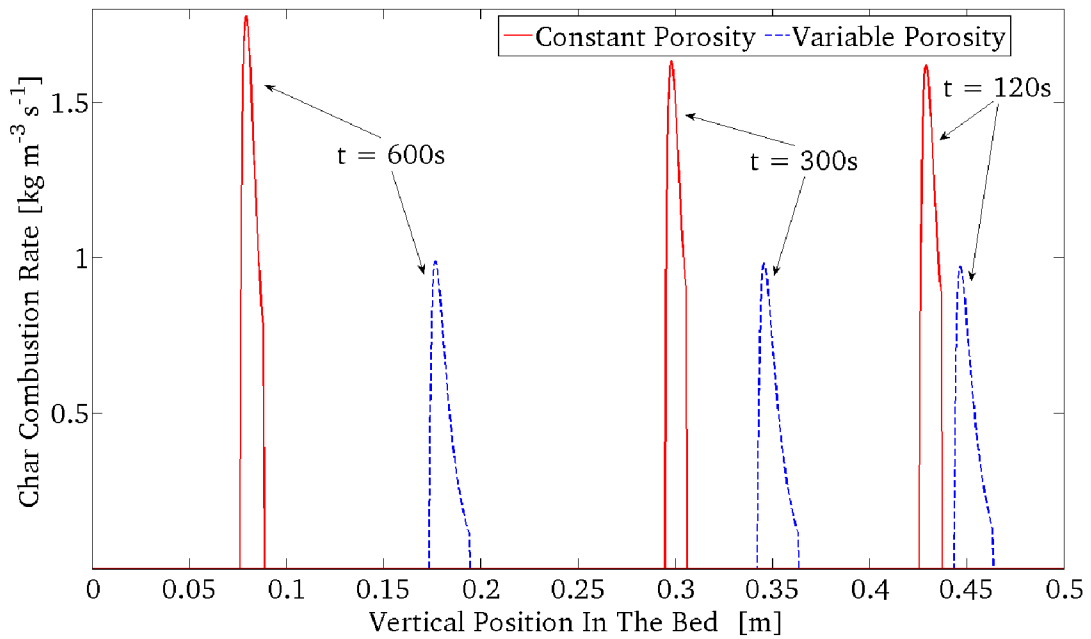


Figure 7.3: Comparison of propagation of char combustion reaction fronts as predicted by constant- and variable-porosity models.

seen in the case of 4-mm particles for the variable-porosity compared to the reaction zone from the simulation with the constant-porosity model (Figure 7.3). This unexpected behavior can be caused by low volumetric surface of particles, which in turn has impact on the interphase heat transfer. Fuel particles shrink during the combustion, but in fact the effect is the same as in case of large particles, which is in contradiction.

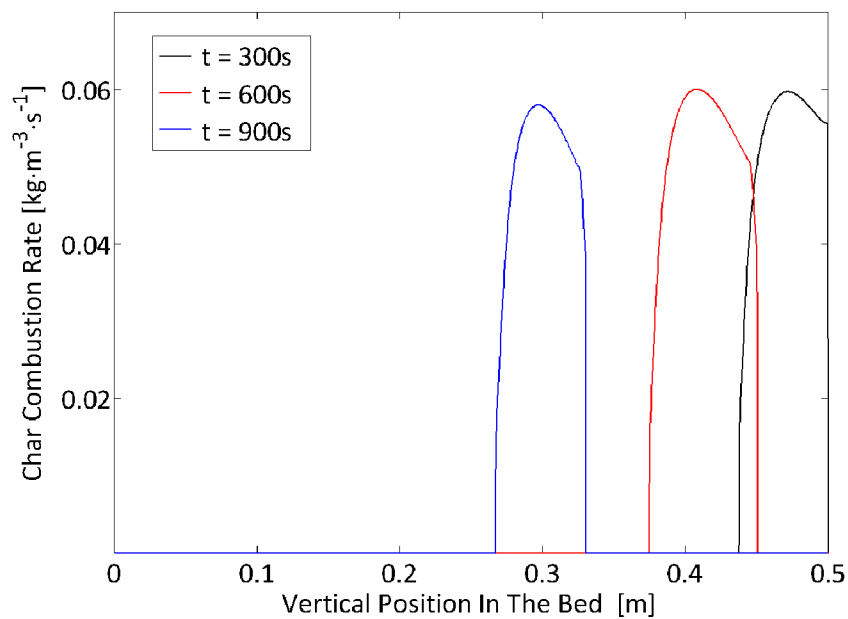


Figure 7.4: Propagation of char combustion reaction front as predicted by the variable-porosity model for 20-mm particles.

Bed porosity and particle size belong to a set of packing conditions parameters, which have impact on heat and mass transfer, propagation and thickness of reaction front in the bed. Propagation of char combustion reaction fronts during wheat straw combustion have been compared for two cases – a constant-porosity bed model and variable-porosity bed model. Results from simulations qualitatively match experimental and theoretical results of other researchers to a certain extent, i.e. at low primary air flow rates, the burning rate decreases with increasing porosity. However, the variable-porosity model produced larger reaction zone than the constant-porosity model, which is in contradiction with the fact that volume of particles shrinks. To remedy this effect, internal particle porosity should be considered.

## 7.2 Numerical issues

Numerical methods and algorithms affect both stability of the solution procedure and accuracy of results. Since a bed model is expected to provide a quality input data for the freeboard CFD model, developed 1D transient bed model has been extended and used to check the conservativeness of the bed model and analyse the effect of some basic solver parameters on simulation results. Presented results have, to the author's knowledge, not been published and, therefore, contribute to the understanding of numerical modelling of fixed-bed combustion.

First, sources of errors in numerical simulations are summarized in 7.2.1. The analysis is based on a balance method, which is described together with the implementation in 7.2.2. Results from the analysis are presented in 7.2.4.

### 7.2.1 Sources of errors in numerical simulations

Combustion in packed beds has already been studied by many authors both experimentally and theoretically by means of detailed numerical models (e.g. [49, 67, 72]). In general, good agreement of experimental data with results from simulations has been reported in all works. Eventual deviations of measurements from calculated values of certain quantities such as peak bed temperature, CO-to-CO<sub>2</sub> production ratio and process rates have mostly been attributed to either degree of precision of measurements or simplifying assumptions made upon mathematical models.

Beside these two common errors, other errors also contribute more or less to overall inaccuracy of numerical predictions - discretization and truncation errors, round-off errors, errors due to instability of an algorithm and human mistakes. Although CFD models (including bed models) are based on physical conservation laws, the physical quantities are not precisely conserved because of aforementioned errors [12]. Therefore, it is important to limit or avoid these errors. For instance, higher-order discretization schemes tend to approach the exact solution faster than schemes of a lower order as the mesh is refined. Shifting from single precision to double precision calculation improves the accuracy of calculations. However, an inappropriate algorithm or implementation may cause large round-off errors, that lead to very inaccurate results even if a double-precision solver is used. Human mistakes (e.g. errors in a computer code implementation) must, of course, be completely eliminated.

## 7.2.2 Balance-based control method

Relative significance and effects of errors on results from simulations of packed-bed combustion can be examined by the numerical bed model, if appropriate tool is employed. It is crucial to ensure the bed model is conservative, i.e. both gas and solid phase contain correct amount of mass and energy, so that the mass and energy balances over the system is satisfied. Therefore, a balance-based control method has been proposed and implemented to check the conservativeness of the 1D transient bed model.

A balance equation for a conserved quantity  $\phi$  in a control volume can generally be written as

$$\phi^f - \phi^i + \phi^{\text{out}} - \phi^{\text{in}} = 0. \quad (7.1)$$

where superscripts  $i$  and  $f$  denote initial and final conditions and terms  $\phi^{\text{in}}$ ,  $\phi^{\text{out}}$  the amounts of the quantity  $\phi$  flowing into and out of the control volume, respectively. While initial conditions are given explicitly, the terms  $\phi^{\text{in}}$ ,  $\phi^{\text{out}}$  are usually unknown functions of time and therefore must be calculated at the end of each time step. For the gas phase,  $\phi^{\text{in}}$ ,  $\phi^{\text{out}}$  are given by convective fluxes at the inlet and outlet boundaries, respectively. Diffusion is set to zero at both boundaries (at the primary air inlet the convection is dominant transport mechanism based on the Peclet number [46]). On the other hand, since a batch-type simulation is considered and thus no additional fuel is fed to the reactor during the process, only radiative heat flux must be calculated for the solid phase at the top of the bed. Homogenous (zero) Neumann boundary condition is assumed at the grate.

The equation (7.1) is not satisfied exactly due to various errors mentioned before. Therefore, a residual  $R_{\text{bal}}$  of the balance equation and the relative imbalance  $I_r$  are defined as

$$R_{\text{bal}} = \phi^f - \phi^i + \phi^{\text{out}} - \phi^{\text{in}}, \quad (7.2)$$

$$I_r = \frac{|R_{\text{bal}}|}{\phi^i + \phi^{\text{in}}}. \quad (7.3)$$

Let the bulk volume of the packed bed be the control volume. Then mass and energy balance equations can be derived from the equation (7.1) for arbitrary time interval. Initial and final mass contents of the bed are given by mass of the fuel and gas occupying voids of the bed:

$$m^f - m^i = (m_s^f + m_g^f) - (m_s^i + m_g^i). \quad [\text{kg}] \quad (7.4)$$

In a batch mode of combustion, mass flowing into and out of the packed bed is determined from primary combustion air and flue gas leaving the bed:

$$m^{\text{out}} - m^{\text{in}} = A_r \int_{\Delta t} (\epsilon_b^{\text{out}} \rho_g^{\text{out}} v_g^{\text{out}} - \epsilon_b^{\text{in}} \rho_g^{\text{in}} v_g^{\text{in}}) dt, \quad [\text{kg}] \quad (7.5)$$

where  $m_{g(s)}$  is mass of gas (solid) phase [kg],  $\epsilon_b$  is porosity of the bed [-],  $\rho_g$  is gas phase density [kg/m<sup>3</sup>],  $v_g$  is interstitial velocity of gas [m/s],  $A_r$  is the cross-sectional area of the reactor [m<sup>2</sup>] and  $t$  is time [s]. Mass balance over the packed bed is obtained by summing up the equations (7.4) and (7.5).

Energy balance equation is given by a sum of analogous equations, which take into account the lower heating value (LHV) and sensible heat of both fuel and gas. In addition, energy transmitted by radiation between the top of the bed and over-bed environment must be included in the balance as well. So the energy balance over the packed bed reads:

$$E^f - E^i = m_s^f \left( LHV_s^f + \int_{T_{ref}}^{T_s^f} c_{p,s} dT_s \right) + m_g^f \left( LHV_g^f + \int_{T_{ref}}^{T_g^f} c_{p,g} dT_g \right) - m_s^i \left( LHV_s^i + \int_{T_{ref}}^{T_s^i} c_{p,s} dT_s \right) - m_g^i \left( LHV_g^i + \int_{T_{ref}}^{T_g^i} c_{p,g} dT_g \right). \quad [J] \quad (7.6)$$

$$E^{out} - E^{in} = m_g^{out} \left( LHV_g^{out} + \int_{T_{ref}}^{T_g^{out}} c_{p,g} dT_g \right) - m_g^{in} \left( LHV_g^{in} - \int_{T_{ref}}^{T_g^{in}} c_{p,g} dT_g \right) - \int_{\Delta t} A_r \epsilon_r \sigma (T_{env}^4 - T_s^4) dt. \quad [J] \quad (7.7)$$

where the quantities have the following physical meanings and units:  $c_{p,s(g)}$  is constant-pressure specific heat capacity of the solid (gas) phase [J/kgK],  $LHV_{g(s)}$  is lower heating value of gas (solid) [J/kg],  $\epsilon_r$  is emissivity of the radiation heat source [-],  $\sigma$  is Stefan-Boltzman constant [ $W/m^2K^4$ ],  $T$  is temperature [K] ( $T_{env}$  is temperature of environment, i.e. radiation heat source temperature).

The equations (7.4)-(7.7) have been implemented in a discrete form as a subroutine `mass_en_balance.m` of the computer code `GRATECAL1D`. The algorithm of mass and energy balance evaluation is divided into three steps, which are shown on Figure 7.5 and described in detail in the following text:

1. **Initialization.** Initial mass and energy content of fuel and gas in the reactor must be determined prior to the simulation. LHV of the fuel is calculated from HHV, which is usually correlated with elemental composition and proximate analysis of the fuel. In this work, equations (4.2)-(4.3) are used to determine HHV and LHV of the fuel. LHV of gas species must be determined prior to the simulation as well, because a large proportion of the volatile volume leaves the bed due to incomplete combustion as unburnt gas species in flue gas carrying away certain amount of chemical energy.
2. **Time-loop assignments.** At the end of each time step, mass and heat entering and leaving the fuel bed are calculated. Also, unscaled residuals of discretized mass and energy transport equations as defined by (5.9) and (5.12) are stored. The sum of the residuals over simulated time will give total mass and energy residuals as an estimate of the upper bound of the overall error.
3. **Conservativeness check.** When the simulation is finished, mass and energy content of gas and fuel left in the reactor is computed. Overall mass and energy imbalances are evaluated and compared to values of total residuals of discretized mass and energy transport equations as a measure of imperfect conservation. If either of imbalances is not covered by the corresponding total residual, then the bed model does not conserve the physical quantity and contains an error.

All terms in equations (7.4)-(7.7) as well as quantities  $R_{bal}$ ,  $I_r$  and unscaled residuals  $R_u$  are recorded in a log file at the end of a simulation to allow for analysis of various errors.

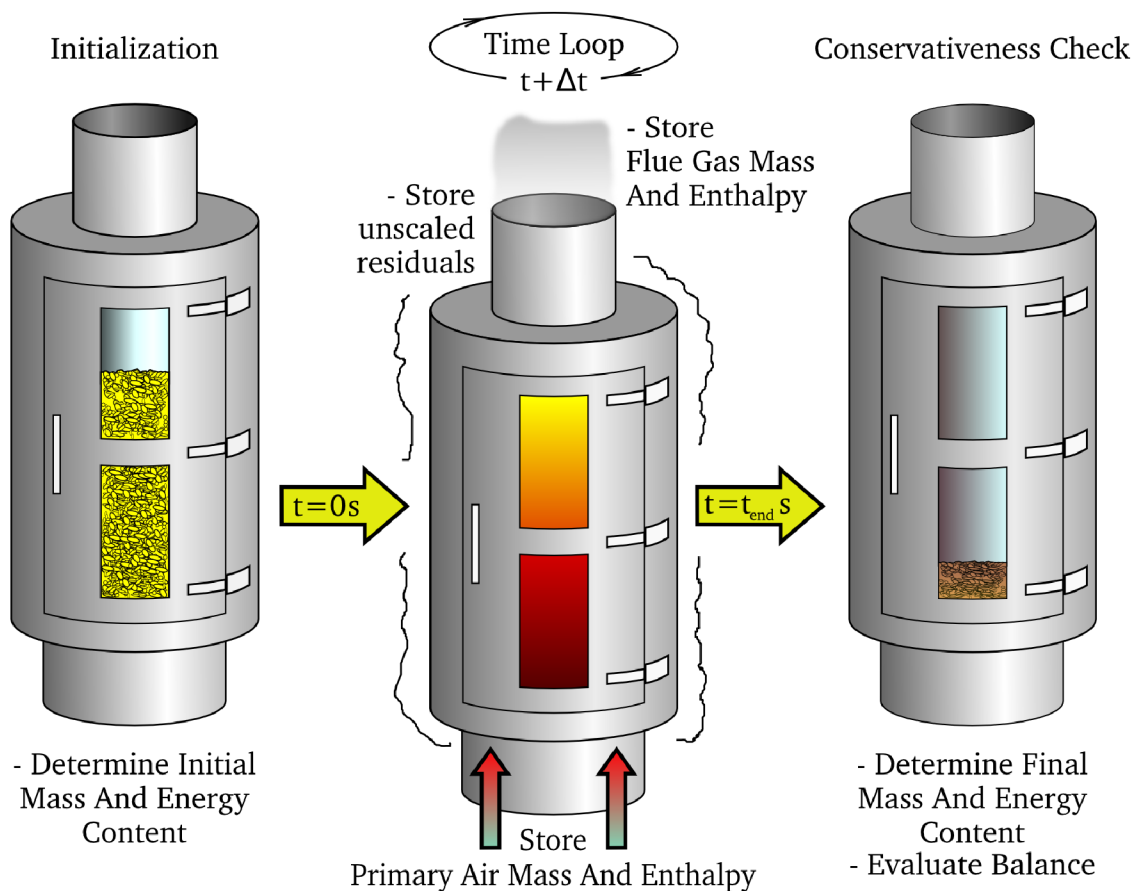


Figure 7.5: The algorithm of verification of a bed model conservativeness.

The correctness of implementation of the initialization step has been checked by a simple spreadsheet calculation using Microsoft<sup>®</sup> Excel software to ensure that the code itself does not contain any errors.

### 7.2.3 Test studies

The balance-based control method has been used to verify correctness of the GRATECAL 1.3 code implementation in two test studies. Conditions common to all cases are listed in the table 7.3.

Fuel	Bed porosity	Bed height	Initial fuel mass	Primary air mass flux	Number of grid cells
Wheat straw	0.58	0.5 m	1.4 kg	0.1 kg/m <sup>2</sup> s	250

Table 7.3: Values of parameters common to all test studies.

#### Pure convection test

Gas within the bed is preheated to temperature 398 K, while the primary air temperature is 298 K. The radiation heat source is turned off and the coefficient of convective heat

transfer between gas and solid phases is set to zero. The fuel is dry thus no interphase mass transfer takes place either (temperatures are too low to initiate pyrolysis) and heat transfer is also switched off, so the solid temperature keeps constant through the simulation. The preheated gas is gradually purged by colder primary air, so that the sensible heat of gas leaving the bed is finally equal to initial energy content of the gas phase. Only a negligible energy imbalance is observed after 2 minutes of simulated time and it corresponds with the order of convergence error ( $R_{\text{bal}} = 7.31 \text{ J}$ ,  $I_r = 0.000031\%$ ,  $R_u = 7.30 \text{ J}$ ). Note that using power-law scheme for convection terms instead of 1st-order upwind scheme results in slightly reduced errors ( $R_{\text{bal}} = 5.41 \text{ J}$ ,  $I_r = 0.000023\%$ ,  $R_u = 5.40 \text{ J}$ ). Both schemes are 1st-order accurate, however the upwind scheme overestimates diffusion in case of dominant convection (here,  $Pe \approx 10$ ), which could explain worse accuracy [46].

### Pure drying test

The primary air is preheated to temperature 398 K, while the initial temperature for gas and solid phase is 298 K. The radiation heat source is turned off. Simulation shows under these conditions, that the fuel bed is dried up in approximately 1160 s. This test revealed an error in definition of source terms in the gas species transport equation as published in [91]. According to [91], the source term is defined as  $\epsilon_b r_i$ , where  $\epsilon_b$  is bed porosity and  $r_i$  is the rate of production/consumption of species  $i$ . The mass balance shows that the mass loss of moisture in solid phase is  $\epsilon_b$  times faster than production of water vapour in the gas phase. Mass imbalance is computed as  $R_{\text{bal}} = -0.053223 \text{ kg}$ ,  $I_r = 1.024624\%$  and the sum of unscaled residuals of gas species is  $R_u = 0.002662 \text{ kg}$ . (This error is also reflected in the energy balance.) If the source term is replaced by  $r_i$ , correct amount of mass of water vapour in gas phase is calculated ( $R_{\text{bal}} = 0.00125 \text{ kg}$ ,  $I_r = 0.02406\%$ ,  $R_u = 0.003111 \text{ kg}$ ). Note that the model presented in the chapter 3 is already reconciled, because the source term  $\epsilon_b \sum_j r_{i,j}$  represents only mass that is formed or consumed in homogenous reactions, whereas  $r_i$  comes from either drying, devolatilization or char oxidation reaction.

### 7.2.4 Effects of convergence criteria

The balance-based method has been used to analyse effects of convergence criteria on mass and energy imbalance of the modelled system. Such an investigation is motivated by the fact, that the system of governing equations is solved by an iterative procedure and iterations are continued until convergence criteria are met. However, whenever a process is stopped not reaching its limiting value, a truncation error is introduced, so the incomplete convergence generates mass and energy imbalance in the system. This effect becomes more important in unsteady simulations, in which truncation errors cumulate at the end of each time step. Another reason to carry out this kind of parametric study is to determine a *sufficiently small value* of the relative error for judging the convergence, which, otherwise, is not specified in literature on general iterative numerical methods and depends on the nature of the solved problem.

The effect of convergence criteria on mass and energy balances is studied through a series of simulations of heat-up and pyrolysis as essential stages of combustion of dry wheat straw in an experimental fixed-bed reactor. Since combustible volatiles are released during pyrolysis, even a small mass imbalance in the system can lead to large errors in the energy conservation. This also follows from equations (7.6)-(7.7), where an error in mass is am-



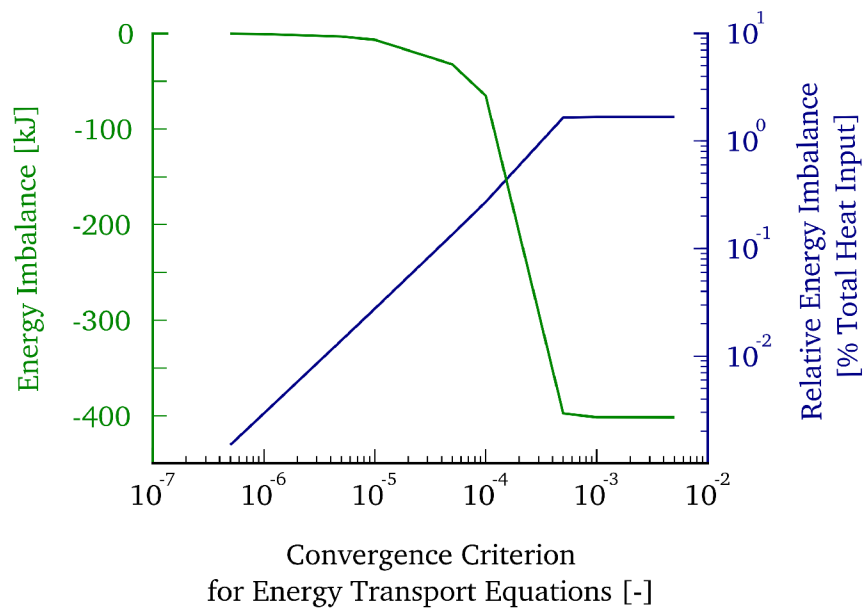


Figure 7.6: Total and relative energy imbalances as obtained by simulations of heat-up of dried wheat straw by preheated primary air (398 K) and over-bed radiation.

plified by the order of magnitude of energy parameters such as LHV of combustible gases. Values of convergence criteria are varied in the interval  $(10^{-7}, 10^{-2})$  with a step of a half of an order. Convergence is judged by scaled residuals as defined by equations (5.10) and (5.13).

The effect of scaled residuals for energy transport equations on the energy imbalance during heat-up of wheat straw by primary air (398 K) and over-bed radiation is shown on figure 7.6. The convergence criterion for gas species transport equations is fixed to  $10^{-3}$ . It can be seen that the energy imbalance significantly increases for values of energy scaled residual greater than  $10^{-5}$  and keeps very low for values less than or equal to  $10^{-6}$ , which is the default value for the energy equation in ANSYS FLUENT [14].

However, the value  $10^{-3}$  of scaled residuals for gas species transport equations seems to be too low to obtain sufficiently low energy imbalance after volatile matter (approximately 1.1 kg, 79.28wt% on dry basis) is completely pyrolysed as shown on figure 7.7. Although the convergence criterion for energy transport equations is fixed to  $10^{-6}$ , mass imbalance produces relatively large energy imbalance as long as scaled residuals are greater than  $10^{-6}$ . In order to obtain sufficiently accurate results from in-bed simulations in terms of mass and energy conservation within the packed bed, it is, therefore, suggested to require all the scaled residuals to drop to as low as  $10^{-6}$  or lower.

### 7.2.5 Inverse application of the method

The presented method offers an alternative to setting of convergence criteria, which is interesting from practical point of view. Instead of defining scaled residuals, the convergence criteria could be set in terms of the total mass and energy imbalance of the system. Such a requirement is somehow more natural than a drop of a nondimensional quantity, as the error is defined by physical quantities, that are commonly used in engineering analyses.

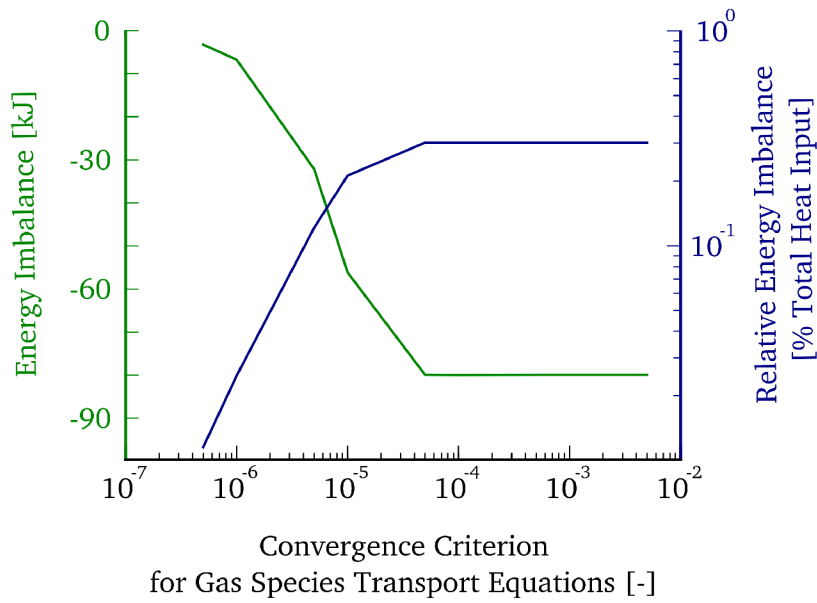


Figure 7.7: Total and relative energy imbalances as obtained by simulations of pyrolysis of dried wheat straw by preheated primary air (698 K) and over-bed radiation.

However, the physical limits would have to be set very carefully, since too strict requirement on the magnitude of imbalance might lead to undesirable long computational times due to very low equivalent scaled residuals. For this purpose, more accurate discretization methods and fast converging iterative schemes would have to be used or developed in order to achieve low imbalances in reasonable computational times.

### 7.3 Summary

The capability of the simulation tool has been demonstrated on a series of simulations. Among the physical issues considered, analysis of propagation of drying and combustion reaction fronts in the bed of wheat straw particles have been done. Results from simulations qualitatively agree with data available in literature. It has been suggested to include modelling of particle internal porosity in order to obtain correct reaction zone thickness, if porosity of the bed is allowed to change during combustion.

In order to check the conservativeness of the bed model, mass and energy balance method has been implemented in the code providing for detailed analysis of various errors arising during a simulation. The method has revealed certain errors in the definition of source terms in models adopted from literature. This has been done to reconcile the base model to yield a conservative model. A parametric study of the effects of convergence criteria on total mass and energy imbalance of the system has been carried out. From the results, it has been suggested to set the criteria on the scaled residuals for all variables to  $10^{-6}$  or lower in order to obtain acceptably low mass and energy imbalance.

## Chapter 8

# C library of functions for coupled bed-freeboard modelling in ANSYS FLUENT

ANSYS FLUENT [14] is one of the leading commercial CFD softwares for modelling a wide range of physical problems. The integrated database of numerous material properties, selection of chemical reaction schemes and radiation models make it suitable for solving reactive flows in combustion systems. The applicability is further extended by use of the so-called user defined functions (UDF), which allow a user to define custom models or modify the existing ones, making it even more flexible.

By means of UDF's, a bed model can be coupled with a freeboard model, so that heat and mass fluxes leaving the bed form the inlet boundary conditions for the freeboard, while radiation heat flux obtained from the solution of the freeboard can be passed onto the bed model. If this procedure is repeated iteratively, converged solutions of both models can be reached, when the radiation heat flux ceases to fluctuate.

There are two major steps in the development of such a coupled model. First, a stand-alone bed model must be developed and implemented into a computer code written in C programming language. Second, an interface must be created to allow for data exchange between the two models. Before the attention is turned to the interface issues, generation of a standalone C code from MATLAB codes for the bed models is briefly described. The rest of the chapter is devoted to the implementation of the interface as a C-programmed library of functions, that can be loaded into ANSYS FLUENT as UDF for coupling the codes. The purpose of the code generation is to test the functionality of the UDF and it is demonstrated on an example using a model of an industrial grate furnace.

### 8.1 Generation of C code from MATLAB code of GRATECAL

Matlab Coder utility provides for translation of MATLAB code into C/C++ code. Generated codes are portable and readable, therefore can be embedded in other projects and compiled together. Several important steps must precede the translation (provided that appropriate compiler is already installed in the system):

1. A main function, which is called in order to run the whole generated code, must be defined and marked with `%#codegen` directive. Should the function accept or return some parameters, these must be declared as well in the function.
2. Some MATLAB data types and functions are not supported for the code generation. These must be either removed, or replaced by supported ones.
3. All variables must be declared prior to the first use, because, unlike MATLAB, C programming language is static.

GRATECAL 1.3 is chosen for the code generation as it is more robust than the 2D version. The original code for GRATECAL 1.3 is modified to meet the three requirements. Among functions, that are not supported for code generation are functions for plotting data. Therefore, plotting of residuals and displaying results have to be completely removed. In fact, these are not really needed for the testing of the interface. Neither functions for printing text messages in the terminal (command line or prompt) are supported. However, these can be replaced by functions from the standard C library defined in `stdio.h`. In addition, two other issues related to passing user and ANSYS FLUENT data have to be solved.

### 8.1.1 Fluent data

The original MATLAB code for the bed model allows a user to set duration of the simulation and a length of a time step. In the walking-column approach (see 2.3), time scale is transformed to space through the velocity of the grate (equation (2.8)). Therefore, both duration of the simulation and time steps are no longer set by a user, but determined from geometry and mesh properties of the grate such that  $t = L_G/v_G$  [s], where  $L_G$  is the grate length and  $\Delta t = t/N_f$ , where  $N_f$  is the number of faces, that discretize the grate along its length. If a computed time step exceeds 0.5 s, then the code finds a number  $n_{\Delta t} > 1$  such that  $\Delta t/n_{\Delta t} \leq 0.5 < \Delta t/(n_{\Delta t} - 1)$ , so that a solution for each face is obtained in  $n_{\Delta t}$  time sub-steps to ensure numerical stability.

Velocity and length of the grate as well as the number of faces is passed to the main function from ANSYS FLUENT in a structure `fluentDataStruct`. The following table 8.1 describes all fields of the structure. (note that a different terminology is used for names of the fields - cell is used instead of face):

### 8.1.2 GRATECAL data

When a simulation of in-bed combustion is finished, data at the top of the bed must be returned to ANSYS FLUENT to macros of the UDF, which set the boundary conditions at the inlet of the furnace. Since these data are shared by both codes as in case of `fluentDataStruct`, a special data type must be defined. The following table 8.2 describes all fields of the structure `bedTopDataStruct`, which stores calculated values of fluxes for the boundary conditions:

### 8.1.3 User data

Since MATLAB graphical user interfaces are not supported for code generation, user data must be specified another way. The number of parameters needed for a simulation

Field	Description	Data Type
path2file	Path to a text file specifying gas and fuel properties and solver settings	emxArray_char_T *
grateL	Length of the grate [m]	real_T
grateW	Width of the grate [m]	real_T
grateV	Velocity of the grate [m/s]	real_T
nGrateCells	Number of cells along the grate [-]	uint16_T
Acell	Surface area of a face on the grate [m/s]	real_T
Tenv	Temperature of the environment, i.e. temperature profile above the layer [K]	emxArray_real_T *

Table 8.1: Fields of `fluentDataStruct` structure. The structure is passed to GRATECAL from ANSYS FLUENT.

Field	Description	Data Type
Ts	Temperature of fuel at the top of the bed [K]	emxArray_real_T *
Tg	Temperature of flue gas leaving the bed [K]	emxArray_real_T *
vg	Velocity of flue gas leaving the bed [m/s]	emxArray_real_T *
mass_flux	Mass flux of flue gas leaving the bed [kg/m <sup>2</sup> s]	emxArray_real_T *
wig	Mass fractions of gas species leaving the bed [kg/kg]	emxArray_real_T *
radHeat	Energy radiated from the top of the bed into the freeboard [W/m <sup>2</sup> K <sup>4</sup> ]	emxArray_real_T *
c	Indicator of convergence of the bed model [-]	boolean_T

Table 8.2: Fields of `bedTopDataStruct` structure. The structure is returned from GRATECAL to ANSYS FLUENT for setting of boundary conditions.

is quite large and it would be very inconvenient to set them through the ANSYS FLUENT prompt. Therefore, effort has been made to allow a user to specify data in a text file, which would be read after the call of GRATECAL. However, MATLAB functions for text file operations are not supported for code generation either, so a C-function has been written to read the file and assign values to a structure carrying the user-specified data. Although the C-function has been tested on many files and no errors occurred, MATLAB Coder has not been able to compile the MATLAB code with the function, so the user data have been specified in another MATLAB function and, therefore, when the whole project has been compiled, data have remained fixed. The only way to specify a different set of input values is to change values in `loadData.m` and rebuild the whole project.

#### 8.1.4 Generated code

The generated code consists of 57 source code files (with the extension `.c`) and 59 header files (extension `.h`).

## 8.2 Coupled modelling methodology in detail

The coupled methodology is based on the idea, that a fuel bed can be physically separated from the freeboard, however, logically connected by the common interface, through which either of the models accepts data passed from the other one based on the current solution within the particular model. Transmitted data form dynamic boundary conditions for each model, so that solutions of both models are not independent of each other underlying the fact, that processes above the fuel bed are strongly influenced by, and therefore coupled to, in-bed processes and vice versa.

This concept has been used in a few studies on grate combustion of solid fuels, e.g. [32, 52, 79, 89]. In simulations of combustion of a single wood log as documented in [16], while the mean mass loss rates were overestimated by a solid-phase model alone, acceptable agreements with experimental measurements were obtained by the coupled methodology. However, important issues related to a technique of coupling of the two models are not discussed much in detail. Therefore, the discussion is provided first in the following text.

### 8.2.1 Placement of the interface

Physical separation of the two models has one major implication. It must be decided, where the freeboard model is cut off, i.e. where the interface is positioned. A correct way is to cutoff the freeboard right at the top of the bed. Since most CFD models of real furnaces also include zones with a fuel feeder and ashpit, these either would have to become parts of the bed model (this obviously would be a complicated task in general), or the interface would have to be precisely adjusted to the geometry of zone boundaries (this is, on the other hand, very inconvenient). Neither of the ways provides an easy setup of the coupled model, which seems to be impractical.

From a practical point of view, an optimal way of coupling the two models is to define the plane of a grate as the interface, where primary air properties entering the furnace were originally prescribed for boundary conditions. Of course, it is an approximation of a real situation, since the part of the furnace volume occupied by a fuel layer is now left void allowing the flue gas species to react with the secondary combustion air closer to the grate.

Despite the approximation of the second approach, it is chosen as a base in the first stage of coupled model development as it provides an easier way to realize the coupling.

### 8.2.2 Radiation heat flux

Another important issue in the coupled modelling methodology is treatment of radiation heat flux. The top of the bed is ignited by the over-bed radiation, so the value of the heat flux should be passed to the bed model as the boundary condition for the energy equation. The hot bed top also radiates energy into the freeboard. This can be taken into account by setting a black body temperature within the inlet boundary conditions. However, the value is fixed and no UDF can change it in order to reflect changes of bed top temperature. A possible solution is to change the black body temperature artificially using the inlet emissivity, for which a UDF can be defined. Beside this complication, a heat flux from inside the furnace must be obtained through another UDF. Therefore, in order to test the functionality of the programmed interface, i.e. calling GRATECAL from ANSYS FLUENT, solving combustion inside the fuel bed by GRATECAL and passing parameters of flue gas

from in-bed simulation back to ANSYS FLUENT, the radiation heat transfer at the bed top is simplified such that a temperature profile along the bed length for calculation of the heat flux is predefined and set constant.

### 8.2.3 Main descriptive parameters of a grate

Since the grate is chosen as the interface for data exchange, inlet boundary conditions must be defined at the grate boundary zone. Figure 8.1 shows an outline of a model of a municipal solid waste incinerator which is run in TERMIZO, Liberec. Previously (within a framework of research plan No. MSM 0021630502 "Waste and Biomass Utilization focused on Environment Protection and Energy Generation"), combustion in the furnace was modelled using a coal substitute for the waste and mass and energy source terms as calculated from mass and energy balance of the fuel were placed to a cell zone immediately above the grate. It can be seen, that the grate is divided into four boundary zones, for each of which different inlet properties of the primary air can be defined as the boundary conditions. A detail of the meshed grate is shown on Figure 8.2. Faces are grouped into the boundary zones, for each of which a set of boundary conditions must be defined. ANSYS FLUENT associates each boundary zone with a boundary zone ID, an integer number, which can be found in the panel for definition of boundary conditions. This number is important for setting the boundary conditions by means of UDF.

Following the walking-column approach described in 2.3, transient solutions of the 1D model are related with corresponding positions on the grate (i.e. faces) according to the equation (2.8) and a series of faces along the grate length represents a series of transient solutions of the experimental reactor. The velocity of the grate  $v_G$  is another important parameter of the grate. Also an information on the orientation of the grate with respect to the coordinate system must be provided in order to properly match transient solutions with corresponding faces. It is assumed, that the furnace is oriented such that the grate declines in a direction of one of the coordinate axes (if the grate is not inclined, then the direction from the feeder to the ashpit must correspond with either of coordinate axes direction). The axes  $x, y, z$  are denoted by numbers 0, 1, 2, respectively.

In summary, parameters needed to describe the grate for the purpose of matching transient solutions to proper correct positions on the grate, are as follows:

- Boundary zone ID's.
- Velocity of the grate  $v_G$  [m/s].
- ID number of the coordinate axis, along which the grate declines. ID numbers are assigned to axes as follows: 0  $\rightarrow$   $x$ , 1  $\rightarrow$   $y$ , 2  $\rightarrow$   $z$ .

## 8.3 Working with UDF

Since the UDF must be compiled inside ANSYS FLUENT, the whole library of C-functions must be placed at the same location, where `.cas` and `.dat` files are placed. The library contains a large number of files, each of which has to be loaded into ANSYS FLUENT. Therefore, in order to make it easier, a journal file `gc1D.jou` has been written, which also has to be put in the same folder as other files. When the journal is selected and run through

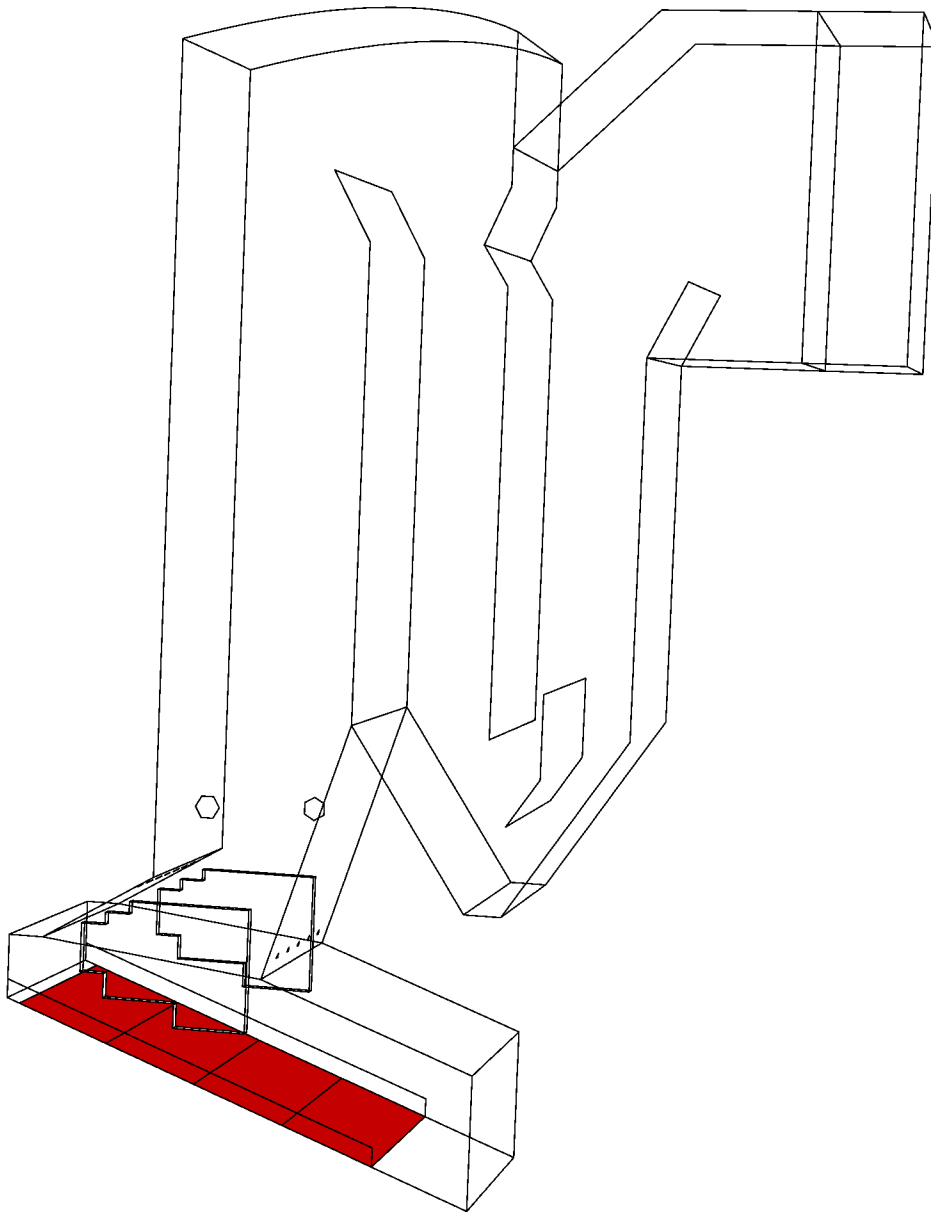


*Figure 8.1: Outline of a model of municipal solid waste incinerator. The grate is divided into four sections.*

File→Read→Journal, all source code files are loaded and compiled at once. Should any error appear (e.g. due to missing source code file), the library can be rebuilt again using `gc1D_rebuild.jou`.

The main source code file of the UDF is `udf_gc1D.c`, which contains several `DEFINE` macros and a number of functions, that are called by macros in order to initialize data and process results from GRATECAL to set profiles of boundary conditions. A user first must set the main descriptive parameters of the grate in `fluentData.h` as described in 8.2.3. A



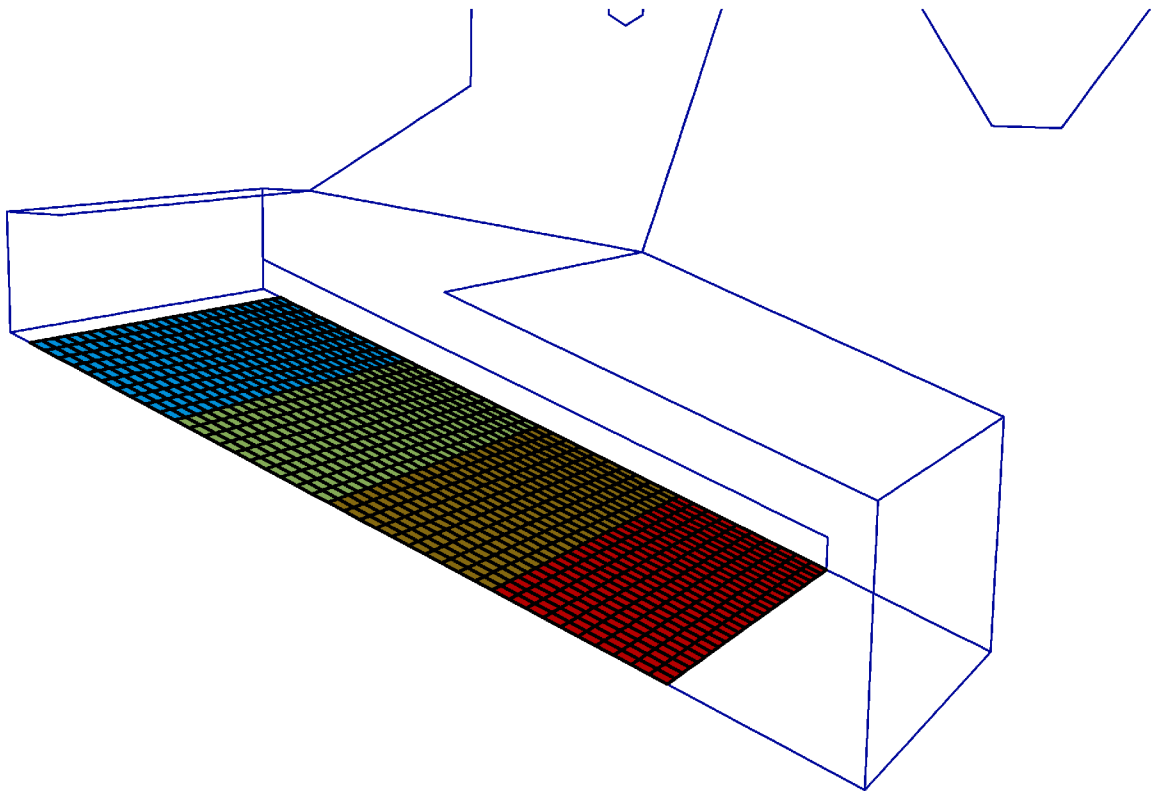


Figure 8.2: Close-up of grate boundary zones.

valid full path to the file `gcData.txt`, that contains information on settings of GRATECAL including gas and fuel properties etc., must be provided. The default total number of gas species in the simulation must not be changed.

Three `DEFINE_PROFILE` macros are available in the UDF, by means of which boundary conditions can be modified. Note, that the UDF for boundary conditions for all variables must be defined. These include:

- `udf_inlet_species` for all gas species, see Figure 8.3, where the inlet boundary condition is being defined for CO). Gas species may be ordered in the list of mixture arbitrarily provided, that  $N_2$  is the last item in the list.
- `udf_inlet_m_flux` for mass flux in units of  $[\text{kg}/\text{m}^2 \text{ s}]$ .
- `udf_inlet_temp` for gas temperature.

The UDF for boundary conditions can be selected through a corresponding menu as shown on the figure 8.3 .

When selection of boundary conditions is confirmed, the UDF is executed for the first time to initialize values of boundary conditions. At this moment, the C-function `initialize_data`, which is declared and defined in `udf_gc1D.c`, is called to load and initialize data about the grate. The main data, that have been initialized, are displayed at the ANSYS FLUENT prompt, e.g. geometric properties of the grate and the time interval, that is needed to cover the entire length of the grate by the walking-column method.

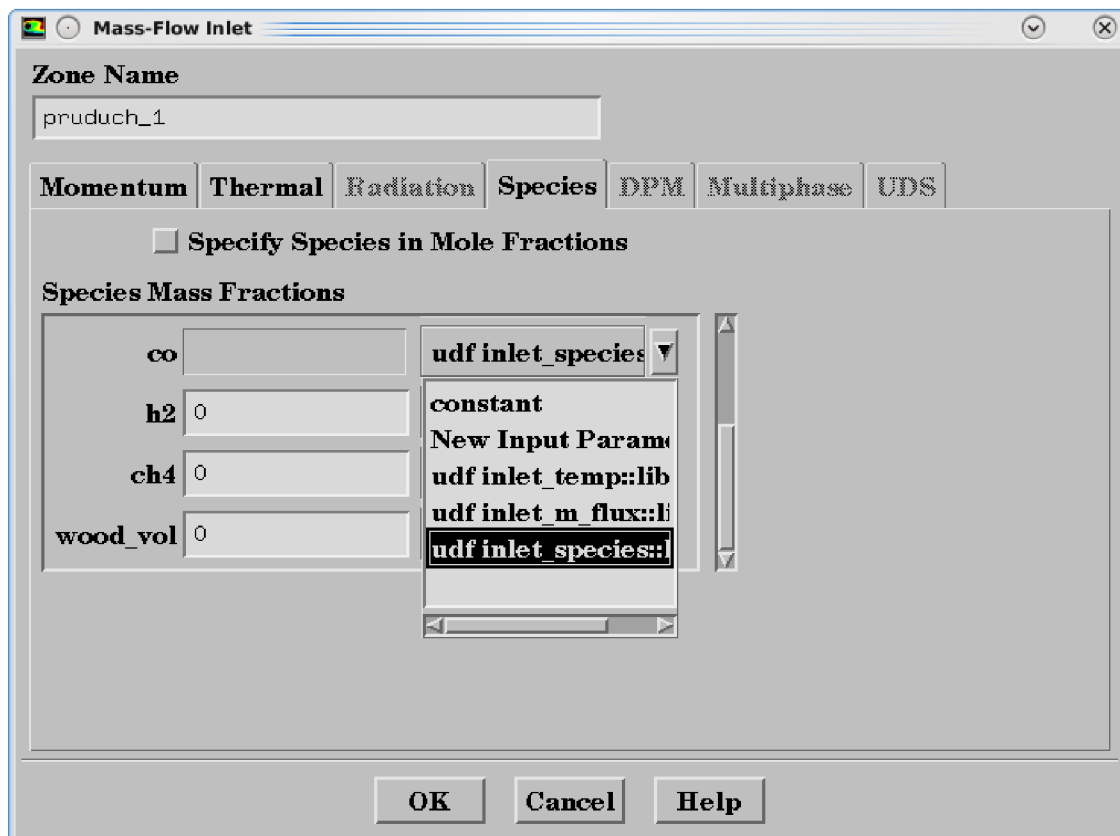


Figure 8.3: Definition of mass-flow inlet boundary conditions for gas species.

When the whole simulation is started, the control is passed on to GRATECAL, which solves combustion in the fuel bed first and return results back to ANSYS FLUENT to update inlet boundary conditions of the freeboard model. The progress of iterations can be watched during the simulation in the ANSYS FLUENT prompt.

## 8.4 Summary

The coupled methodology has been described. Using MATLAB Coder, a C code has been generated from MATLAB source files in order to use the program as a tool for calculation of the boundary conditions at the grate (inlet). An interface for coupling the bed and freeboard models has been developed and implemented into a library of C-functions as a user-defined function, which can be loaded into ANSYS FLUENT to set and modify boundary conditions at the furnace inlet, providing for a one-way coupling of the two models. The UDF can be used for a wide range of grate furnace CFD models. It has also been shown, how to load the UDF into ANSYS FLUENT and run coupled simulation.

# Chapter 9

## Conclusions and future work

The present work is concerned with numerical modelling of grate combustion of solid fuels, especially biomass and municipal solid waste. The scope of investigated topics is restricted to modelling of processes, that take place within a fuel bed on a grate, as knowledge of the process dynamics in the bed is essential for optimization and development of grate-firing technologies. This is emphasized by the fact that results from CFD simulations of grate combustion depend on the quality of input data including information on temperature, mass flux and chemical composition of flue gas leaving the bed. Therefore, the attention is turned to development of a reliable numerical model of packed-bed combustion as it may help improve both results from simulations and knowledge of principles of solid fuel combustion in fixed or moving beds.

Based on a review of existing bed models, a one-dimensional transient numerical model of combustion in an experimental reactor has been developed. The fuel bed is treated as a porous layer consisting of gas and solid phase. The model is described on macroscale, so processes within an individual fuel particles are neglected. Such an assumption is very practical from computational point of view, since beds of industrial furnaces contain many fuel particles and solution on such a large set of entities would be very demanding in terms of computational times. A comprehensive description and discussion on parameters of governing equation has been provided. Parameters that have been critically reviewed with respect to generality and validity under combustion conditions, include effective mass and thermal dispersion coefficient, effective heat capacity, heat and mass transfer coefficients, packing condition parameters such as porosity, particle size and shape, process rates for drying, pyrolysis, char combustion, fuel mixing coefficient as well as particle volume shrinkage factors.

The model has been implemented into a computer program called GRATECAL 1.3 with a graphical user interface, which solves governing equations numerically by the finite volume method. Discretization methods and techniques have been described, especially methods, that have been found helpful in obtaining the convergence. A special numerical treatment of process rates based on physical limitations has been introduced.

During development of the model, emphasis has been put on the conservativeness of the model. A method for control of mass and energy balance over the system has been developed, by means of which the model can be checked and corrected for errors to yield a conservative model. The method has been applied to a series of case studies, which have revealed certain errors in definitions of mass source terms, so that data adopted from literature have been reconciled. The method has been formulated with respect to combustion

in an experimental reactor, it can be extended to other applications as it is based on basic physical principles such as balancing of mass and energy. Therefore, the idea can be helpful in development of any numerical model.

The model has been used in analysis of some physical and numerical issues. Propagation of drying and char combustion reaction fronts have been analysed, demonstrating the capabilities of the developed simulation tool. A parametric study on effects of convergence criteria on total mass and energy imbalance of the system due to incomplete convergence has been carried out using the mass and energy balance method. The presented results have not been published by other authors yet and therefore contribute to better understanding of numerical modelling of packed-bed combustion.

The second part of the work has been devoted to implementation of an interface, through which the bed model can be coupled with the freeboard model created in ANSYS FLUENT. The interface has been programmed in C programming language and implemented as a user defined function, that can be loaded into ANSYS FLUENT to set and update boundary conditions at the furnace inlet at each iteration. The interface is general enough to be used for a wide range of models of grate furnaces. In order to test its functionality, a C code has been generated from GRATECAL 1.3 using MATLAB Coder utility and the coupling has been demonstrated.

## 9.1 Future work

The capabilities of one-dimensional transient model should be extended to account for modelling of gaseous reactions and bed volume reduction. Although the current version has gaseous reactions implemented, in a standalone module, its usage is very limited due to convergence problems. Once these problems are solved, the database of chemical reactions should be extended in order to model other pollutant species formation such as  $\text{NO}_x$  and  $\text{SO}_x$ . Beside this model, a two-dimensional steady model has also been developed and implemented as GRATECAL 2.0. However, much work has yet to be done to improve numerical stability of the 2D simulation tool.

In the area of coupled simulations, future work should be concentrated on a implementation of full, i.e. two-way coupling of the computational model. The presented one-way coupling may serve for setting the boundary conditions at the inlet only once at the beginning of a simulation, since the incident radiation heat flux is fixed. The processes inside and above the bed should be fully coupled to provide for a better estimate of profiles of temperature, mass flux and concentrations of gas leaving the bed.

Finally, the presented results of simulations could not be compared quantitatively to experimental measurements due to unavailability of detailed data. Results were validated only on qualitative level according to published literature. However, for proper quantitative model validation, it is necessary to perform a series of experimental measurements. This is the matter of a proposed future project (Czech Science Foundation), within which an experimental reactor is planned to be constructed.

# References

- [1] BIOBIB - a database for biofuels, [on-line], [last cited 17 September 2012], available at <http://www.vt.tuwien.ac.at/biobib/biobib.html>.
- [2] ASTHANA, A., MÉNARD, Y., SESSIECQ, P., AND PATISSON, F. Modeling On-Grate MSW incineration with experimental validation in a batch incinerator. *Industrial & Engineering Chemistry Research* 49 (2010), 7597–7604.
- [3] BASU, P. *Combustion and gasification in fluidized beds*. Taylor & Francis, London, UK, 2006, ISBN 0-8493-3396-2.
- [4] BELLAIS, M. *Modelling of the pyrolysis of large wood particles*. PhD thesis, KTH - Royal Institute of Technology, Stockholm, 2007.
- [5] BLONDEAU, J., JEANMART, H., RYCKMANS, Y., ALLARD, P., AND ROCHAYA, D. Biomass combustion in pulverized-fuel boilers: use of apparent pyrolysis parameters in CFD codes. *Proceedings of the 9th European Conference on Industrial Furnaces and Boilers 9* (2011), 10 pp., ISBN 978-972-99309-6-6.
- [6] BORMAN, G. L., AND RAGLAND, K. W. *Combustion Engineering*, 1st ed. McGraw-Hill, Boston, 1998, ISBN 0-07-006567-5.
- [7] BRYDEN, K. M., RAGLAND, K. W., AND RUTLAND, C. J. Modeling thermally thick pyrolysis of wood. *Biomass & Bioenergy* 22 (2002), 41–53.
- [8] CHANEY, J., LIU, H., AND LI, J. An overview of CFD modelling of small-scale fixed-bed biomass pellet boilers with preliminary results from a simplified approach. *Energy Conversion and Management* (2012), 8 pp., <http://dx.doi.org/10.1016/j.enconman.2012.01.036>.
- [9] CHARTIER, J., GUERNION, P., AND MILO, I. CFD modelling of municipal solid waste incineration. *Progress in Computational Fluid Dynamics* 7 (2007), 19–24.
- [10] CHEVANAN, N., WOMAC, A. R., BITRA, V. S. P., IGATHINATHANE, C., YANG, Y. T., MIU, P. I., AND SOKHANSANJ, S. Bulk density and compaction behavior of knife mill chopped switchgrass, wheat straw, and corn stover. *Bioresource Technology* 101 (2010), 207–214.
- [11] COLLAZO, J., PORTEIRO, J., PATIÑO, D., AND GRANADA, E. Numerical modeling of the combustion of densified wood under fixed-bed conditions. *Fuel* 93 (2012), 149–159.
- [12] DAHLQUIST, G., AND ÅKE BJÖRCK. *Numerical Methods*, 1st ed. Prentice-Hall, Englewood Cliffs, New Jersey, USA, 1974, ISBN 0-486-42807-9.

- [13] FJELLERUP, J., AND HENRIKSEN, U. Heat transfer in a fixed bed of straw char. *Energy & Fuels* 17 (2003), 1251–1258.
- [14] FLUENT 6.3.26. *User's Guide*. Fluent Inc., Lebanon, USA, 2006.
- [15] FOUHENY, E. A., KULKARNI, A., ROSHANI, S., AND VATANI, A. Elucidation of pressure drop in packed-bed systems. *Applied Thermal Engineering* 16 (1996), 195–202.
- [16] GALGANO, A., AND DI BLASI, C. Coupling a CFD code with a solid-phase combustion model. *Progress in Computational Fluid Dynamics* 6, Nos. 4/5 (2006), 287–302.
- [17] GOFF, J. A. A. saturation pressure of water on the new Kelvin temperature scale. *Transactions of the American society of heating and ventilating engineers* (1957), 347–354.
- [18] GOH, Y. R., YANG, Y. B., ZAKARIA, R., SIDDALL, R. G., NASSERZADEH, V., AND SWITHEENBANK, J. Development of an incinerator bed model for municipal solid waste incineration. *Combustion Science and Technology* 162 (2001), 37–58.
- [19] GORT, R. *On the propagation of a reaction front in a packed bed: thermal conversion of municipal solid waste and biomass*. PhD thesis, University of Twente, The Netherlands, 1995.
- [20] GREEN, D. W., AND PERRY, R. H. *Perry's Chemical Engineers' Handbook*, 8th ed. ed. McGraw-Hill, USA, 2008, ISBN 0-07-142294-3.
- [21] GRØNLI, M. G. *A theoretical and experimental study of the thermal degradation of biomass*. PhD thesis, The Norwegian University of Science and Technology, Trondheim, Norway, 1996.
- [22] GUBBA, S. R., INGHAM, D. B., LARSEN, K. J., MA, L., POURKASHANIAN, M., TAN, H. Z., WILLIAMS, A., AND ZHOU, H. Numerical modelling of the co-firing of pulverised coal and straw in a 300 MWe tangentially fired boiler. *Fuel Processing Technology* (2012), 8 pp., <http://dx.doi.org/10.1016/j.fuproc.2012.05.011>.
- [23] GUPTA, M., YANG, J., AND ROY, C. Density of softwood bark and softwood char: procedural calibration and measurement by water soaking and kerosene immersion method. *Fuel* 81 (2002), 1379–1384.
- [24] HANKALIN, V., AHONEN, T., AND RAIKOO, R. On thermal properties of a pyrolysing wood particle. *Finnish-Swedish Flame Days pp. 16* (2009).
- [25] HIRSCH, C. *Numerical Computation of Internal and External Flows - Volume 1: Fundamentals of Numerical Discretization*, 1st ed. John Wiley & Sons, New Jersey, USA, 2001, ISBN 0-471-92385-0.
- [26] HOROVÁ, I., AND ZELINKA, J. *Numerické metody*, 2nd ed. ed. Masarykova Univerzita, Brno, Czech Republic, 2004, ISBN 80-210-3317-7.
- [27] HÁJEK, J. State of the art in fixed bed combustion experiments. *Sborník 56. konference chemického a procesního inženýrství* 56 (2009), B5.6, pp. 12, ISBN 978–80–86059–51–8.

- [28] INCROPERA, F. P., AND DEWITT, D. P. *Fundamentals of Heat and Mass Transfer*, 5th ed. John Wiley & Sons, New Jersey, USA, 2002, ISBN 0-471-38650-2.
- [29] JOHANSSON, R., THUNMAN, H., AND LECKNER, B. Sensitivity analysis of a fixed bed combustion model. *Energy & Fuels* 21 (2007), 1493–1503.
- [30] KÆR, S. K. *Numerical Investigation of Ash Deposition in Straw-fired Boilers*. PhD thesis, Aalborg University, Denmark, 2001.
- [31] KÆR, S. K. Numerical modelling of a straw-fired grate boiler. *Fuel* 83 (2004), 1183–1190.
- [32] KÆR, S. K., ROSENDAHL, L. A., AND BAXTER, L. L. Towards a CFD-based mechanistic deposit formation model for straw-fired boilers. *Fuel* 85 (2006), 833–848.
- [33] KAUSLEY, S. B., AND PANDIT, A. B. Modelling of solid fuel stoves. *Fuel* 89 (2010), 782–791.
- [34] KLASON, T., AND BAI, X. S. Combustion process in a biomass grate fired industry furnace: a CFD study. *Progress in Computational Fluid Dynamics* 6 (2006), 278–286.
- [35] MANDØ, M., ROSENDAHL, L., YIN, C., AND SØRENSEN, H. Pulverized straw combustion in a low-NO<sub>x</sub> multifuel burner: Modeling the transition from coal to straw. *Fuel* 89 (2010), 3051–3062.
- [36] MARIAS, F. A model of a rotary kiln incinerator including processes occurring within the solid and the gaseous phases. *Computers and Chemical Engineering* 27 (2003), 813–825.
- [37] MASSMAN, W. J. A review of the molecular diffusivities of H<sub>2</sub>O, CO<sub>2</sub>, CH<sub>4</sub>, CO, O<sub>3</sub>, SO<sub>2</sub>, NH<sub>3</sub>, N<sub>2</sub>O, NO and NO<sub>2</sub> in air, O<sub>2</sub> and N<sub>2</sub> near STP. *Atmospheric Environment* 32 (1998), 1111–1127.
- [38] MATHUR, S. R., AND MURTHY, J. Y. Pressure boundary conditions for incompressible flow using unstructured meshes. *Numerical Heat Transfer, Part B: Fundamentals* 32 (1997), 283–298.
- [39] MATLAB R2011A. *User's Guide*. MathWorks Inc., USA, 2011.
- [40] MCKENDRY, P. Energy production from biomass (part 1): overview of biomass. *Biore-source Technology* 83 (2002), 37–46.
- [41] MILTNER, M., MAKARUK, A., HARASEK, M., AND FRIEDL, A. Computational fluid dynamics simulation of a solid biomass combustor: modelling approaches. *Clean Technologies and Environmental Policy* 10 (2008), 165–174.
- [42] MODEST, M. F. *Radiative Heat Transfer*, 2nd ed. Elsevier Science, USA, 2003, ISBN 0-12-503163-7.
- [43] MURTHY, J. Y., AND MATHUR, S. R. Draft notes to ME 608 Numerical methods in heat, mass, and momentum transfer, 2002, [last cited 4 October 2012], available at <https://engineering.purdue.edu/ME608/webpage/main.pdf>.

- [44] OBERNBERGER, I., BRUNNER, T., AND BÄRNTHALER, G. Chemical properties of solid biofuels-significance and impact. *Biomass and Bioenergy* 30 (2006), 973–982.
- [45] OBERNBERGER, I., AND THEK, G. Physical characterisation and chemical composition of densified biomass fuels with regard to their combustion behaviour. *Biomass and Bioenergy* 27 (2004), 653–669.
- [46] PATANKAR, S. V. *Numerical Heat Transfer and Fluid Flow*, 1st ed. Hemisphere Publishing Corporation, USA, 1980, ISBN 0-89116-522-3.
- [47] PETERS, B. *Thermal Conversion of Solid Fuels*, 1st ed. WIT Press, Southampton, UK, 2003, ISBN 1-85312-953-4.
- [48] PETERS, B., DZIUGYS, A., RASLAVICIUS, L., AND NARBUTAS, L. Prediction of straw gasification on a forward acting grate. *Proceedings of 20th International Congress of Chemical and Process Engineering* 59 (2012), A6.8, ISBN 978–80–905035–1–9.
- [49] PETERS, B., SCHRÖDER, E., BRUCH, C., AND NUSSBAUMER, T. Measurements and particle resolved modelling of heat-up and drying of a packed bed. *Biomass and Bioenergy* 23 (2002), 291–306.
- [50] RECMAN, M., HÁJEK, J., AND STEHLÍK, P. Review of thermo-physical properties of biomass for grate combustion modelling. *Summaries 4 PRES and System Engineering* 34 (2008), 1596–1597, ISBN: 978–80–02–02051–6.
- [51] RYAN, J. S., AND HALLETT, W. L. H. Packed bed combustion of char particles: experiments and an ash model. *Chemical Engineering Science* 57 (2002), 3873–3882.
- [52] RYU, C., SHIN, D., AND CHOI, S. Combined simulation of combustion and gas flow in a grate-type incinerator. *Journal of the Air & Waste Management Association* 52 (2002), 174–185.
- [53] RYU, C., YANG, Y. B., KHOR, A., YATES, N. E., SHARIFI, V. N., AND SWITHEBANK, J. Effect of fuel properties on biomass combustion: Part I. Experiments—fuel type, equivalence ratio and particle size. *Fuel* 85 (2006), 1039–1046.
- [54] SAASTAMOINEN, J., AND RICHARD, J.-R. Simultaneous drying and pyrolysis of solid fuel particles. *Combustion and Flame* 106 (1996), 288–300.
- [55] SALEM, A., AHMADLOUIEDARAB, M., AND GHASEMZADEH, K. CFD approach for the moisture prediction in spray chamber for drying of salt solution. *Journal of Industrial and Engineering Chemistry* 17 (2011), 527–532.
- [56] SCHAFFEL-MANCINI, N., MANCINI, M., SZLEK, A., AND WEBER, R. Novel conceptual design of a supercritical pulverized coal boiler utilizing high temperature air combustion (HTAC) technology. *Energy* 35 (2010), 2752–2760.
- [57] SCHARLER, R., FORSTNER, M., BRAUN, M., BRUNNER, T., AND OBERNBERGER, I. Advanced CFD analysis of large fixed bed biomass boilers with special focus on the convective section. *Proceedings of the 2nd World Conference and Exhibition on Biomass for Energy, Industry and Climate Protection* 1 (2004), 1357–1360, ISBN 88–89407–04–2.



- [58] SCHARLER, R., AND OBERNBERGER, I. Numerical modelling of biomass grate furnaces. *Proceedings of the 5th European Conference on Industrial Furnaces and Boilers* (2000), pp. 17, ISBN 972-8034-04-0.
- [59] SHIN, D., AND CHOI, S. The combustion of simulated waste particles in a fixed bed. *Combustion and Flame* 121 (2000), 167-180.
- [60] SKÁLA, Z., AND OCHODEK, T. Energetické parametry biomasy: Projekt GAČR 101/04/1278, [on-line], 2007, [last cited September 17 2012], available at <http://www.oei.fme.vutbr.cz/enparbio.pdf>.
- [61] SMITH, J. M., AND VAN NESS, H. C. *Introduction to chemical engineering thermodynamics*, 4th ed. ed. McGraw-Hill, USA, 1987, ISBN 0-07-058703-5.
- [62] SMOOT, L. D., AND PRATT, D. T. *Pulverized-Coal Combustion and Gasification*, 1st ed. Plenum Press, New York, 1979, ISBN 0-306-40084-7.
- [63] SYAMLAL, M., ROGERS, W., AND O'BRIEN, T. J. *MFIX Documentation Theory Guide*, [on-line], 1993, [last cited September 17 2012], available at <https://mfix.netl.doe.gov/documentation/Theory.pdf>.
- [64] THUNMAN, H., AND LECKNER, B. Influence of size and density of fuel on combustion in a packed bed. *Proceedings of the Combustion Institute* 30 (2005), 2939-2946.
- [65] THUNMAN, H., LECKNER, B., NIKLASSON, F., AND JOHNSON, F. Combustion of wood particles - a particle model for eulerian calculations. *Combustion and Flame* 129 (2002), 30-46.
- [66] TURNER, I., AND MUJUMDAR, A. S. *Mathematical modeling and numerical techniques in drying technology*. Marcel Dekker, Inc., New York, 1997, ISBN 0-8247-9818-X.
- [67] VAN DER LANS, R. P., PEDERSEN, L. T., JENSEN, A., GLARBORG, P., AND DAM-JOHANSEN, K. Modelling and experiments of straw combustion in a grate furnace. *Biomass & Bioenergy* 19 (2000), 199-208.
- [68] VAN KUIJK, H. A. J. A. *Grate Furnace Combustion: a Model for the Solid Fuel Layer*. PhD thesis, Eindhoven University of Technology, 2008.
- [69] VAN LOO, S., AND KOPPEJAN, J. *The Handbook of Biomass Combustion and Co-firing*, 2nd ed. Earthscan, London, 2008, ISBN 978-1-84407-249-1.
- [70] VERSTEEG, H. K., AND MALALASEKERA, W. *An introduction to computational fluid dynamics: The finite volume method*, 1st ed. Longman Scientific & Technical, Harlow, England, 1995, ISBN 0-582-21884-5.
- [71] WAKAO, N., AND KAGUEI, S. *Heat and mass transfer in packed beds*. Gordon & Breach Science Publishers, London, 1982, ISBN 0-677-05860-8.
- [72] WURZENBERGER, J. C. *A Combined Packed Bed and Single Particle Model Applied to Biomass Combustion*. PhD thesis, Technische Universität Graz, 2001.

- [73] YAGI, S., AND KUNII, D. Studies on effective thermal conductivities in packed beds. *AIChE Journal* 3 (1957), 373–381.
- [74] YANG, W., RYU, C., AND CHOI, S. Unsteady one-dimensional model for a bed combustion of solid fuels. *Proceedings of the Institution of Mechanical Engineers, Part A: Journal of Power and Energy* 218 (2004), 589–598.
- [75] YANG, Y. B., GOH, Y. R., ZAKARIA, R., NASSERZADEH, V., AND SWITHEBANK, J. Mathematical modelling of MSW incineration on a travelling bed. *Waste Management* 22 (2002), 369–380.
- [76] YANG, Y. B., GOODFELLOW, J., GOH, Y. R., NASSERZADEH, V., AND SWITHEBANK, J. Investigation of channel formation due to random packing in a burning waste bed. *Process Safety and Environmental Protection* 79 (2001), 267–277.
- [77] YANG, Y. B., LIM, C. N., GOODFELLOW, J., SHARIFI, V. N., AND SWITHEBANK, J. A diffusion model for particle mixing in a packed bed of burning solids. *Fuel* 84 (2005), 213–225.
- [78] YANG, Y. B., NASSERZADEH, V., GOODFELLOW, J., AND SWITHEBANK, J. Simulation of channel growth in a burning bed of solids. *Chemical Engineering Research and Design* 81 (2003), 221–232.
- [79] YANG, Y. B., NEWMAN, R., SHARIFI, V., JIM SWITHEBANK, AND ARISS, J. Mathematical modelling of straw combustion in a 38 MWe power plant furnace and effect of operating conditions. *Fuel* 86 (2007), 129–142.
- [80] YANG, Y. B., RYU, C., KHOR, A., SHARIFI, V. N., AND SWITHEBANK, J. Fuel size effect on pinewood combustion in a packed bed. *Fuel* 84 (2005), 2026–2038.
- [81] YANG, Y. B., RYU, C., KHOR, A., YATES, N. E., SHARIFI, V. N., AND SWITHEBANK, J. Effects of fuel properties on biomass combustion. Part II. Modelling approach - identification of the controlling factors. *Fuel* 84 (2005), 2116–2130.
- [82] YANG, Y. B., SHARIFI, V. N., AND SWITHEBANK, J. Effect of air flow rate and fuel moisture on the burning behaviours of biomass and simulated municipal solid wastes in packed beds. *Fuel* 83 (2004), 1553–1562.
- [83] YANG, Y. B., SHARIFI, V. N., AND SWITHEBANK, J. Numerical simulation of the burning characteristics of thermally-thick biomass fuels in packed-beds. *Process Safety and Environmental Protection* 83 (2005), 549–558.
- [84] YANG, Y. B., SHARIFI, V. N., SWITHEBANK, J., MA, L., DARVELL, L. I., JONES, J. M., POURKASHANIAN, M., AND WILLIAMS, A. Combustion of a single particle of biomass. *Energy & Fuels* 22 (2008), 306–316.
- [85] YANG, Y. B., YAMAUCHI, H., NASSERZADEH, V., AND SWITHEBANK, J. Effects of fuel devolatilisation on the combustion of wood chips and incineration of simulated municipal solid wastes in a packed bed. *Fuel* 82 (2003), 2205–2221.
- [86] YIN, C., ROSENDAHL, L., CLAUSEN, S., AND HVID, S. L. Characterizing and modeling of an 88MW grate-fired boiler burning wheat straw: Experience and lessons. *Energy* 41 (2012), 473–482.

- 
- [87] YIN, C., ROSENDAHL, L., KÆR, S. K., CLAUSEN, S., HVID, S. L., AND HILLE, T. Mathematical Modeling and Experimental Study of Biomass Combustion in a Thermal 108 MW Grate-Fired boiler. *Energy & Fuels* 22 (2008), 1380–1390.
- [88] YIN, C., ROSENDAHL, L. A., AND KÆR, S. K. Grate-firing of biomass for heat and power production. *Progress in Energy and Combustion Science* 34 (2008), 725–754.
- [89] YU, Z., MA, X., AND LIAO, Y. Mathematical modeling of combustion in a grate-fired boiler burning straw and effect of operating conditions under air- and oxygen-enriched atmospheres. *Renewable Energy* 35 (2010), 895–903.
- [90] ZHAO, W., LI, Z., ZHAO, G., ZHANG, F., AND ZHU, Q. Effect of air preheating and fuel moisture on combustion characteristics of corn straw in a fixed bed. *Energy Conversion and Management* 49 (2008), 3560–3565.
- [91] ZHOU, H., JENSEN, A. D., GLARBORG, P., JENSEN, P. A., AND KAVALIAUSKAS, A. Numerical modeling of straw combustion in a fixed bed. *Fuel* 84 (2005), 389–403.
- [92] ZHOU, H., JENSEN, A. D., GLARBORG, P., AND KAVALIAUSKAS, A. Formation and reduction of nitric oxide in fixed-bed combustion of straw. *Fuel* 85 (2006), 705–716.



# Nomenclature

Symbol	Unit	Meaning
$a$	various	Regression coefficient
$A$	[1/s]	Pre-exponential factor
$A$	[m <sup>2</sup> /m <sup>3</sup> ]	Volumetric surface
$A$	[m <sup>2</sup> ]	Cross-flow area
$b$	various	Right hand side of discretized equations, or regression coefficient
$Bi$	[-]	Biot number
$c$	various	Regression coefficient
$c_p$	[J/kg K]	Specific heat capacity at constant pressure
$c_{p,s(g)}$	[J/kg K]	Specific heat capacity of solid (gas)
$d$	various	Regression coefficient
$d$	[m]	Particle or reactor diameter
$D$	[m <sup>2</sup> /s]	Diffusivity, dispersion coefficient, fuel mixing coefficient
$E_a$	[J/mol]	Activation energy
$f$	[N/m <sup>3</sup> ]	Body force
$f$	[-]	Particle shrinkage factor
$F$	[kg/m <sup>2</sup> s]	Mass flux
$h_c$	[W/m <sup>2</sup> K]	Convective heat transfer coefficient
$h_{g(s)}$	[J/kg]	Specific sensible enthalpy of gas (solid)
$h_{vap}$	[J/kg]	Heat of vaporization
$\Delta h$	[J/kg]	Enthalpy of reaction, enthalpy of phase change
$HHV$	[J/kg]	Higher heating value
$I$	[-]	Imbalance
$k_c$	[kg/m <sup>2</sup> s atm]	Kinetic rate constant
$k_d$	[m/s]	Mass transfer coefficient
$k_D$	[kg/m <sup>2</sup> s atm]	Mass transfer coefficient
$L$	[m]	Characteristic length
$LHV$	[J/kg]	Lower heating value
$m$	[kg]	Mass
$M$	[kg/mol]	Molecular weight
$\bar{M}$	[kg/mol]	Mean molecular weight
$n$	[-]	Number of time sub-steps
$N$	[-]	Number of faces
$p$	[Pa],[atm]	Pressure, partial pressure
$Pe$	[-]	Peclet number

Symbol	Unit	Meaning
Pr	[-]	Prandtl number
Nu	[-]	Nusselt number
$\dot{q}$	[W/m <sup>3</sup> ]	General heat transfer rate
$r$	[m]	Particle or reactor radius
$r$	[kg/m <sup>3</sup> s]	Reaction or process rate
R	[-]	Residual
R	[J/mol K]	Universal gas constant ( $\approx 8.314$ )
Re	[-]	Reynolds number
S	[m <sup>2</sup> ]	Surface area
S	various	Source term
Sc	[-]	Schmidt number
Sh	[-]	Sherwood number
$t$	[s]	Time
$T$	[K]	Temperature
$\tilde{T}$	[K]	Temperature
$\mathbf{v}$	[m/s]	Velocity vector
$v$	[m/s]	Velocity
$V$	[m <sup>3</sup> ]	Volume
$x$	[m]	Spatial coordinate
$y$	[m]	Spatial coordinate
$Y$	[kg/kg]	Mass fraction
$z$	[m]	Spatial coordinate
$\alpha$	[-]	Relaxation factor, Stoichiometric coefficient
$\alpha$	[mol]	Stoichiometric coefficient
$\Gamma$	various	General diffusion coefficient
$\epsilon$	[-]	Porosity, emissivity
$\eta$	[-]	Degree of biomass conversion
$\sigma$	[W/m <sup>2</sup> K <sup>4</sup> ]	Steffan-Boltzman constant ( $\approx 5.67 \cdot 10^{-8}$ )
$\lambda$	[W/m K]	Thermal conductivity, thermal dispersion coefficient
$\mu$	[kg/m s]	Dynamic viscosity
$\rho$	[kg/m <sup>3</sup> ]	Density
$\phi$	various	General transported quantity

Subscript	Meaning
0	Initial, or without fluid flow
1	First iteration
a	Activation (energy)
air	Primary air
amb	Ambient
ash	Ash
b	Bed
bal	Balance (equation)
c	Convective
C	Char, or constant part of a source term

<b>Subscript</b>	<b>Meaning</b>
CH <sub>4</sub>	Methane
C <sub>x</sub> H <sub>y</sub> O <sub>z</sub>	Tar
CO	Carbon monoxide
CO <sub>2</sub>	Carbon dioxide
COCO <sub>2</sub>	CO-to-CO <sub>2</sub> formation ratio
dry	Drying
e	Effective
<i>e</i>	Eastern face of a control volume
<i>E</i>	Eastern neighbour
end	End of simulation
env	Environment
f	Reaction front, or face of a control volume
fuel	Fuel
g	Gas phase
G	Grate
H	Hydrogen
H <sub>2</sub> O	Water vapour, or moisture
<i>i</i>	Index of species
in	Inner (diameter, radius, etc.)
<i>j</i>	Index of species
lim	Limiter
m	Molecular part
mix	Mixing (fuel)
<i>n</i>	Northern face of a control volume
<i>N</i>	Northern neighbour
N <sub>2</sub>	Nitrogen
NO	Nitrogen oxide
NO <sub>x</sub>	Nitrogen oxides
O	Oxygen
O <sub>2</sub>	Oxygen
out	Outer (diameter, radius, etc.)
onset	Onset (temperature)
p	Particle, constant pressure
plot	Plotting (time intervals)
pyr	Pyrolysis
<i>P</i>	Central coefficient, or linear part of a source term
r	Reactor, or relative
rad	Radiation
ref	Reference
s	Solid phase
s	Scaled
sb	Solid bulk (density)
s	Southern face of a control volume
surf	Surface
S	Sulphur
S	Southern neighbour

<b>Subscript</b>	<b>Meaning</b>
SO <sub>x</sub>	Sulphur oxides
t	Tube, or turbulent part
top	Bed top
u	Unscaled
vap	Vaporization
vol	Volatile matter
VF	Virgin fuel
w	Wall
w	Western face of a control volume
W	Western neighbour
x	X-coordinate position or direction, or stoichiometric coefficient
y	Y-coordinate position or direction, or stoichiometric coefficient
z	Stoichiometric coefficient
$\phi$	General transported quantity

<b>Superscript</b>	<b>Meaning</b>
0	Initial (condition)
f	Final state
i	Initial state
in	Inlet
iter	Iteration
new	New (the most current)
out	Outlet
sat	Saturation
$\phi$	General transport variable
+	Always positive part
-	Always negative part
*	Previous iteration
/	Correction

<b>Acronym</b>	<b>Meaning</b>
1D	One-Dimensional (transient)
2D	Two-Dimensional (steady)
CFD	Computational Fluid Dynamics
GRATECAL	Grate Calculator
GUI	Graphical User Interface
HHV	Higher Heating Value
MFIX	Multiphase Flow with Interphase Exchanges
LHV	Lower Heating Value
MSW	Municipal Solid Waste
SIMPLE	Semi-Implicit Method for Pressure-Linked Equations



# Annex I

## List of author's publications

- [1] HÁJEK, J., AND JUŘENA, T. Modelling of 1 MW solid biomass combustor: simplified balance-basedbed model coupled with freeboard CFD simulation. *Chemical Engineering Transactions* 29 (2012), 745–750, ISSN 1974–9791.
- [2] JUŘENA, T., AND HÁJEK, J. Computational system for CFD simulation of drying and devolatilization of biomass in 1D experimental fixed bed reactor. *Sborník 56. konference chemického a procesního inženýrství 56* (2009), pp. 17, ISBN 978–80–86059–51–8.
- [3] JUŘENA, T., AND HÁJEK, J. Mathematical modelling of biomass combustion: packing conditions issues. *Chemical Engineering Transactions* 21 (2010), 1105–1110, ISSN 1974–9791.
- [4] JUŘENA, T., AND HÁJEK, J. Energy considerations in CFD modelling of biomass combustion in an experimental fixed-bed reactor. *Chemical Engineering Transactions* 25 (2011), 803–808, ISSN 1974–9791.
- [5] JUŘENA, T., AND HÁJEK, J. Note on convergence criteria for energy and mass in CFD model of fixed-bed combustion. *MCS-7 Seventh Mediterranean Combustion Symposium - Proceedings* (2011), pp. 1, ISBN 978–88–88104–12–6.
- [6] JUŘENA, T., HÁJEK, J., AND KROPÁČ, J. Physical and chemical properties of biomass for CFD modelling of grate combustion. *Sborník 58. konference chemického a procesního inženýrství 58* (2011), pp. 12, ISBN 978–80–905035–0–2.
- [7] JUŘENA, T., RECMAN, M., AND HÁJEK, J. Simulation of biomass drying in fixed bed of experimental grate combustion reactor. *Chemical Engineering Transactions* 19 (2009), 599–604, ISSN 1974–9791.



## **Annex II**

# **Source codes of GRATECAL**

All source codes of bed models including GRATECAL 1.3 and GRATECAL 2.0 are available on the enclosed CD-ROM.



## **Annex III**

# **Source codes of UDF**

All source codes related to UDF for ANSYS FLUENT are available on the enclosed CD-ROM.